Late-Quaternary paleoclimate of Mount Field, Tasmania

by

Andrew Rees

BSc University of New Brunswick, 2005

BA University of New Brunswick, 2005

A Dissertation Submitted in Partial Fulfillment
of the Requirements for the Degree of

Doctor of Philosophy

in the Graduate Academic Unit of Biology

Supervisor: Les Cwynar, PhD

Examining Board: Joseph Culp, PhD, Department of Biology
Tillmann Benfey, PhD, Department of Biology
Joseph White, PhD, Department of Earth Sciences

External Examiner: James Shulmeister, PhD, School of Geography, Planning and Environmental Management, University of Queensland, Australia

This dissertation is accepted by the
Dean of Graduate Studies

THE UNIVERSITY OF NEW BRUNSWICK

May, 2014

Dedication

To my families Rees and Hickey

Together we've overcome many hardships and,

Without whose love and support,

I could not have persevered

Abstract

The mid-latitudes of the Southern Hemisphere possess a complex history of paleoenvironmental change. I address two objectives using lake sediment records from Tasmania, one of the few landmasses situated within this critical region of the "Water Hemisphere". First, cosmogenic dates from terminal moraines and sea surface temperatures (SST) suggest the climate of south-eastern Australia warmed rapidly after the Last Glacial Maximum, whereas pollen records indicate temperatures only began to increase at the onset of the Holocene, roughly 11.5 thousand calibrated years before present (cal ka BP). To explicitly address this discrepancy, I surveyed the modern environmental drivers of chironomid (Insecta: Diptera) distributions in Tasmania and developed an independent proxy of temperature. Second, a large body of literature has emerged invoking the Southern Westerly Winds (SWW) and El Niño/Southern Oscillation (ENSO) as major drivers of paleoenvironmental change. Some researchers have hypothesized that the SWW governed broad scale precipitation patterns from 14 to 5 cal ka BP, when ENSO became the main control of synoptic climate. Using a suite of lacustrine proxies, I investigated the nature of the transition from a SWW- to ENSO-dominated climate regime.

In terms of the first objective, pH explains most of the variance in the modern chironomid distributions. This environmental variable delineates between two geological provinces in Tasmania: one province has infertile, acidic soils and the other has soils generally richer in clay, possessing a greater buffering capacity. However, temperature of the warmest quarter (TWARM) explains most of the variance in the chironomid fauna within either

geological province. Consequently, I applied a chironomid-based transfer function for TWARM to a pair of fossil chironomid records from Mount Field National Park. Temperatures were at or above modern values early in the record, from about 15 to 13 cal ka BP, supporting the evidence from the cosmogenic dates and SST. After a prolonged cooling, temperatures again returned to modern, supporting a mid-Holocene thermal maximum between 6.7 and 4.6 cal ka BP. I used another lake sediment record from Mount Field to address the second objective. Based on lacustrine proxies, SSW controlled precipitation from 12 to 4.9 cal ka BP, fluctuating from wet to dry conditions around 8.4 cal ka BP. The abrupt shift to a generally dry though variable climate at 4.9 cal ka BP was characterized by an increased fire frequency. Considering all of the proxies, their transitions were nearly simultaneous and concurrent with the onset of ENSO activity in Ecuador, highlighting close links between the equatorial Pacific and south-eastern Australia.

Acknowledgments

I would like to start by thanking my supervisor and mentor, Dr. Les Cwynar. Where I am details-oriented, and sometimes cannot see the forest for the trees, Les was always able to help me see the big picture; he outlined the sandbox, but let me choose how to play. With this freedom, I was able to cultivate a toolset particular to the paleolimnologist's trade and develop templates of environmental change for parts of Tasmania. These templates can be used to generate specific climate questions, bringing me to the most important lesson. Les always stressed the significance of asking good research questions, and I look forward to putting this lesson to use throughout my career. I also appreciate the advice, feedback, and open doors of my other supervisory committee members, Dr. Steve Heard and Dr. Donald Baird.

This research was made possible by the generosity of many funding agencies. I am thankful to the Natural Sciences and Engineering Research Council of Canada, the Dr. John S. Little International Study Fellowship, The O'Brien Fellowship and the various funding opportunities provided by the University of New Brunswick.

I am also grateful to my wonderful lab mates who made the tedium of core subsampling and chironomid sorting bearable. Thank you Phil Brown, Katie and Kristie Richardson, Laura Bursey, Nancy Zhou, Daniel Lebouthillier, and Emily Higgins. On the other side of the microscope, I am indebted to Joshua Kurek for interspersing advice with fishing tips and to Stefen Engels for expanding my numerical literacy while simultaneously reducing my brain cell count at "Metal Mondays". Thank you Roger Smith and Bong Yoo for enlightening the photo shoot of sediment cores and terrestrial macrofossils. And a special thanks to my colleagues who made life inside and outside of

Bailey Hall fun: Fonya Irvine, Stephan Köning, Bridgette Clarkston, Julie Ryu, Laura Grace, Katrina Chu, Jeff Crocker and David Armanini.

Many thanks to Margaret Blacquier, Melanie Lawson, Rose Comeau, and Marni Turnbull for cheerfully dealing with my administrative and financial ineptitudes. I am also appreciative of Mike Casey for venturing outside of the Apple ecosystem to help me with technical issues of a PC nature.

To Sean and Heather, thank you for supplying a second home and the psychological nurture only best friends can provide. I will finally admit that our associations are based on more than geographical location! Also, thank you Adam, Nicole, Trevor, Janice, Andrew, Helen, Gabe, and Shawn for making Fredericton such an extraordinary place.

I am especially grateful for the best of all possible families. Mom, Dad, Katie, and Tim, thank you for putting up with my rants, encouraging my decisions, and being unwavering in your support; a person could not ask for a better clan. And finally, to my moon and stars, your love gives me the strength to attempt any challenge, your understanding the courage to pursue seemingly unattainable goals, and your patience the opportunity to finish this thesis! Thank you.

Table of Contents

List of Tables

List of Figures

List of Common Abbreviations

ACR: Antarctic Cold Reversal

cal ka BP: calibrated thousands of years before present

CCA: canonical correspondence analysis

DCA: detrended correspondence analysis

ENSO: El Niño/Southern Oscillation

GLM: generalised linear model

ITRAX: high resolution X-ray fluorescence

LGIT: last glacial-interglacial transition

LGM: Last Glacial Maximum

LOI: loss-on-ignition

PCA: principal components analysis

PLS: partial least squares

PRECIP: annual precipitation

r^2_{jack}: jack-knifed coefficient of determination

RMSEP: root mean square error of prediction

SST: sea surface temperature

SWW: Southern Westerly Winds

TWARM: temperature of the warmest quarter

VIF: variance inflation factor

WA-PLS: weighted averaging partial least squares

YD: Younger Dryas

Chapter 1 Introduction

The significance of Tasmania to Quaternary research in the Southern Hemisphere

With this thesis, I address two questions of major paleoenvironmental consequence associated with the mid-latitudes of the Southern Hemisphere. First, does the last glacial-interglacial transition (LGIT) of the mid-latitudes possess a temperature sequence resembling the Northern Hemisphere, the Southern Hemisphere, or something distinctive to the mid-latitudes? Second, when and how long did it take to transition from a climate dominated by the Southern Westerly Winds (SWW) to one dominated by the El Niño/Southern Oscillation (ENSO) during the mid-Holocene? Tasmania is an ideal location to investigate both questions.

In terms of the first question, global conditions became glacial between 29 and 20 ka BP (thousand years before present), with ice reaching maximum development around 21±3 ka BP. After the Last Glacial Maximum (LGM), ice retreat was rapid, though distinct cold reversals punctuated warming; these reversals occurred at different times in either hemisphere. Climate amelioration was interrupted by the Younger Dryas (12.8 ka BP) in the Northern Hemisphere and the Antarctic Cold Reversal (14.5 ka BP) in the Southern Hemisphere (Raynaud et al., 2000). Indeed, the "bipolar seesaw" paradigm (Broecker, 1998) hypothesizes that the LGIT temperature sequence was anti-phased between hemispheres. That is, warm episodes in the south corresponded to cooling in the north and vice versa. However, this paradigm was developed from ice core proxies, and therefore its applicability to the mid-latitudes of either hemisphere remains debatable.

Tasmania is located within the critical latitudinal range for ice building during glacial and stadial periods. Further, the island is situated between two important controls of synoptic-scale climate: Antarctica to the south and the Western Pacific Warm Pool to the north. Therefore, the island should register shifts in major climate systems. Evidence from pollen records, sea surface temperatures (SST), and cosmogenic dates suggests that Tasmania did not experience any major temperature reversals during the LGIT, favouring a sequence that is unique from Northern and Southern Hemisphere ice cores. However, where the SST and cosmogenic dates highlight rapid warming after the LGM (Barrows et al., 2002; Mackintosh et al., 2006; Sikes et al., 2009), the pollen records indicate temperatures approached modern values much later, around 11.5 ka BP (Macphail, 1979; Markgraf et al., 1986). I developed an independent proxy of temperature to specifically address this debate.

The second major transition I address involves the shift from a SWW- to ENSO-dominated climate, hypothesized to have occurred 5 ka BP (Fletcher and Moreno, 2012). This transition has major implications for interpreting vegetation and precipitation records from the mid-latitudes. Currently, Tasmania's climate is strongly affected by both the SWW and ENSO. In terms of the westerlies, precipitation is positively correlated with wind speed in western Tasmania, whereas eastern regions possess either no or negative relationships (Garreaud, 2007). Regarding ENSO, El Niño (La Niña) years result in anomalously dry (wet) conditions island-wide (Hill et al., 2009). Consequently, Tasmania is well-positioned to characterize the transition between these different drivers of synoptic climate. However, an understanding of paleoenvironments is often garnered from modern analogues, requiring a deep knowledge of the contemporary setting.

Tasmania and its (paleo)climate

Tasmania (Fig. 1.1) is a small island-state (68,018 km^2; Australian Bureau of Statistics) located on the south-eastern tip of the Australian continental plate. It possesses a maritime climate with only slight continentality on the Central Plateau. Temperatures for the capital city, Hobart (pop. 216,276 for Greater Hobart; Australian Bureau of Statistics), range from 18.9°C in the summer to 11.9°C in the winter (Hobart meteorological station, Australian Government Bureau of Meteorology). Tasmania lies on the boundary of the Roaring Forties - strong zonal westerlies that deliver precipitation to the island year-round. Because of north-south trending mountain ranges near the west coast, there is a marked decrease in rainfall across the island. Moisture bearing winds undergo orographic lift, dropping between 2,500 and 3,500 mm of rain annually on western ranges and generating an appreciable rain-shadow in the east. The midlands of east-central Tasmania generally receive less than 760 mm of precipitation annually (Macphail, 1979).

Tasmania possesses a complex geology, housing a wide variety of old and new landforms with an array of geological formations. Generally speaking, western Tasmania is characterized by quartzose basement sediments that have been extensively folded and reworked by erosion. Soils in these regions are typically shallow, infertile and acidic (Jackson, 2005). In central and eastern regions of the island, extensive faulting has occurred; Permian mudstones and Triassic siltstones overlie older basement rock. Both of these features have been extensively modified by doleritic intrusions (Fig. 1.1b, c, e), generating soils richer in clay and generally more fertile than those in the west (Jackson, 2005).

The vegetation of Tasmania consists of endemics (amongst vascular plants, there are about 330 endemics of 1,488 native species; Buchanan, 1995) mixed with Gondwanaland and Australian components. Species distributions broadly mirror the discontinuities in rainfall and geology. Regions with high annual rainfall in the west support rainforest communities typically dominated by *Nothofagus cunninghamii*. Low soil fertility generates breaks in the canopy, permitting the establishment of shade-intolerant and mesophytic species. Where fire is prominent, expansive communities of button grass moorland prevail (Macphail, 1979). Moving east, reductions in annual rainfall along with improved soil quality drive the vegetational gradient. Rainforest gives way to wet sclerophyllous communities dominated by *Eucalyptus* species (Fig. 1.1a). Further east, in the rain-shadow of the western mountain ranges, dry sclerophyllous *Eucalyptus* forests (Fig. 1.1d) are replaced by savanna woodland (Macphail, 1979).

Repeated glacial episodes during the Quaternary carved out much of the Tasmanian landscape, generating countless cirque and valley lakes (Colhoun, 2004). The sediments of these systems archive past climate change dating back to the LGIT and, in regions that remained unglaciated, to the previous interglacial 120 ka BP. However, despite the suite of lakes and its sensitivity to hemispheric-scale climate events, most of the previous paleoclimate studies from Tasmania focused on qualitative or semi-quantitative interpretations of pollen records (Macphail, 1979; Colhoun and van de Geer, 1986; Markgraf et al., 1986; van de Geer et al., 1989). These studies generally indicate increasing temperature and moisture between roughly 14 and 11.5 ka BP. Temperature and precipitation gradually reached maxima between 11.5 and 6.8 ka BP with values slightly greater than modern. After these maxima, climate cooled to its modern state

(Macphail, 1979; Markgraf et al., 1986; Harrison, 1993). Although these studies were pioneering, they suffer from poor chronological control, lack of modern analogues, lags in response time of certain plant taxa and the insensitivity of local vegetation's response to broad scale climate change. Consequently, we decided to verify these results with quantitative inferences derived from an independent proxy - chironomids.

Chironomids and the transfer function approach

Chironomids are non-biting midges belonging to the order Diptera. They are holometabolic organisms that undergo complete metamorphosis. Female adults lay eggs in a hydrophilous jelly mass atop the water's surface or as a jelly string attached to a substrate by one end. The eggs hatch into aquatic larvae that undergo four stages, moulting between each instar (Brooks et al., 2007; Fig. 1.2). The larvae of some subfamilies are free-living (e.g., Tanypodinae); however, most species dwell in silken tubes spun by organs located on the ventromentum. These tubes serve to hide larvae from predators as well as perform respiratory functions. The larva undulates in the tube, drawing oxygenated water into the mouth end and flushing out deoxygenated water from the anterior. Tube-dwelling chironomids may be mobile, transporting their case with them, or sedentary. Most larvae burrow into sediments or live attached to macrophytes or stones. This is the dominant phase of the insect's lifecycle. Large species inhabiting the profundal region of lakes may require more than one year developing into pupae. On the other hand, smaller species living in warm, shallow water may be uni-, bi- or multivoltine (Brooks et al., 2007).

Larvae mature into pupae, a stage that generally lasts 3-4 days. Metamorphosed, pharate adults swim upwards where they breach the meniscus and remain suspended on the water's surface; a fully developed, winged adult emerges. Adults usually do not feed and typically live for only a few days. Males congregate in mating swarms to attract females (Brooks et al., 2007).

Chironomids are the most widely-distributed and often most abundant group of insects found in freshwater systems (Armitage et al. 1995); the remains (typically head capsules; Fig. 1.3) of several hundred individuals may be present in just a few grams of sediment. They also inhabit a variety of other biotopes: some species are terrestrial, colonizing moist leaf litter; some are marine and have been found in the stomach contents of cod (Chernovskii, 1949); some chironomid species can tolerate hot springs that reach 40°C (Pinder, 1995); while others inhabit volcanic lakes with pH values as low as 1.4 (Yamamoto, 1986). Most chironomid larvae are either detritivores, collecting particulate matter in silken webs, or grazers, feeding on bacteria or algae that grow on aquatic macrophytes or the surface of submerged stones. Members of the family have adopted any of six feeding strategies: they are either scrapers, shredders, filter-feeders, deposit-feeders, predators or a mixture (Berg, 1995).

Chironomid larvae possess many traits that make them useful paleoecological indicators. A large number of taxa are stenotopic, meaning they have narrow ecological optima. As previously mentioned, the family Chironomidae is ubiquitous and abundant, occurring in virtually all aquatic biotopes in sufficient number to satisfy the statistical prerequisites of many numerical methods. Chironomid larvae also deposit chitinous head capsules that are usually preserved in good condition in lacustrine sediments (Fig. 1.3).

Most specimens are identifiable to genus or species-group levels, making the distinction between ecologically sensitive taxa possible. However, most importantly, chironomids are sensitive to local environmental change and, because of their short generation times and winged adult phase, effectively respond to perturbations instantaneously with respect to the sampling resolution of most paleoecological studies (Brooks et al., 2007).

Chironomids have been statistically linked to a host of environmental variables: pH (Rees et al., 2010), water depth (Barley et al., 2006), dissolved oxygen (Quinlan and Smol 2001), salinity (Heinrichs et al., 2001), and heavy metals (Brooks et al., 2005) to name a few. Most important for reconstructing past climate, temperature plays a dominant role in every stage of the chironomid lifecycle. Temperature governs egg development and the number of larvae that successfully hatch, it affects how larvae and pupae develop and it controls many adult behaviours, for instance, emergence time and duration, the number and size of mating swarms, and sexual activity (Pinder, 1986; Armitage et al., 1995).

The transfer function approach capitalizes on the aforementioned relationships between environmental variables and modern chironomid distributions. A transfer function is a mathematical model that applies these modern relationships to abundance data from the fossil record to quantitatively infer past changes in the environmental variable of interest (Fig. 1.4). Fossil taxa abundances are effectively synthesized, within a reasonable margin of error, into a single, important environmental variable. Transfer functions are generally developed by sampling a number of lakes across environmental gradients (e.g., temperature). Each taxon is ascribed a coefficient to convert abundances

into units of measurement (e.g., °C, metres, μg/L); these conversion factors are then applied to fossil communities in order to quantitatively estimate environmental variables.

Thesis organization and objectives

My thesis is divided into two parts: one focused on "neoecology" (Chapters 2 and 3) and the other on paleoecology (Chapters 4 and 5). The first part explores the modern relationships between chironomid distributions and the complex suite of environmental variables that comprise the Tasmanian landscape. The main goal was to develop a transfer function to reconstruct past temperature change. The second part of my thesis centers on applying the transfer function to two fossil records collected from Mount Field National Park, located in south-central Tasmania. In these chapters, I describe the temperature and hydrological fluctuations that characterize the region's deglacial and postglacial sequences, with records extending to about 16 ka BP.

Chapter 2 presents chironomid-based transfer functions developed to reconstruct temperature of the warmest quarter (TWARM) in Tasmania. In recent decades, the use of chironomid remains in paleoecology has made excellent progress in the Northern Hemisphere. Unfortunately, incomplete knowledge of the chironomid fauna, a lack of ecological data, and logistical problems have hampered the application of this technique south of the equator. In building the transfer functions, I worked alongside Dr. Peter S. Cranston, an eminent chironomid specialist, to establish a working taxonomy for the larval remains. These inference models are the first of their kind for the Australian region and will serve to quantitatively address specific hypotheses regarding the LGIT.

Chapter 3 builds on the foundation laid in the preceding section. Previous analyses revealed that pH explained the majority of variance in the modern chironomid distributions. In Tasmania, pH correlates with broad scale differences between western and eastern lake districts, effectively integrating congruent geologic, climatic, and vegetational change over a narrow corridor, called Tyler's Line. With this in mind, the objectives of this chapter were threefold: 1) to test the hypothesis that chironomid community composition changes across Tyler's Line and to identify indicator taxa of either lake district, 2) to determine critical breakpoints on the pH scale where these changes take place, and 3) to create an inference model to estimate the natural variability of pH. These models can be used to establish a baseline of pre-industrial pH fluctuations, putting the impact of anthropogenic effects in context. Further, identifying modern pH indicator taxa will help assess the reliability of temperature reconstructions based on fossil chironomids.

In the paleoecology chapters, I apply the previously developed models and taxonomic knowledge to fossil records from Mount Field National Park, Tasmania; Chapter 4 focuses on inferred temperatures and Chapter 5 on paleohydrology. In Chapter 4, I applied the temperature transfer function to fossil chironomid records extending to the Late Pleistocene/Holocene transition. The goal was to quantitatively characterize the LGIT in Tasmania and to assess the variability of climate throughout the Holocene. Specifically, I was looking for evidence of the Antarctic Cold Reversal (ACR) and Younger Dryas (YD) to determine if Tasmania had a temperature sequence similar to either the Northern or Southern Hemisphere pattern. Alternatively, Tasmania could have a unique sequence, as supported by the pollen records, SST, and cosmogenic dates. If this

is the case, I hope to identify evidence supporting either an early (cosmogenic dates, SST) or late (pollen) postglacial warm period. I also tried to constrain the Holocene thermal maximum and assess if past temperatures have exceeded modern values in recent history.

In my final research chapter, I use multiple proxies to qualify past changes in moisture regime at Mount Field. Since Tasmania is on the boundary of the Roaring Forties and within the zone of ENSO influence, the island should be sensitive to broad changes in both phenomena. As organisms with a dominant aquatic phase, chironomids are responsive to changes in lake depth (Heiri, 2004), and hence shifts in assemblages should mirror these hydrological features.

Statement of contributions

I developed the ideas comprising this thesis and carried out all of the data analysis, interpretation, and manuscript preparation with guidance from Dr. Les Cwynar (all Chapters), Dr. Peter Cranston (Chapter 2), and Dr. Michael-Shawn Fletcher (Chapter 5). Dr. Les Cwynar and I conducted the majority of the fieldwork, collecting water samples for chemical analysis (Chapters 2 and 3), surface samples for chironomid and loss-on-ignition (LOI) analyses (Chapters 2 and 3), and long cores for climate reconstructions (Chapters 4 and 5); additional contributions are acknowledged in each chapter. Chironomid remains were picked by me, Phil Brown, Katie and Kristie Richardson, Laura Bursey, Nancy Zhou, and Daniel Lebouthillier. I identified all of the remains using a taxonomy developed in conjunction with Dr. Peter Cranston. I collected the remaining data with instruction from Dr. Les Cwynar (e.g., LOI, material for

radiometric dating), except for the ITRAX (high resolution X-ray fluorescence) and charcoal results presented in Chapter 5. The former were collected by Dr. Pierre Francus and the latter were collected by Emily Higgins, Kristen Fulton, and Heather Hickey.

This thesis has redundancies in information among chapters, particularly introduction and methods sections, because each data chapter was written as a stand-alone publication.

References

Armitage, P., Cranston, P.S., Pinder, L.C.V., 1995. The Chironomidae: The Biology and Ecology of Non-Biting Midges. Chapman and Hall, London.

Barley, E.M., Walker, I.R., Kurek, J., Cwynar, L.C., Mathewes, R.W., Gajewski, K., Finney, B.P., 2006. A northwest North American training set: distribution of freshwater midges in relation to air temperature and lake depth. Journal of Paleolimnology 36, 295-314.

Barrows, T.T., Stone, J.O., Fifield, L.K., Cresswell, R.G., 2002. The timing of the Last Glacial Maximum in Australia. Quaternary Science Reviews 21, 159-173.

Berg, H.B., 1995. Larval food and feeding behaviour. In: Armitage, P.D., Cranston, P.S., Pinder, L.C.V. (Eds.), The Chironomidae: The Biology and Ecology of Non-Biting Midges. Chapman & Hall, London, pp. 136-168.

Birks, H.J.B., 2003. Quantitative palaeoenvironmental reconstructions from Holocene biological data. In: Mackay, A., Battarbee, R., Birks, H.J.B., Oldfield, F. (Eds.), Global Change in the Holocene. Oxford University Press, New York, pp. 107-123.

Brodersen, K.P., Anderson, N.J., 2000. Subfossil insect remains (Chironomidae) and lake-water temperature inference in the Sisimuit-Kangerlussuaq region, southern West Greenland. Geology of Greenland Survey Bulletin 186, pp. 78-82.

Broecker, W.S., 1998. Paleocean circulation during the Last Deglaciation: a bipolar seesaw? Paleoceanography 13, 119-121.

Brooks, S.J., Udachin, V., Williamson, B.J., 2005. Impact of copper smelting on lakes in the southern Ural Mountains, Russia, inferred from chironomids. Journal of Paleolimnology 33:229-241.

Brooks, S.J., Langdon, P.G., Heiri, O., 2007. Using and Identifying Chironomid Larvae in Palaeoecology. QRA Technical Guide no. 10. Quaternary Research Association, London, UK.

Buchanan, A.M., 1995. A Census of the Vascular Plants of Tasmania and Index to the Student's Flora of Tasmania. Tasmanian Herbarium, Tasmanian Museum and Art Gallery, Hobart.

Chernovskii, A.A., 1949. A Key to Larvae of the Family Tendipedidae. Keys to the Fauna of the USSR. Zoological Museum of the USSR Academy of Sciences, Moscow, Leningrad.

Colhoun, E.A., 2004. Quaternary glaciations of Tasmania and their ages. In: Ehlers, J., Gibbard, P.L. (Eds.), Quaternary Glaciations - Extent and Chronology, Part 3. Elsevier, Amsterdam, pp. 353-371.

Colhoun, E.A., van de Geer, G., 1986. Holocene to Middle Last Glaciation vegetation history at Tullabardine Dam, western Tasmania. Proceedings of the Royal Society of London B29, 177-207.

Fletcher, M.-S., Moreno, P.I., 2012. Have the Southern Westerlies changed in a zonally symmetric manner over the last 14,000 years? A hemisphere-wide take on a controversial problem. Quaternary International 253, 32-46.

Garreaud, R.D., 2007. Precipitation and circulation covariability in the extratropics. Journal of Climate 20, 4789-4797.

Harrison, S.P., 1993. Late Quaternary lake-level changes and climates of Australia. Quaternary Science Reviews 12, 211-231.

Heinrichs, M.L., Walker, I.R., Mathewes, R.W., 2001. Chironomid-based paleosalinity records in southern British Columbia, Canada: a comparison of transfer functions. Journal of Paleolimnology 26:147-159.

Heiri, O., 2004. Within-lake variability of subfossil chironomid assemblages in shallow Norwegian lakes. Journal of Paleolimnology 32: 67-84.

Hill, K.J., Santoso, A., England, M.H., 2009. Interannual Tasmanian rainfall variability associated with large-scale climate modes. Journal of Climate 22, 4383-4397.

Jackson, W.D., 2005. The Tasmanian environment. In: Reid, J.B., Hill, R.S., Brown, M.J., Hovenden, M.J. (Eds.), Vegetation of Tasmania. Australian Biological Resources Study, Tasmania, Australia, pp. 11-34.

Mackintosh, A.N., Barrows, T.T., Colhoun, E.A., Fifield, L.K., 2006. Exposure dating and glacial reconstruction at Mt. Field, Tasmania, Australia, identifies MIS 3 and MIS 2 glacial advances and climatic variability. Journal of Quaternary Science 21, 363-376.

Macphail, M.K., 1979. Vegetation and climates in southern Tasmania since the Last Glaciation. Quaternary Research 11, 306-341.

Markgraf, V., Bradbury, J.P., Bubsy, J.R., 1986. Paleoclimates in southwestern Tasmania during the last 13,000 years. Palaios 1, 368-380.

Pinder, L.C.V., 1995. The habitats of chironomid larvae. In: Armitage, P.D., Cranston, P.S., Pinder, L.C.V. (Eds.), The Chironomidae: The Biology and Ecology of Non-Biting Midges. Chapman & Hall, London, pp. 107-135.

Pinder, L.C.V., 1986. Biology of freshwater Chironomidae. Annual Review of Entomology 31, 1-23.

Quinlan, R., Smol, J.P., 2001. Chironomid-based inference models for estimating end-of-summer hypolimnetic oxygen from south-central Ontario lakes. Freshwater Biology 46:1529-1551.

Raynaud, D., Barnola, J.-M., Chappellaz, J., Blunier, T., Indermühle, A., Stauffer, B., 2000. The ice record of greenhouse gases: a view in the context of future changes. Quaternary Science Reviews 19, 9-17.

Rees, A.B.H., Cwynar, L.C., 2010. A test of Tyler's Line - response of chironomids to a pH gradient in Tasmania and their potential as a proxy to infer past changes in pH. Freshwater Biology 55, 2521-2540.

Sikes, E.L., Howard, W.R., Samson, C.R., Mahan, T.S., Robertson, L.G., Volkman, J.K., 2009. Southern Ocean seasonal temperature and Subtropical Front movement on the South Tasman Rise in the late Quaternary. Paleoceanography 24, PA2201. doi: 10.1029/2008PA001659.

van de Geer, G., Fitzsimons, S.J., Colhoun, E.A., 1989. Holocene to Middle Last Glaciation vegetation history at Newall Creek, western Tasmania. New Phytologist 111, 549-558.

Yamamoto, M., 1986. Studies of the Japanese *Chironomus* inhabiting high acidic water (Diptera, Chironomidae) I. Kontyu 54, 324-332.

Figure 1.1: Snapshots of Tasmanian environments. a) Wet sclerophyll forest dominated by *Eucalyptus oliqua* near Lake Chisholm, north-western Tasmania; the catchment consists of sedimentary carbonate and siliclastic rocks. b) Eastern alpine vegetation characterized by heathland with minor sedgeland, cushion moorland and grassland; Quaternary colluvium and Jurassic dolerite prevail in eastern highlands. c) and d) Dry *Eucalyptus* forest, dominated by *E. coccifera* with a stunted *E. subcrenulata* understory, characterizes the catchment of Platypus Tarn (the smaller lake to the right in panel c), Mount Field National Park; Mount Field is capped by Tasmanian dolerite. e) The Tarn Shelf, also located in Mount Field National Park, consists of cushion moorland and alpine coniferous heathland.

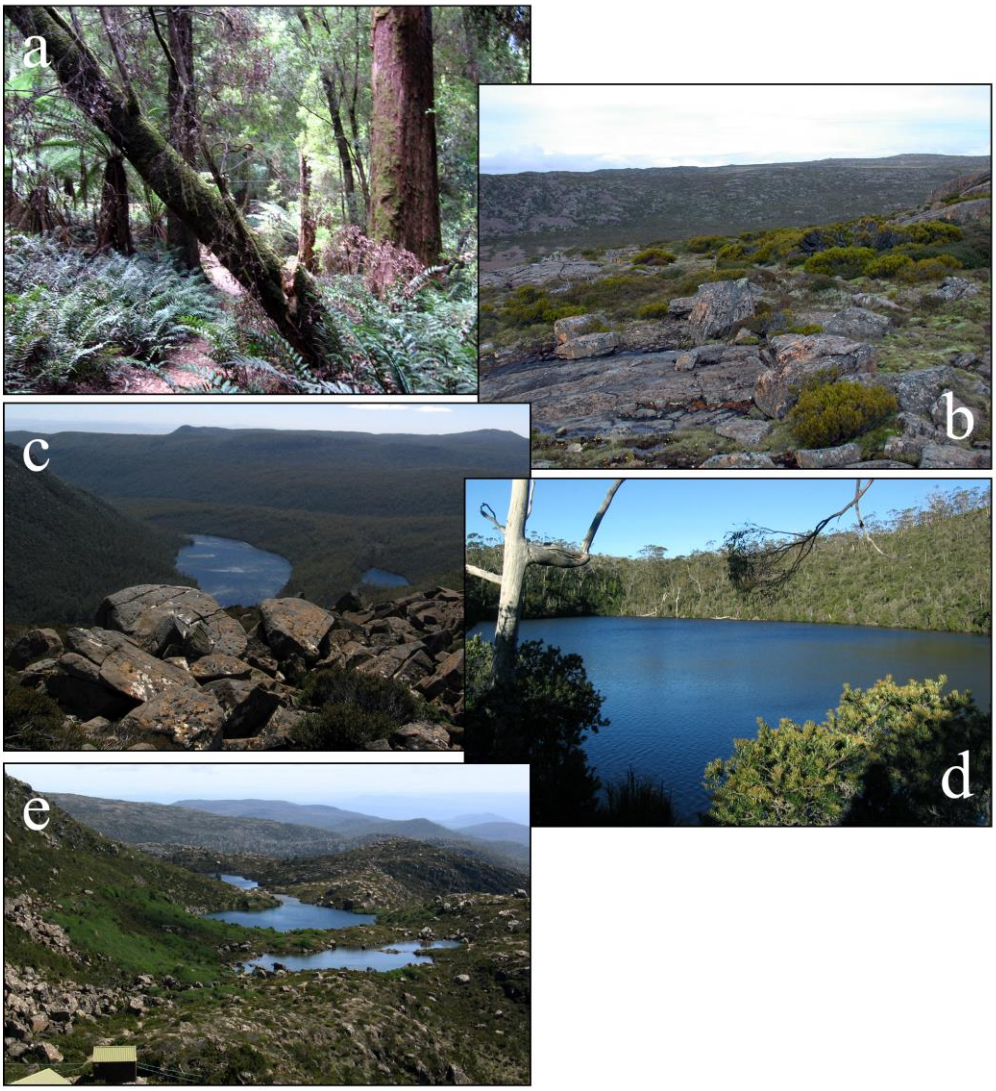

Figure 1.1: Snapshots of Tasmanian environments.

Pictures taken by Andrew Rees from January to February of 2006 in Tasmania, Australia.

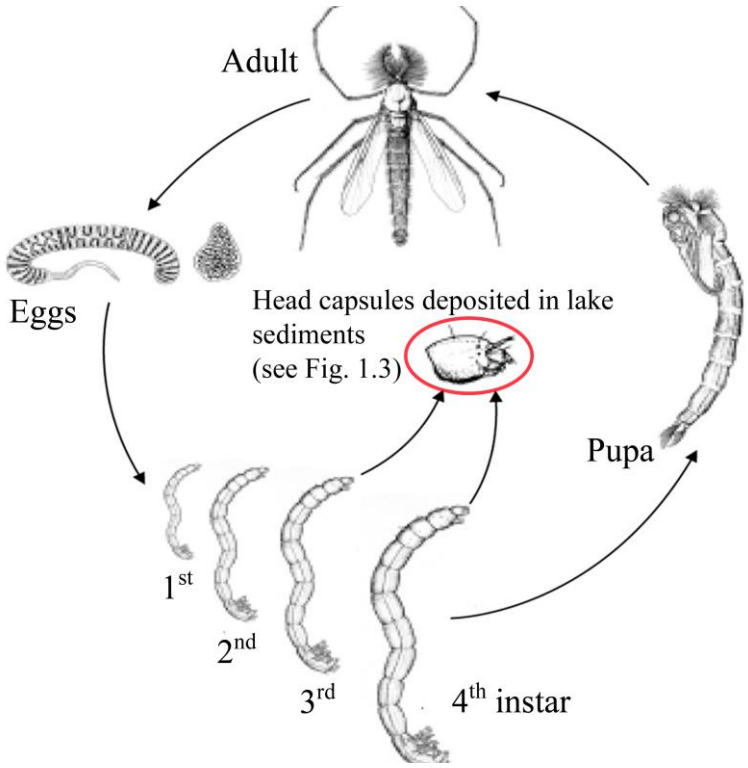

Figure 1.2: Schematic of the chironomid life cycle.

Typically the head capsules preserved in lake sediments can be identified to either genus or species levels (modified from Brodersen and Anderson, 2000).

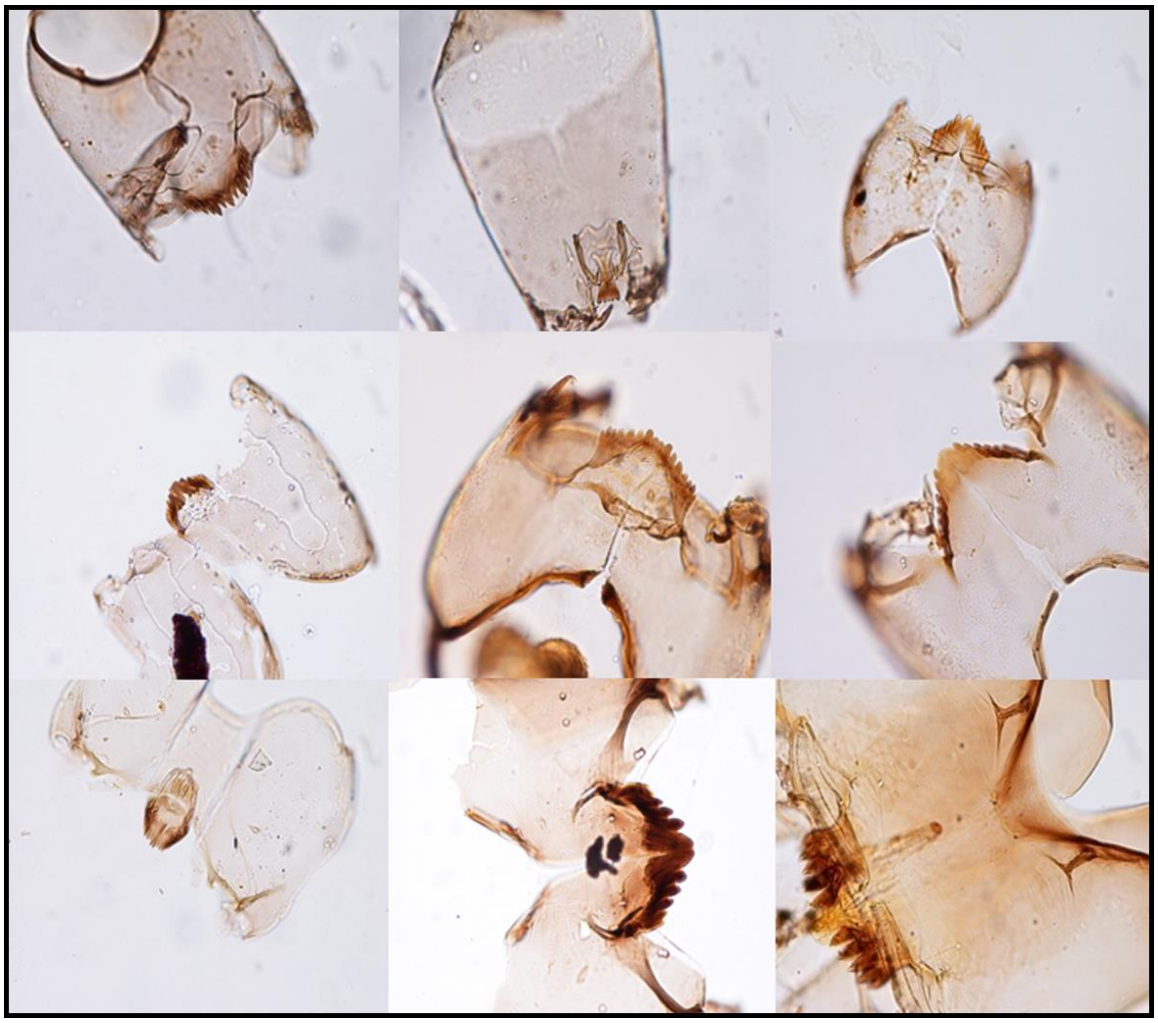

Figure 1.3: Variability of chironomid taxa from Tasmanian sediments.

From left-to-right and top-to-bottom: *Chironomus*, Pentaneurini (early instar), *Paratanytarsus*, worn *Paralimnophyes* morphotype 1, *Stictochironomus*, *Cricotopus*, *Parochlus*, *Botryocladius*, and *Tanytarsus* morphotype 2. Pictures taken by Andrew Rees during the winter and spring of 2006 at the University of New Brunswick, Canada.

Figure 1.4: Schematic of the transfer function approach. a) Modern chironomid remains (typically head capsules) are collected from the upper centimetre of lake sediment; this process is repeated for many lakes (47 in the case of the temperature transfer function developed in Chapter 2). These data are modelled with contemporary environmental information from each site to create a transfer function. The model essentially assigns each taxon a coefficient to convert percent abundance into the desired unit of measure (e.g., °C, metres, µg/L, etc.). This approach reduces a complete species assemblage into a single point estimate. b) Fossil chironomid remains are collected from a sediment core; the deeper one samples through the core, the further back in time one goes. Typically, age estimates are derived from radiometrically dated plant macrofossils. c) The fossil chironomid samples are run through the transfer function to reconstruct past changes in the environmental variable of interest (modified from Birks, 2003).

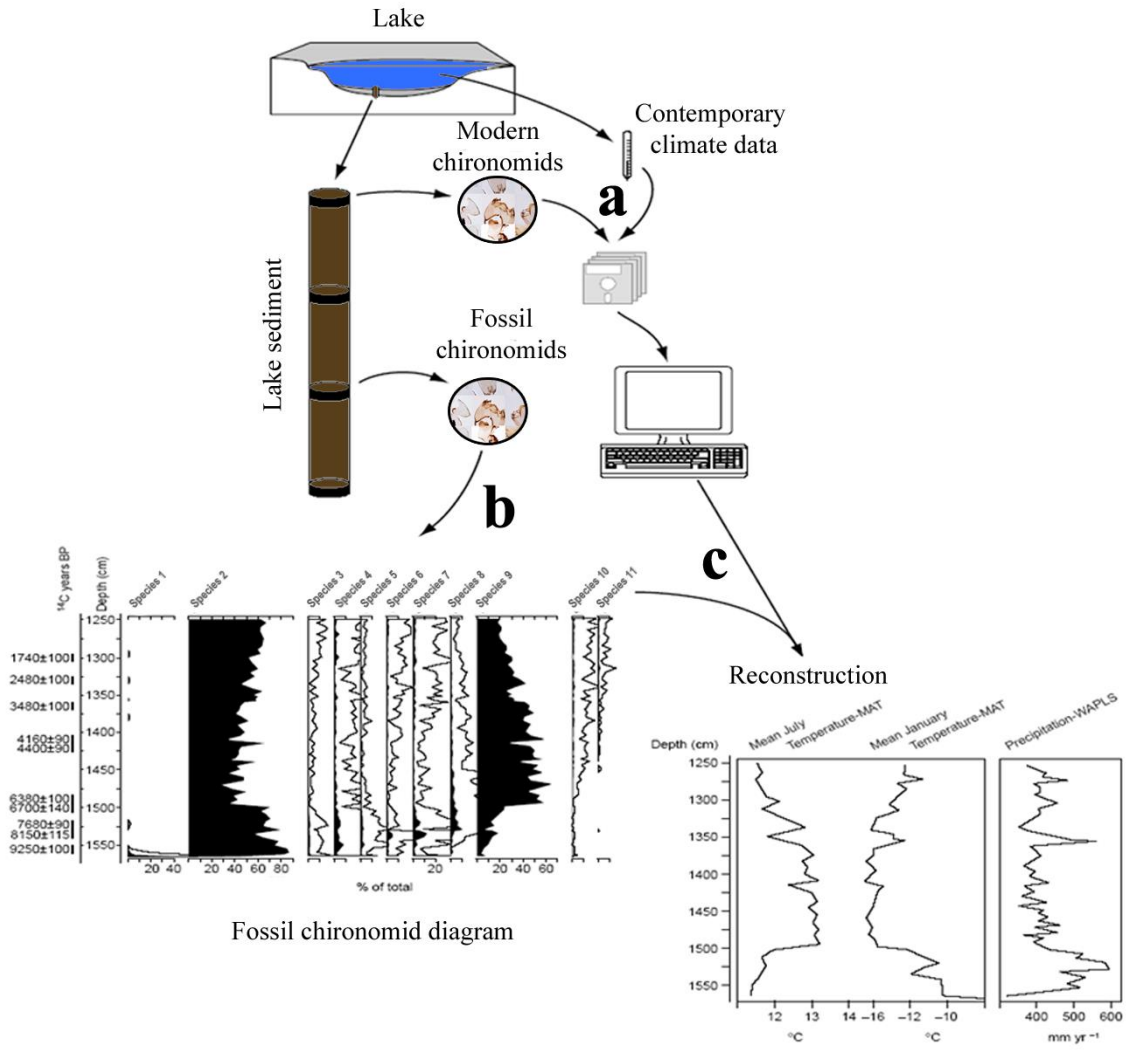

Figure 1.4: Schematic of the transfer function approach.

Chapter 2 Midges (Chironomidae, Ceratopogonidae, Chaoboridae) as a temperature proxy: a training set from Tasmania, Australia

Citation for published manuscript: Rees, A.B.H., Cwynar, L.C., Cranston, P.S., 2008. Midges (Chironomidae, Ceratopogonidae, Chaoboridae) as a temperature proxy: a training set from Tasmania, Australia. Journal of Paleolimnology 40, 1159-1178.

Abstract

Chironomid and ceratopogonid head capsules, along with *Chaoborus* mandibles, were used to model mean temperature of the warmest quarter (TWARM) in Tasmania. Our transfer function is based on midge assemblages and 21 environmental variables sampled from 47 lakes. Canonical correspondence analysis (CCA) revealed seven variables that account for a significant ($P \leq 0.05$) portion of the explainable variance. In order of explanatory power, these were pH, TWARM, annual radiation, magnesium, annual precipitation, SiO_2, and depth. TWARM was modelled using weighted averaging partial least squares (WA-PLS) and generated a model with dissolved TKN = 0.72 and RMSEP = 0.94°C. Advances in chironomid paleoecology are progressing very quickly in the Southern Hemisphere. Chironomid identification guides and autecological data are available for many regions, highlighting the potential for developing midge-based quantitative models to address hemispheric and interhemispheric climate hypotheses.

Keywords: Chironomids, Midges, Tasmania, Paleoclimate, Temperature, Transfer function, Australia

Introduction

The degree to which Northern Hemisphere paleoclimate affected its southern counterpart during the most recent deglaciation (20-10 ka BP) is a hotly debated issue (Turney et al., 2006; Alloway et al., 2007). Hypotheses are difficult to test with the few quantitative paleoclimate reconstructions currently available from south of the equator. Compounding the issue in terms of terrestrial records, only 2% of the Southern Hemisphere landmass is located within temperate regions corresponding to latitudes of extensive glaciation in the Northern Hemisphere (Clapperton, 1990). At 41-44°S, the island-state of Tasmania, Australia (Fig. 2.1), is situated within this critical latitudinal range.

Tasmania is ideally located to detect synoptic-scale climate change within the Southern Hemisphere because it is positioned between two important controls of both atmospheric and oceanic circulation patterns: Australasia continental shelf regions to the north and Antarctica to the south (Kershaw and Nanson, 1993). In addition, Tasmania may be distant enough from Northern Hemisphere ice sheet feedbacks and insolation-forcing mechanisms to register a genuinely Southern Hemisphere climate signal from the previous glaciation.

During the Last Glacial Maximum (LGM), icecaps, along with valley and cirque glaciers, developed in western and central parts of Tasmania, covering ca. 1,000 km^2 (Colhoun, 1985; Colhoun and Shulmeister, 2006). With more ice coverage than mainland Australia, Tasmania's glaciers generated numerous lakes containing continuous sediment records dating to the Last Glacial Termination (LGT) and, where regions remained

unglaciated, to the previous interglacial (120 ka BP). This presents a unique opportunity to address regional and hemispheric research questions. For example, what evidence is there from Tasmania for the Antarctic Cold Reversal (ACR) or Younger Dryas cooling event? Were there abrupt climate reversals during the Holocene? Does Tasmania register a hemispheric climate signal, i.e., how similar are Tasmanian records to those of Southern Hemisphere marine and ice cores? Does Tasmania's climate history show any similarity to other important Southern Hemisphere landmasses such as New Zealand or Patagonia? Obtaining answers to these questions is impeded by the lack of inference models based on terrestrial proxies that can provide quantifiable estimates of past climate change.

Chironomids (Diptera: Chironomidae) are particularly useful environmental indicators, especially for reconstructing changes in temperature (Brooks and Birks, 2001; Walker et al., 1997) and they are the most widely-distributed and often most abundant group of insects found in freshwaters (Armitage et al., 1995). The majority of species have short generation times and winged adults. Furthermore, as insects, chironomids respond to temperature during all stages of their lifecycle (Ward and Stanford, 1982).

Although chironomid paleoecology has made tremendous progress over the past two decades in temperate regions of the Northern Hemisphere, progress in the Southern Hemisphere has lagged until recently. Chironomid-based, paleoecological studies in the tropics and Southern Hemisphere traditionally have remained relatively scarce because of an incomplete knowledge of the chironomid faunas, a lack of ecological data, and logistical problems that have prevented the development of calibration sets (Verschuren and Eggermont, 2006). Because of these handicaps, many attempts to use chironomids

for core-based paleoclimate/paleoenvironmental reconstructions in South America (Massaferro and Brooks, 2002; Massaferro et al., 2005), Africa (Mees et al., 1991), and New Zealand (Deevey, 1955) have been qualitative (see Verschuren and Eggermont, 2006 for review). However, chironomid identification guides (e.g., Cranston, 2000; Cranston and Dimitriadis, 2004) and autecological data (e.g., Paterson and Walker, 1974; Kokkin, 1986) are available for many regions of the Southern Hemisphere, creating opportunities to develop robust, quantitative inference models.

While none of the earlier efforts in the Southern Hemisphere resulted in a quantitative temperature inference model, one of the first detailed studies to apply multivariate statistics to chironomid fossil data was conducted in New Zealand. Boubée (1983) used principal components analysis on modern chironomid remains to constrain down-core interpretations of fossil taxa. Similarly in New Zealand, Schakau (1986) applied classification techniques down-core in order to interpret shifts in fossil chironomid abundances qualitatively. Since these initial studies, there have been major improvements both in the statistics used in paleoecology and in the taxonomic resolution of New Zealand chironomids, culminating in two transfer functions for temperature (Woodward and Shulmeister, 2006; Dieffenbacher-Krall et al., 2007) and one for chlorophyll a (Woodward and Shulmeister, 2006).

The first quantitative study of chironomid paleoecology in Australia was conducted by Dimitriadis and Cranston (2001) who calibrated subfossil assemblages using chironomid survey and physico-chemical data collected from eastern Australian lakes. With these data, they created a Holocene climate reconstruction from a tropical lake in north-eastern Queensland using mutual-climate-ranges (MCRs), a technique

common to beetle paleoecology (Elias, 1997). This method has encountered criticisms (see Birks, 2003; Verschuren and Eggermont, 2006 for a review), resulting in the need for a more robust approach to reconstructing the paleoclimates of Australia.

Here we present a temperature transfer function based on subfossil assemblages of Chironomidae (non-biting midges), Ceratopogonidae (biting midges), and Chaoboridae (phantom midges) from 47 Tasmanian lakes. This is the first such transfer function built for Australia and will add to the paleoclimatological tools available for testing climate hypotheses in the Southern Hemisphere.

Study area

Tasmania is located at the southern-most extent of the Australasian continental plate. During glacial stages, the island was connected to Australia by a land bridge; otherwise, Tasmania is separated from the mainland by the 250 km wide Bass Strait (Jackson, 2005). Despite its association with a flat and dry continent, Tasmania possesses a predominately maritime climate and a mountainous landscape preserving many glacial features. The geology, climate, lake chemistry, and vegetation all change abruptly at what has been called "Tyler's Line" by Shiel et al. (1989) and roughly coincides with the 146th meridian. The ensuing descriptions of climate, geology, and vegetation follow Jackson (2005) and Macphail (1979).

Climate

Westerlies known as the Roaring Forties provide western Tasmania with year-round precipitation. Migration of a subtropical high pressure system over Australia governs the position of the Roaring Forties, forcing the westerlies south of Tasmania

during summer months and across the island during winter (Harrison, 1993), resulting in wet winters and relatively dry summers. In conjunction with Tasmania's orography, the Roaring Forties produce a strong, west-east precipitation gradient. On the west coast, annual precipitation typically ranges from 1,029 to 1,270 mm. Rain-bearing winds move inland where they meet western mountain ranges, resulting in annual precipitation usually ranging between 2,540 and 3,560 mm on western mountains and a rain-shadow eastward. Consequently, the Midlands of east-central Tasmania typically receive less than 760 mm of precipitation annually. Above approximately 910 m, precipitation generally falls as snow during the winter months.

Tasmania's climate is also moderated by the ocean, resulting in a maritime climate with only slight continentality on the Central Plateau. Mean austral summer and winter temperatures for Hobart (51 m a.s.l.), the capital city of Tasmania, are 18.9 and 11.7°C, respectively (Hobart meteorological station, Australian Bureau of Meteorology). However, like precipitation, temperature also is controlled by orography. For example, annual temperatures from a meteorological station in Liawenee (1,065 m a.s.l.), located on the Central Plateau, range from 16.1 (summer) to 5.3°C (winter). Irregular incursions of cold air from high latitudes can produce snow and frost at any time of the year. On the other hand, warm, dry air from continental Australia occasionally causes extremely hot days in excess of 41°C.

Geology and vegetation

In western Tasmania, quartzose basement sediments have been intensely folded and reworked by erosion. This side of the island consists of jagged Precambrian siliceous

rocks, namely quartzite, schist, and phyllite. In certain regions, older basement rock has been overlain by sedimentary limestones, sandstones, siltstones, and mudstones. However, extensive erosion has excised softer strata, leaving the hard quartzite rocks behind and filling valleys with the erosional by-products. In general, soils in the west are shallow, infertile, and acidic.

High annual precipitation in the west supports temperate, podocarp-broadleaf rainforests with *Nothofagus cunninghamii* present from sea level to tree line. Low soil fertility produces breaks in the canopy, allowing the establishment of shade-intolerant mesophytic species such as *Eucryphia lucida*, *Anodopetalum biglandulosum*, and *Phyllocladus aspleniifolius*. Fire regimes encourage expansive communities of button grass moorland dominated by *Gymnoschoenus sphaerocephalus*.

In central and eastern Tasmania, extensive faulting has occurred with vertical down-drops of up to 1.5 km. Permian mudstones and Triassic siltstones, both modified by Jurassic doleritic intrusions, overlie the older basement rock. The younger strata weather rapidly, generating soils that are richer in clay and relatively more fertile than those in the west.

Reductions in moisture, along with enhanced soil fertility, drive the vegetational gradient from west to east. Temperate rainforests merge into a wet sclerophyll ecotone. In these landscapes, *N. cunninghamii*-dominated forests give way to *Eucalyptus* forests containing an understory of *Pomaderris apetala* and the tree fern, *Dicksonia antarctica*. Wet sclerophyllous species are quick to colonize fire-cleared rainforest west of the ecotone.

Further east, in the rain-shadow of the western mountains, dry sclerophyllous *Eucalyptus* forests contain an understory of small trees like *Casuarina*, *Acacia,* and *Banksia*, along with shrubs of the Epacridaceae, Proteaceae, and Asteraceae. This vegetation is eventually replaced by savanna woodland. Open *Eucalyptus* forests dominate inland of the east coast.

Materials and methods

Midge collection and analysis

Sediment from 54 lakes was collected in replicates using a mini-Glew corer (Glew, 1991) during the austral summer months of January and February, 2006 and 2007. Samples were obtained from the deepest part of each lake. The upper 0-1 and 1-2 cm of each replicate were extruded on site, packaged in separate Whirl-Pak® sample bags (Nasco, Fort Atkinson, WI, USA), and kept cool until analysis. Lakes were selected along an altitudinal range to ensure a strong temperature gradient. While there was no strict cut-off in terms of lake depth, small and shallow lakes were preferentially sampled to ensure a close relationship between bottom water temperature and air temperature (Livingstone et al., 1999). Sampling deep, stratified lakes should be avoided in order to prevent the effect of hypolimnetic anoxia on chironomid assemblages (Little and Smol, 2001). However, due to the lack of bathymetric data for the majority of Tasmanian lakes, this was not always possible (Table 2.1).

In the laboratory, midge analysis was conducted according to the protocol established by Walker et al. (1991). Lake sediment was volumetrically sampled, deflocculated in hot 10% KOH, and washed with distilled water through a screen with 95

μm meshes. Aliquots of the residue were poured into a Bogorov tray and examined under a dissecting microscope at 50x magnification. Chironomid and ceratopogonid head capsules, along with *Chaoborus* mandibles, were hand-picked using fine forceps until the entire sample was processed. This procedure was repeated until a minimum of 100 head capsules was obtained per sample, which required, on average, 12 mL of wet sediment.

Quinlan and Smol (2001) suggest between 40 and 50 head capsules as sufficient for use in inference models where diversity is low. However, Heiri and Lotter (2001) caution against extrapolating this minimum count size to other geographical locations, arguing that minimum count size is model dependent. Therefore, rarefaction analysis was conducted using RAREPOLL (Birks and Line, 1992) to estimate the taxon richness of samples processed with varying sampling effort. In total, three runs were performed, holding samples at constant counts of 50 (recommended count size), 77 (minimum count size of this study), and 144 (average count size of this study) chironomid head capsules, which captured an average of 84.3%, 92.8%, and 99.3% of actual taxonomic richness, respectively (Fig. 2.2).

Head capsules were positioned ventral-side up on a coverslip and mounted with Entellan® (Merck, Darmstadt, Germany). Identification was conducted with a compound, light microscope at 400x magnification, following Wiederholm (1983), Oliver and Roussel (1983), and identification guides by Cranston (2000). Samples are archived with L. C. Cwynar's collection at the University of New Brunswick for eventual deposition in The Australian National Insect Collection, Canberra.

Environmental variables

Lake water for chemical analyses was sampled approximately 0.5 m below the water surface. A 250-mL plastic bottle was filled with lake water and kept cool until analysis. This particular sample was used to measure Na, K, Ca, Mg, Fe, Mn, Cu, Zn, Cl, SiO_2, SO_4, HCO_3, total organic carbon (TOC), turbidity (TURB), conductivity (CON), and pH. A 125-mL glass bottle was nearly filled with filtered (Sarstedt®, 0.45 μm syringe filter) lake water; 1 mL of 30% H_2SO_4 was added for preservation, and the bottle was kept cool until analysis. This sample was used to measure dissolved total Kjeldahl nitrogen (dissolved TKN) and dissolved total phosphorus (dissolved TP). Both general water chemistry protocols and dissolved TKN and dissolved TP protocols were conducted at the Research Productivity Council (RPC) located in Fredericton, New Brunswick, Canada.

Climate variables (Table 2.1) were acquired using the program BIOCLIM (Houlder et al., 2003). BIOCLIM uses a continent-wide, thin-plate smoothing spline derived from all available climate stations with adequate records (minimum of 30 years). For any given parameter, the software predicts point values for a specific latitude, longitude, and elevation within Australia. Of the 35 possible variables to choose from, we opted to use temperature of the warmest quarter (TWARM), annual precipitation (PRECIP), and annual radiation (RAD). Temperature estimates for Tasmania were based on 76 meteorological stations, which were a minimum, maximum, and average distance of 1.9, 35.5, and 19.8 km away from sampling sites, respectively. The standard errors associated with temperature vary from 0.2 to 0.4°C (Houlder et al., 2003).

Water depth (DEPTH) was acquired by sounding at the geographical centre of each lake until a maximum depth was found. Loss-on-ignition (LOI), a coarse indication of the organic content of lake sediment, was measured on 1 mL of wet sediment, dried overnight at 100°C, then ashed at 550°C for 4 h following Dean (1974).

Data screening and transformations

Prior to the ordinations, species count data were transformed into percentages. To remove noise, rare taxa, here defined as having a maximum abundance less than 2% and/or occurring in fewer than 2 lakes, were removed. Where applicable (i.e., detrended and canonical correspondence analyses), species count data were square root-transformed and rare taxa were downweighted.

Prior to ordinations, environmental data were assessed for normality using the Kolmogorov-Smirnov normality test and measurements of skewness and kurtosis (Zar, 1999). Four transformations were considered in order to normalize the environmental data: square root, inverse square root, log 10, and inverse. LOI, pH, RAD, and dissolved TKN did not need to be transformed. K and TOC were best normalized by inverse square root transformations whereas DEPTH, Ca, Fe, Mn, Zn, SiO_2, and TURB were best normalized by log 10 transformations. Na, Mg, Cl, dissolved TP, and CON were best normalized by inverse transformations. In the situation where no transformation normalized the data or significantly reduced skewness, the environmental parameter was left untransformed; this included TWARM, PRECIP, Cu, and SO_4.

Pearson's correlation tests and canonical correspondence analyses (CCAs) were run to assess the collinearity of the environmental variables. Variables with variance

inflation factors (VIFs) greater than 20 were manually removed to reduce the redundancy of the training set. Variables with the highest VIFs were removed sequentially until all were less than 20 (ter Braak and Šmilauer, 2002). Based on this criterion, only Na was removed; the Pearson's correlation test revealed that Na was highly correlated ($P \leq 0.01$) with pH, TWARM, K, Mg, Fe, Cl, SO_4, dissolved TKN, TOC, and CON.

Sites with fewer than 50 chironomid head capsules were removed from modelling exercises. Only four of the 54 lakes failed to meet this criterion (after processing all of the sediment, Menamatta Tarns 1 and 2 and Baker Lakes 1 and 2 all had fewer than 10 head capsules). A detrended correspondence analysis (DCA) of species data and a principal components analysis (PCA) of environmental data were run for the remaining 50 lakes. Sites with sample scores lying outside of one standard deviation from the means of axes 1 and 2 of both the DCA and PCA were considered for elimination. Although lakes Duckhole, Fortuna, Central Plateau 1, and Roberts Tarn were identified as outliers by the DCA and lakes Strahan, Ashwood, and Chisholm were identified as outliers by the PCA, no lake was identified as an outlier by both.

A final consideration for site removal involved assessing the difference between observed versus predicted temperatures from weighted averaging partial least squares models (see Model development) constructed in C2 version 1.4 (Juggins, 2003). The predicted temperatures for lakes Duckhole, Chisholm, and Little Basin were all considerably greater than the observed temperatures, whereas the predicted temperature for Menamatta Tarn 3 was considerably lower. Lakes Duckhole and Chisholm are both sinkhole lakes with thick organic mats of coarse wood and leaves lining their basins; the basins possess little other sediment and high concentrations of Mg, Fe, TOC, and

dissolved TP. Menamatta Tarn 3 is an ephemeral lake that periodically dries out; the tarn is shallow and highly turbid. All three of these lakes were removed from the data set. Since there was no ecological reason to remove Little Basin Lake, it was retained for further analyses.

Ordinations

Ordinations were conducted using CANOCO version 4.5 (ter Braak and Šmilauer, 2002). Relationships between midge distributions and environmental variables were assessed using CCA. Manual forward selection along with Monte Carlo permutation tests (999 unrestricted permutations) allowed identification of statistically significant ($P \leq 0.05$) environmental variables. Variables were selected such that each subsequent choice explained the highest proportion of the remaining variance. To test the robustness of the significant variables, a series of partial canonical correspondence analyses (pCCAs) were performed with and without the remaining significant variables included as covariables. The relationship between significant environmental variables and ordination axes was assessed with canonical coefficients, their associated t-values, and the interset correlations of the environmental variables with respective axes.

Taxon response models were constructed in CanoDraw, a component of CANOCO, using generalized linear models (GLM) set to a quadratic degree and Poisson distribution (ter Braak and Šmilauer, 2002). The GLMs were used to identify significant relationships between taxa and the significant environmental parameters detected by the CCA (Table 2.2).

Model development

A midge transfer function was developed for temperature of the warmest quarter (TWARM) using the software package C2, version 1.4. A DCA was performed to assess the response of subfossil taxa across the gradients captured by our training set. The gradient length of DCA axis 1 was 2.206, indicating that either linear or unimodal methods could adequately model species response (Birks, 1998). Hence, both partial least squares (PLS) and weighted averaging partial least squares (WA-PLS) techniques were employed. We used leave-one-out, cross-validation as this technique is more robust for data sets with fewer than 80 sites (Kim and Han, 1997). Models were tested with 1,000 cycles and evaluated based on the performance of the jack-knifed coefficient of determination (r^2_{jack}), average bias of jack-knifed predictions ($AveBias_{jack}$), maximum bias of jack-knifed predictions ($MaxBias_{jack}$), and root mean square error of prediction (RMSEP). The number of components included in the final model was selected based on reducing the RMSEP by at least 5% (Birks, 1998).

Results

Midge analysis

After data screening, a total of 49 non-rare, midge taxa were identified from 47 Tasmanian lakes (Table 2.2). The minimum, maximum, and average count sizes were 77, 257, and 144 whole head capsules, respectively. Taxa restricted to cooler, high elevation sites include *Botryocladius*, *Cricotopus* 'parbicintus', *Parakiefferiella* types 3 and 4, *Paralimnophyes* type 2, *Cladopelma*, *Cladotanytarsus*, *Polypedilum vespertinus*, *Polypedilum watsoni*, and *Tanytarsus* types 3 and 4 (Fig. 2.3). Taxa typifying warmer,

low elevations include *Kiefferulus martini*, *Stempellina*, *Tanytarsus* nr. *chinyensis*, *Chaoborus*, and Ceratopogonid type 2 (Fig. 2.3). The majority of the remaining taxa reflect more cosmopolitan distributions. In several cases, these taxa are comprised of multiple species with broad ecological ranges, including *Procladius*, *Chironomus*, and the undifferentiated Pentaneurini, Macropelopini, and Tanytarsini.

Ordinations

CCAs were performed on the 49 non-rare, midge taxa, 21 remaining environmental parameters, and 47 lakes. Of the 21 environmental variables, seven accounted for a significant ($P \leq 0.05$) portion of the explainable variance. In order of explanatory power, these were pH (19.1%), TWARM (10.3%), RAD (7.5%), Mg (7.1%), PRECIP (5.6%), SiO_2 (5.4%), and DEPTH (4.3%). All seven parameters retained their significance after testing with pCCAs (Table 2.3).

Combined, the first four axes of the reduced CCA (with only the seven significant explanatory variables) account for 30.3% of the variance in the species data (Table 2.4). All of the variables, except for DEPTH, are significantly correlated with the first ordination axis whereas only Mg and SiO_2 are not correlated with the second. pH shows the strongest positive correlation with the first axis while both TWARM and DEPTH are strongly associated with the second (Table 2.4).

A biplot of the CCA sample scores shows a clear west-east dichotomy (Fig. 2.4a). In the majority of cases, lakes sampled west of Tyler's Line plot in the left quadrants while those east of the line plot in the right quadrants. Low elevation lakes (sites 1-5) plot

in the upper, left quadrant, which is associated with warmer temperatures and coastal effects.

CCA species scores are indicative of taxa optima with respect to particular environmental variables (Fig. 2.4b). Warm-adapted taxa plot in the upper, left of the figure and are typical of low elevations (<600 m). Taxa plotting out in this quadrant of the figure and showing a significant relationship to temperature as indicated by the GLMs (Table 2.2) include *Kiefferulus martini*, *Parachironomus*, *Stempellina*, *Tanytarsus* nr. *chinyensis*, Ceratopogonid type 2, and *Chaoborus*. Cold-adapted taxa occur on the opposite side of the figure in the lower, right quadrant. These taxa, as identified from the ordination plot and GLMs, include *Botryocladius*, Orthoclad type 4, *Parakiefferiella* type 1, *Paralimnophyes* type 2, and *Tanytarsus* type 4. Based on the ordination and GLMs, some taxa show preferences for deeper lakes, namely *Chironomus* and *Parochlus*. Other taxa prefer acidic lakes, for instance *Parakiefferiella* type 2, *Paralimnophyes* type 1, *Polypedilum* type 1, *Tanytarsus* type 1, and *Dicrotendipes*, whereas *Cricotopus* 'parbicintus', *Cladopelma*, and *Cladotanytarsus* all show a preference for more alkaline conditions.

Model development

Based on the final CCA ordination, TWARM explained the second largest amount of variance after pH. Both partial least squares (PLS) and weighted averaging partial least squares (WA-PLS) models were constructed for temperature. We selected the second component WA-PLS model (Fig. 2.5) as it was the most parsimonious, reducing

the RMSEP by 8.4% and producing a strong r^2_{jack} of 0.72, low $AveBias_{jack}$ of -5.3×10^{-3}, low $MaxBias_{jack}$ of 1.35, and low RMSEP of 0.94 (Table 2.5).

Beta (β) values generated by the model (Table 2.2) can be used as coefficients to construct temperature estimates. With the second component model, *Kiefferulus martini* has the highest coefficient (31.4) whereas *Tanytarsus* type 4 has the lowest (1.7). In general, β values are consistent with the CCA species scores and GLM results mentioned in the previous section.

Discussion

Midge paleoecology in the Australasia region

The small number of transfer functions modelling midge temperature optima of Southern Hemisphere taxa makes it difficult to interpret results across studies. Before we can even compare subfossil chironomid remains from different regions of Australasia, paleoecologists need to develop a consensus on vouchered specimens. Survey and autecological data (e.g., Paterson and Walker, 1974; Kokkin, 1986) as well as identification guides (e.g., Cranston, 2000; Cranston and Dimitriadis, 2004) are available for many regions of the Southern Hemisphere; however, there is a growing need for paleoecologists using fossil chironomids to make use of these resources and create robust, quantitative models in order to address local and regional climate hypotheses.

Although early inventories of chironomid taxa surveyed from Australian lake benthos reported low species richness (Fulton, 1983a, b; Timms, 1985), subsequent studies have shown richness in some Australian lakes to be comparable to lakes in the Northern Hemisphere (Wright and Cranston, 2000; Cranston and Dimitriadis, 2004).

Wright and Burgin (2007) sampled 68 lakes dispersed between tropical northern Queensland, Fraser Island, south-eastern mainland Australia, and Tasmania and discovered more than double the number of taxa that had previously been reported in many early Australian studies. These authors used non-metric multidimensional scaling to evaluate the distribution of chironomid taxa and concluded that geographical location structured chironomid communities more strongly than geomorphic characteristics of lakes.

Within Tasmania, Wright and Burgin (2007) identified 57 species of chironomids based on pupal exuviae from 20 glacially-derived lakes and five dune lakes. At the generic level, the majority of the taxa are consistent with those identified in this study. We identified nine other genera not found in Wright and Burgin's survey while they identified four not found in ours. Furthermore, working with pupal exuviae, Wright and Burgin obtained many more species-level identifications (compare Wright and Burgin, 2007: Table 2 to our Table 2.2).

Geographic location appeared to be more important than geophysical lake characteristics with respect to structuring chironomid communities (Wright and Burgin, 2007). Although this may be the case at their large, semi-continental scale, our data indicate that, at the state level, Tasmania's chironomid communities are structured most strongly by pH. Older, siliceous, rocks of western Tasmania are mantled by peat-forming rainforests and sedgeland, creating dystrophic lakes relative to those situated on the younger, nutrient-rich rock types of the east. Further, the precipitation gradient, driven by the Roaring Forties in conjunction with Tasmania's orography, coincides with the geologic divide. Both factors combine to have a profound influence on Tasmania's flora

and fauna, creating two distinct lake districts separated by the 146th meridian (Tyler, 1992).

At Lake Barrine in northern tropical Queensland, Dimitriadis and Cranston (2001) identified 35 taxa based on pupal exuviae and larval head capsules. Because they used pupal exuviae (which allows for greater taxonomic resolution), MCR techniques, and surveyed a tropical lake, their results differed from ours. Of the taxa common to both studies at the generic level, Dimitriadis and Cranston (2001) found *Cladotanytarsus bilinearis*, *Tanytarsus richardsi*, *Dicrotendipes flexus,* and *Polypedilum convexum* to have warm MCRs whereas *Riethia* sp., *Procladius squamifer*, *Polypedilum kathleenae*, and *Stempellina australiensis* had relatively cold MCRs. A noticeable difference in our study is that *Cladotanytarsus* reconstructs with a relatively cool β coefficient (Table 2.2). In our calibration set, *Cladotanytarsus* (unidentified to species) is restricted to higher elevations. However, *Cladotanytarsus* is known to be a speciose taxon, inhabiting many ecological niches (Dimitriadis and Cranston, 2007). The *Cladotanytarsus* morphotype identified here is more than likely a different species from *Cladotanytarsus bilinearis* identified at Lake Barrine. Dimitriadis and Cranston (2001) also indicate that *Riethia* sp. and *Stempellina australiensis* are cold stenotherms requiring high oxygen concentrations. In our study, *Riethia* is assigned a relatively cool β coefficient (9.4) whereas *Stempellina* is here defined as a warm-adapted taxon. *Stempellina* requires coarse, grainy materials, like sand, to construct its casings. Since the dune lakes in this data set are effectively the warm analogues, *Stempellina* is assigned a warm β coefficient. However, as we can see from Fig. 2.3, *Stempellina* also occurs at higher elevations where it is likely responding to substrate rather than temperature.

Across the Tasman Sea in New Zealand, Woodward and Shulmeister (2006) identified *Cladopelma curtivalva*, *Cricotopus zealandicus*, *Cricotopus aucklandensis*, and *Polypedilum* as typical of warmer sites. At the generic level, all of these taxa differ from Tasmanian equivalents, which prefer intermediate to cool temperatures. Woodward and Shulmeister (2006) also identify *Chironomus*, *Tanytarsus funebris*, *Tanytarsus vespertinus*, and the Macropelopini tribe as taxa dominating high-altitude communities, although these taxa are also abundant at lower elevations. The same is true regarding the distribution of these taxa, at the generic level, in Tasmania (note that *T. funebris* and *T. vespertinus* are not present in Tasmania). Of the taxa common to our training set, at the generic level, Dieffenbacher-Krall et al. (2007) found *Chironomus, Cladopelma*, *Kiefferulus*, *Parachironomus*, *Polypedilum*, *Cricotopus aucklandensis* (which is restricted to New Zealand), and many types of *Tanytarsus* spp. to be significantly related to temperature; only *Kiefferulus martini*, *Parachironomus*, and *Tanytarsus* type 4 are significantly related to temperature in Tasmania.

Woodward and Shulmeister (2006) found *Chironomus* to be abundant at both high-altitude, cool, oligotrophic lakes and low-altitude, warm, eutrophic lakes. Consequently, *Chironomus* reconstructs with an intermediate β coefficient of 12.3°C, underpredicting warm temperatures of lowland lakes and over-predicting cool temperatures of high-altitude lakes. This becomes a problem when *Chironomus* is present in high abundance as in the paleoclimate reconstruction of Lyndon Stream (Woodward and Shulmeister, 2007). In Australia, adult morphology (Freeman, 1961) and cytological variation (Martin, 1979) reveal that *Chironomus* is a genus comprised of many species that cannot readily be distinguished morphologically as larvae. Although *Chironomus* is

not significantly related to temperature in Tasmania, it is clearly most commonly found and most abundant at cooler, high-elevation lakes and has a β coefficient of 8.5°C (Table 2.2).

It is important to note that many New Zealand species are endemic as are some genera (e.g., *Hevelius*, *Kaniwhaniwhanus*, and *Naonella*) and so are not found in Tasmania. There is little endemism in the chironomid fauna of Tasmania at our level of taxonomic resolution. However, at the species level, Wright and Burgin (2007) found Tasmania to have the highest degree of endemism with respect to all four areas surveyed in Australia.

Modelling

The chironomid distributions of the 47 Tasmanian lakes surveyed in this study were strongly influenced by pH, TWARM, RAD, Mg, PRECIP, SiO_2, and DEPTH. Our results indicate that midges are an appropriate tool for modelling the temperature history of Tasmania. Although the r^2_{jack} of our temperature transfer function is lower than that produced by some other models (e.g., Barley et al., 2006; Lotter et al., 1999; Walker et al., 1997), the $AveBias_{jack}$, $MaxBias_{jack}$, and RSMEP (Table 2.5) compare well with other studies. Our lower r^2_{jack} may be the result of a relatively short temperature gradient, which inherently produces lower r^2_{jack} values (Larocque et al., 2001: Table 2.6).

Nevertheless, all models must be interpreted with caution. Errors created by the transfer function approach are partly an artefact of the statistical methods and do not necessarily incorporate errors associated with the data. Since inverse deshrinking is implicit to weighted averaging, there is always a tendency to pull predicted values

towards the mean of the training set, inevitably leading to overestimation of low and underestimation of high observed temperatures (ter Braak and Juggins, 1993). In short, no matter the data entered, the model will still generate results. Therefore, it is important to interpret with scrutiny and test applications of transfer functions with historical data, analogue matching, multi-proxy evidence, and knowledge of the autecology of taxa.

Future directions

Tasmania is a temperate region moderated by a maritime climate. Due to climate, geologic, and vegetation gradients, it may seem difficult to disentangle redundant variables. Furthermore, low to mid elevation sites (300-700 m) are not well represented in our model. The few potential sites within this elevation range are typically located on farms and pasturelands, sites to avoid due to anthropogenic influences. Despite these complications, we have produced a strong model. Observed temperatures from sample sites are significantly correlated with temperatures predicted from 1,000 jack-knifed cycles. However, the model could be improved by adding sites to both increase the gradient length as well as fill in the gap between 300 and 700 m (~12-14°C).

The next step is to apply this transfer function to a long-core record. Our goal is to compare the qualitative pollen-based climate inferences of Colhoun et al. (1999) from Lake Selina, Tasmania, to quantitative midge-inferred temperatures; the reconstruction extends back to the previous interglacial. The pollen record shows close correlation with the Vostok ice core from Antarctica, indicating that Tasmania may be recording climate change at a hemispheric scale. With our model, we will be able to determine quantitative

temperature estimates for this long record and attempt to answer some of the questions posed in the introduction.

Acknowledgments

We would like to thank Rob Wiltshire, Marian McGowen, and Nigella for their friendship, meals to die for, and logistical support; Greg Jordan and Peter Tyler for data contributions and site selection; the Department of Primary Industries, Water and Environment (DPIWE) for letting us collect samples; Fonya Irvine and Joshua Kurek for field assistance; Ian Walker for statistical advice; John S. Little for funding of visits to the University of California - Davis and the 17th International Quaternary Association Congress; and two anonymous reviewers who provided helpful comments and insights. This project was funded by a Natural Sciences and Engineering Research Council of Canada Discovery Grant to L. C. Cwynar. Map data were provided by TASMAP, © State of Tasmania.

References

Alloway, B.V., Lowe, D.J., Barrell, D.J.A., Newnham, R.M., Almond, P.C., Augustinus, P.C., Bertler, N., Carter, L., Litchfield, N.J., McGlone, M.S., Shulmeister, J., Vandergoes, M.J., Williams, P.W., 2007. Towards a climate event stratigraphy for New Zealand over the past 30 000 years (NZ-INTIMATE project). Journal of Quaternary Science 22, 9-35.

Armitage, P., Cranston, P.S., Pinder, L.C.V., 1995. The Chironomidae: The Biology and Ecology of Non-Biting Midges. Chapman and Hall, London.

Barley, E.M., Walker, I.R., Kurek, J., Cwynar, L.C., Mathewes, R.W., Gajewski, K., Finney, B.P., 2006. A northwest North American training set: distribution of freshwater midges in relation to air temperature and lake depth. Journal of Paleolimnology 36, 295-314.

Birks, H.J.B., 1998. Numerical tools in paleolimnology - Progress, potentialities, and problems. Journal of Paleolimnology 20, 307-332.

Birks, H.J.B., 2003. Quantitative palaeoenvironmental reconstructions from Holocene biological data. In: Mackay, A., Battarbee, R., Birks, H.J.B., Oldfield, F. (Eds.), Global Change in the Holocene. Oxford University Press, New York, pp. 107-123.

Birks, H.J.B., Line, J.M., 1992. The use of rarefaction analysis for estimating palynological richness from Quaternary pollen-analytical data. Holocene 2, 1-10.

Boubée, J.A.P., 1983. Past and present benthic fauna of Lake Maratoto, with special reference to the Chironomidae. Ph.D. Thesis, University of Waikato, New Zealand, 151 pp.

Brooks, S.J., Birks, H.J.B., 2001. Chironomid-inferred air temperatures from Lateglacial and Holocene sites in north-west Europe: progress and problems. Quaternary Science Reviews 20, 1723-1741.

Clapperton, C.M., 1990. Quaternary glaciations in the Southern Hemisphere: an overview. Quaternary Science Reviews 9, 299-304.

Colhoun, E.A., 1985. Glaciations of the West Coast Range, Tasmania. Quaternary Research 24, 39-59.

Colhoun, E.A., Shulmeister, J., 2006. Late Pleistocene of the south west Pacific region. In: Elias, S. (Ed.), Encyclopedia of Quaternary Science. Elsevier, pp. 1066-1075.

Colhoun, E.A., Pola, J.S., Barton, C.E., Heijnis, H., 1999. Late Pleistocene vegetation and climate history of Lake Selina, western Tasmania. Quaternary International 57/58, 5-23.

Cranston, P.S., 2000. Electronic guide to the Chironomidae of Australia. http://www.science.uts.edu.au/sasb/chiropage/.

Cranston, P.S., Dimitriadis, S., 2004. The Chironomidae (Diptera) larvae of Atherton Tableland Lakes, north Queensland. Memoirs of the Queensland Museum 49, 573-588.

Dean Jr., W.E., 1974. Determination of carbonate and organic matter in calcareous sediments and sedimentary rocks by loss on ignition: comparison with other methods. Journal of Sedimentary Petrology 44, 242-248.

Deevey, E.S., 1955. Paleolimnology of the upper swamp deposit, Pyramid Valley. Records of the Canterbury Museum 6, 291-344.

Dieffenbacher-Krall, A.C., Vandergoes, M.J., Denton, G.H., 2007. An inference model for mean summer air temperatures in the Southern Alps, New Zealand, using subfossil chironomids. Quaternary Science Reviews 26, 2487-2504.

Dimitriadis, S., Cranston, P.S., 2001. An Australian Holocene climate reconstruction using Chironomidae from a tropical volcanic maar lake. Palaeogeography, Palaeoclimatology, Palaeoecology 176, 109-131.

Dimitriadis, S., Cranston, P.S., 2007. From the mountains to the sea: assemblage structure and dynamics in Chironomidae (Insect: Diptera) in the Clyde River estuarine gradient, New South Wales, south-eastern Australia. Australian Journal of Entomology 46, 188-197.

Elias, S., 1997. The mutual climatic range method of palaeoclimate reconstruction based on insect fossils: new applications and interhemispheric comparisons. Quaternary Science Reviews 16, 1217-1225.

Freeman, P., 1961. The Chironomidae (Diptera) of Australia. Australian Journal of Zoology 9, 611-737.

Fulton, W., 1983a. Macrobenthic fauna of Great Lake, Arthurs Lake and Lake Sorell, Tasmania. Australian Journal of Marine and Freshwater Research 34, 775-785.

Fulton, W., 1983b. Qualitative and quantitative variation in the macrobenthic fauna of the original lake and new lake areas of Great Lake and Arthurs Lake, Tasmania. Australian Journal of Marine and Freshwater Research 34, 786-803.

Glew, J., 1991. Miniature gravity corer for recovering short sediment cores. Journal of Paleolimnology 5, 285-287.

Harrison, S.P., 1993. Late Quaternary lake-level changes and climates of Australia. Quaternary Science Reviews 12, 211-231.

Heiri, O., Lotter, A.F., 2001. Effect of low count sums on quantitative environmental reconstructions: an example using subfossil chironomids. Journal of Paleolimnology 26, 343-350.

Houlder, D., Hutchinson, M., Nix, H.A., McMahon, J., 2003. ANUCLIM User's Guide. Centre for Resource and Environmental Studies, Australian National University, Canberra, Australia.

Jackson, W.D., 2005. The Tasmanian environment. In: Reid, J.B., Hill, R.S., Brown, M.J., Hovenden, M.J. (Eds.), Vegetation of Tasmania. Australian Biological Resources Study, Tasmania, Australia, pp. 11-34.

Juggins, S., 2003. C2 Version 1.4 User Guide. Software for Ecological and Paleoecological Data Analysis and Visualisation. University of Newcastle, Newcastle upon Tyne, UK.

Kershaw, A.P., Nanson, G.C., 1993. The last full glacial cycle in the Australian region. Global and Planetary Change 7, 1-9.

Kim, N., Han, J.K., 1997. Assessing the integrity of cross-validation: a case for small sample-based research. Department of Marketing, Hong Kong University of Science and Technology, Hong Kong, Working Paper Series no. MKTG 97.096.

Kokkin, M., 1986. Identification of two Australian salt-lake chironomid species from subfossil larval head capsules. Palaeogeography, Palaeoclimatology, Palaeoecology 54, 317-328.

Larocque, I., Hall, R.I., Grahn, E., 2001. Chironomids as indicators of climate change: a 100-lake training set from a subarctic region of northern Sweden (Lapland). Journal of Paleolimnology 26, 307-322.

Little, J.L., Smol, J.P., 2001. A chironomid-based model for inferring late-summer hypolimnetic oxygen in southeastern Ontario lakes. Journal of Paleolimnology 26, 259-270.

Livingstone, D.M., Lotter, A.F., Walker, I.R., 1999. The decrease in summer surface water temperature with altitude in Swiss alpine lakes: a comparison with air temperature lapse rates. Arctic, Antarctic, and Alpine Research 31, 341-352.

Lotter, A.F., Walker, I.R., Brooks, S.J., Hofmann, W., 1999. An intercontinental comparison of chironomid paleotemperature inference models: Europe vs. North America. Quaternary Science Reviews 18, 717-735.

Macphail, M.K., 1979. Vegetation and climates in southern Tasmania since the Last Glaciation. Quaternary Research 11, 306-341.

Martin, J., 1979. Chromosomes as tools in taxonomy and phylogeny of Chironomidae (Diptera). Entomologica Scandinavica Supplement 10, 67-74.

Massaferro, J., Brooks, S.J., 2002. Response of chironomids to Late Quaternary environmental change in Taitao Peninsula, southern Chile. Journal of Quaternary Science 17, 101-111.

Massaferro, J., Brooks, S.J., Haberle, S.G., 2005. The dynamics of chironomid assemblages and vegetation during the Late Quaternary at Laguna Facil, Chonos Archipelago, southern Chile. Quaternary Science Reviews 24, 2510-2522.

Mees, F., Verschuren, D., Nijs, R., Dumont, H.J., 1991. Holocene evolution of the crater lake at Malha, Northwest Sudan. Journal of Paleolimnology 5, 227-253.

Oliver, D.R., Roussel, M.E., 1983. The Insects and Arachnids of Canada, Part 11: The Genera of Larval Midges of Canada, Diptera: Chironomidae. Research Branch, Agriculture Canada, Ottawa.

Paterson, C.G., Walker, K.F., 1974. Recent history of *Tanytarsus barbitarsus* Freeman (Diptera: Chironomidae) in the sediments of a shallow saline lake. Australian Journal of Marine and Freshwater Research 25, 315-325.

Quinlan, R., Smol, J.P., 2001. Setting minimum head capsule abundance and taxa deletion criteria in chironomid-based inference models. Journal of Paleolimnology 26, 327-342.

Schakau, B.L., 1986. Preliminary study of the development of the subfossil chironomid fauna (Diptera) of Lake Taylor, South Island, New Zealand, during the younger Holocene. Hydrobiologia 143, 287-291.

Shiel, R.J., Koste, W., Tan, L.W., 1989. Tasmania revisited: rotifer communities and habitat heterogeneity. Hydrobiologia 186/187, 239-245.

ter Braak, C.J.F., Juggins, S., 1993. Weighted averaging partial least squares regression (WA-PLS): an improved method for reconstructing environmental variables from species assemblages. Hydrobiologia 269/270, 485-502.

ter Braak, C.J.F., Šmilauer, P., 2002. CANOCO Version 4.5. Biometris-Plant Research International, Wageningen.

Timms, B.V., 1985. The structure of macrobenthic communities of Australian lakes. The Proceedings of the Ecological Society of Australia 14, 51-59.

Turney, C.S.M., Haberle, S., Fink, D., Kershaw, A.P., Barbetti, M., Barrows, T.T., Black, M., Cohen, T.J., Corrège, T., Hesse, P.P., Hua, Q., Johnston, R., Morgan, V., Moss, P., Nanson, G., van Ommen, T., Rule, S., Williams, N.J., Zhao, J.-X., D'Costa, D., Feng, Y.-X., Gagan, M., Mooney, S., Xia, Q., 2006. Integration of ice core, marine and terrestrial records for the Australian Last Glacial Maximum and Termination: a contribution from the OZ INTIMATE group. Journal of Quaternary Science 21, 751-761.

Tyler, P.A., 1992. A lakeland from the dreamtime: the second founder's lecture. British Phycological Journal 27, 353-368.

Verschuren, D., Eggermont, H., 2006. Quaternary paleoecology of aquatic Diptera in tropical and Southern Hemisphere regions, with special reference to the Chironomidae. Quaternary Science Reviews 25, 1926-1947.

Walker, I.R., Smol, J.P., Engstrom, D.R., Birks, H.J.B., 1991. An assessment of Chironomidae as quantitative indicators of past climatic change. Canadian Journal of Fisheries and Aquatic Sciences 48, 975-987.

Walker, I.R., Levesque, A.J., Cwynar, L.C., Lotter, A.F., 1997. An expanded surface-water palaeotemperature inference model for use with fossil midges from eastern Canada. Journal of Paleolimnology 18, 165-178.

Ward, J.V., Stanford, J.A., 1982. Thermal responses in the evolutionary ecology of aquatic insects. Annual Review of Entomology 27, 97-117.

Wiederholm, T., 1983. Chironomidae of the Holarctic Region. Keys and Diagnoses. Part 1. Larvae. Entomologica Scandinavica Supplement 19.

Woodward, C.A., Shulmeister, J., 2006. New Zealand chironomids as proxies for human-induced and natural environmental change: transfer functions for temperature and lake production (chlorophyll a). Journal of Paleolimnology 36, 407-429.

Woodward, C.A., Shulmeister, J., 2007. Chironomid-based reconstructions of summer air temperature from lake deposits in Lyndon Stream, New Zealand spanning the MIS 3/2 transition. Quaternary Science Reviews 26, 142-154.

Wright, I.A., Cranston, P.S., 2000. Are Australian lakes different? Chironomid and chaoborid exuviae from Lake McKenzie, a coastal temperate dune lake. Internationale Vereinigung Für Theoretische Und Angewandte Limnologie Verhandlungen 27, 303-308.

Wright, I.A., Burgin, S., 2007. Species richness and distribution of eastern Australian lake chironomids and chaoborids. Freshwater Biology 52, 2354-2368.

Zar, J.H., 1999. Biostatistical Analysis. Prentice Hall, Upper Saddle River, New Jersey.

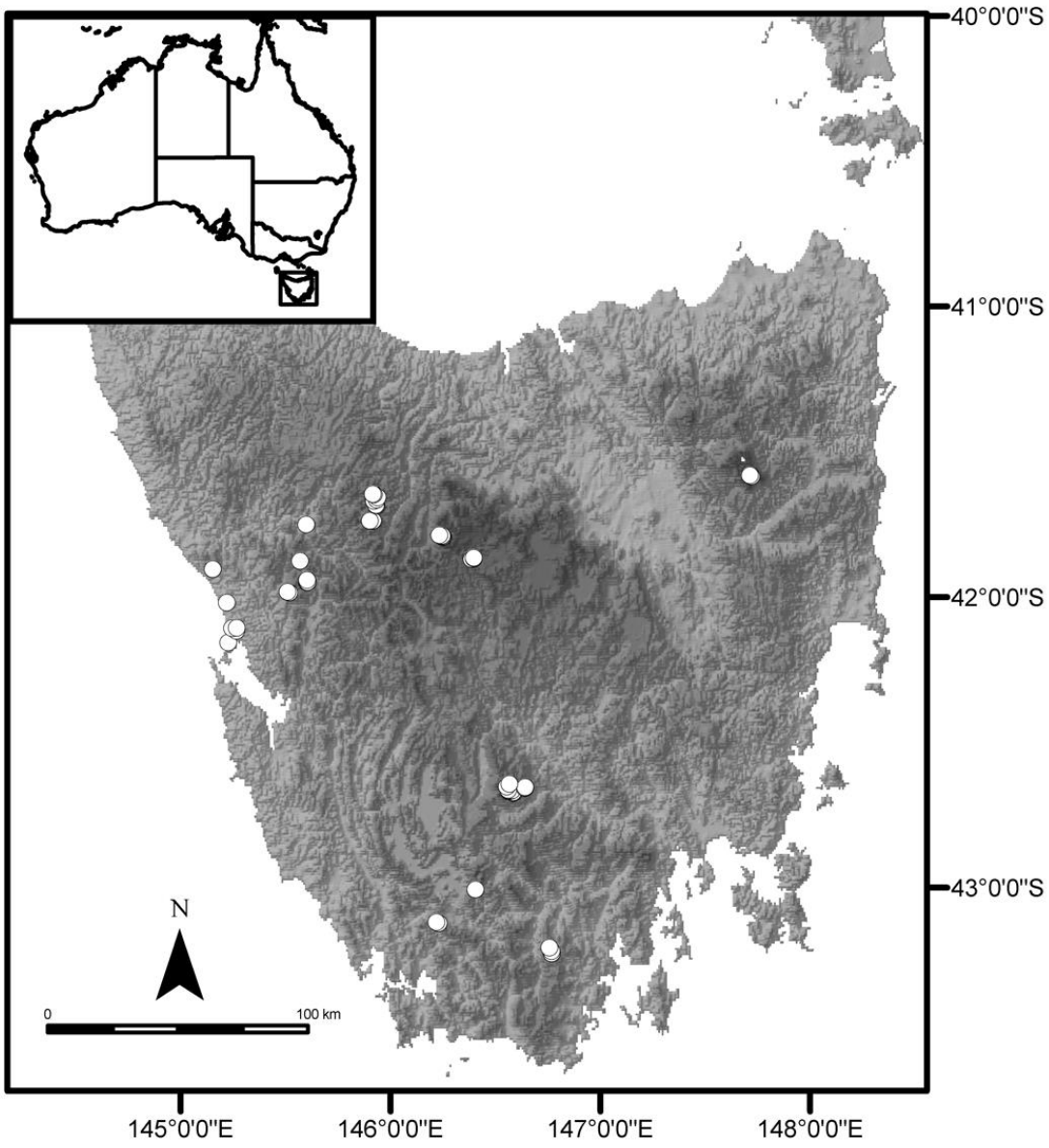

Figure 2.1: Map of Tasmania.

The map includes the 47 lakes comprising the training set. Map data were provided by TASMAP, ©State of Tasmania.

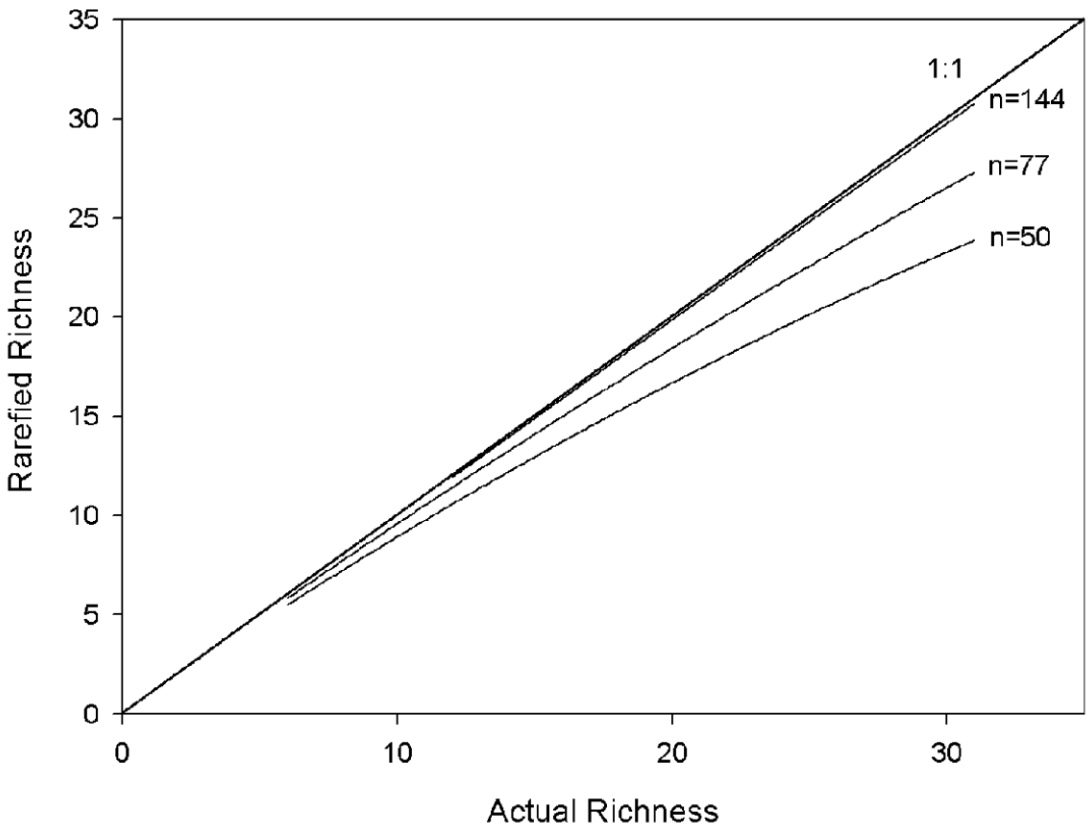

Figure 2.2: Rarefaction plot comparing actual taxon richness to rarefied taxon richness.

Samples were held at constant sizes of 50, 77, and 144 chironomid head capsules, which captured an average of 84.3%, 92.8%, and 99.3% of actual taxonomic richness, respectively.

Figure 2.3: Midge percent abundance diagram. These are the 49 non-rare taxa included in the final model. Elevation is on the y-axis and the zones are based on approximate temperature ranges associated with the elevation gradient.

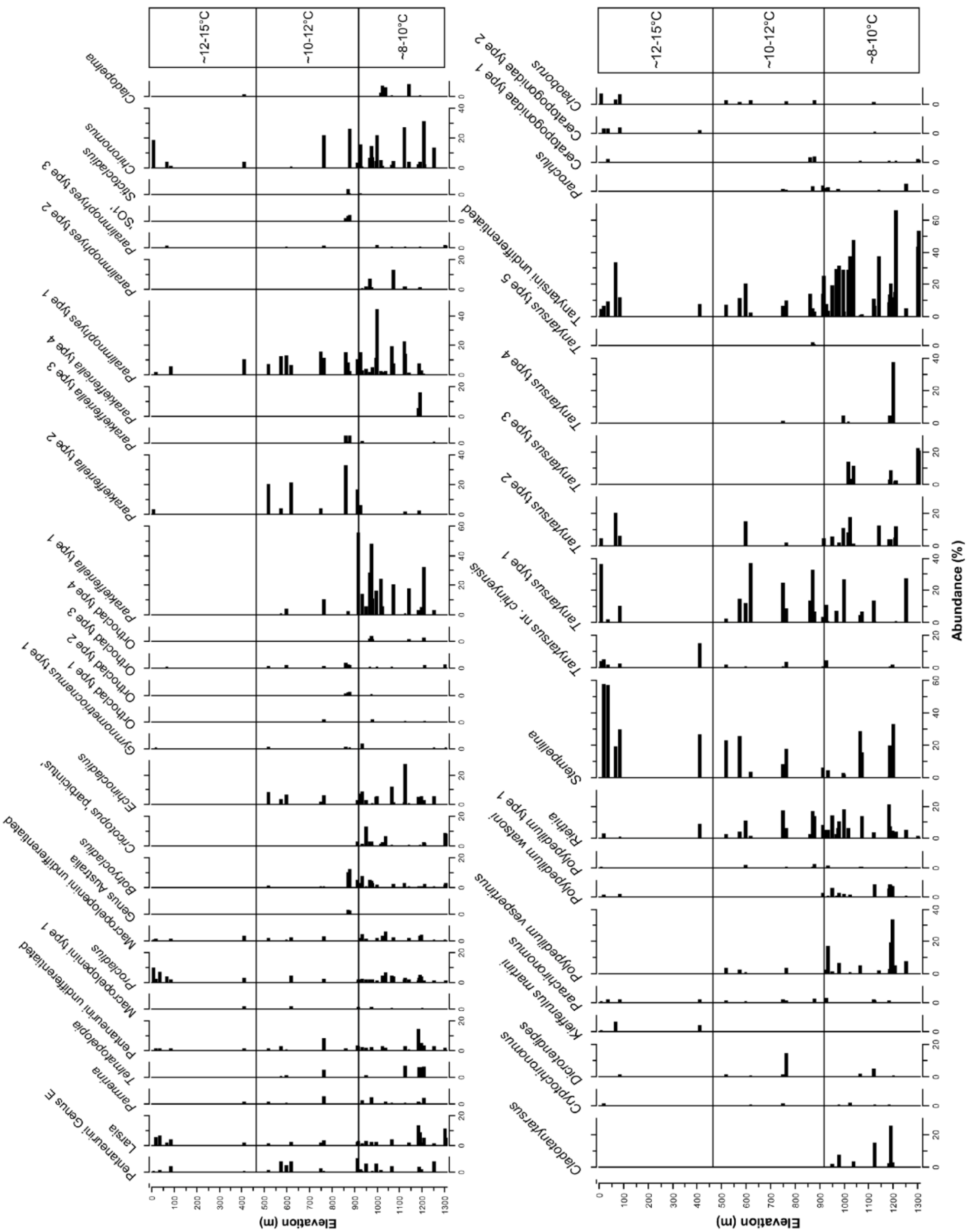

Figure 2.3: Midge percent abundance diagram.

Figure 2.4: Canonical correspondence analysis (CCA) of: a) sample scores for the 47 Tasmanian lakes where circles represent lakes west of Tyler's line and triangles represent lakes east of Tyler's line and b) species scores. Both are plotted relative to the seven significant environmental variables. The numbers in the sample score plot correspond to Table 2.1 while the numbers in the species score plot correspond to Table 2.2.

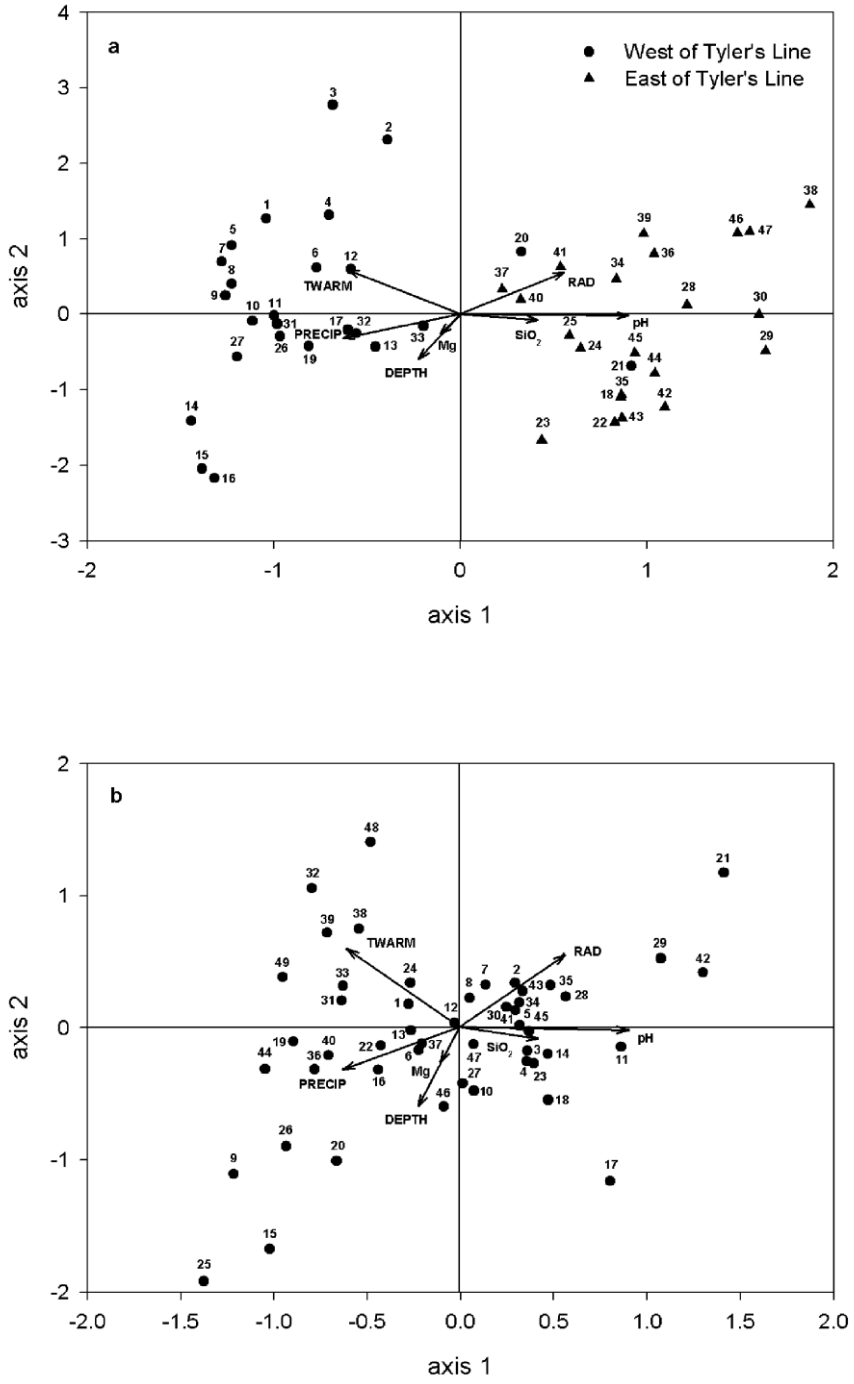

Figure 2.4: Canonical correspondence analysis (CCA).

Figure 2.5: Performance of second component WA-PLS model. Panel a) illustrates the predicted versus observed mean temperature of the warmest quarter and b) illustrates residuals of the predicted versus observed mean temperature of the warmest quarter.

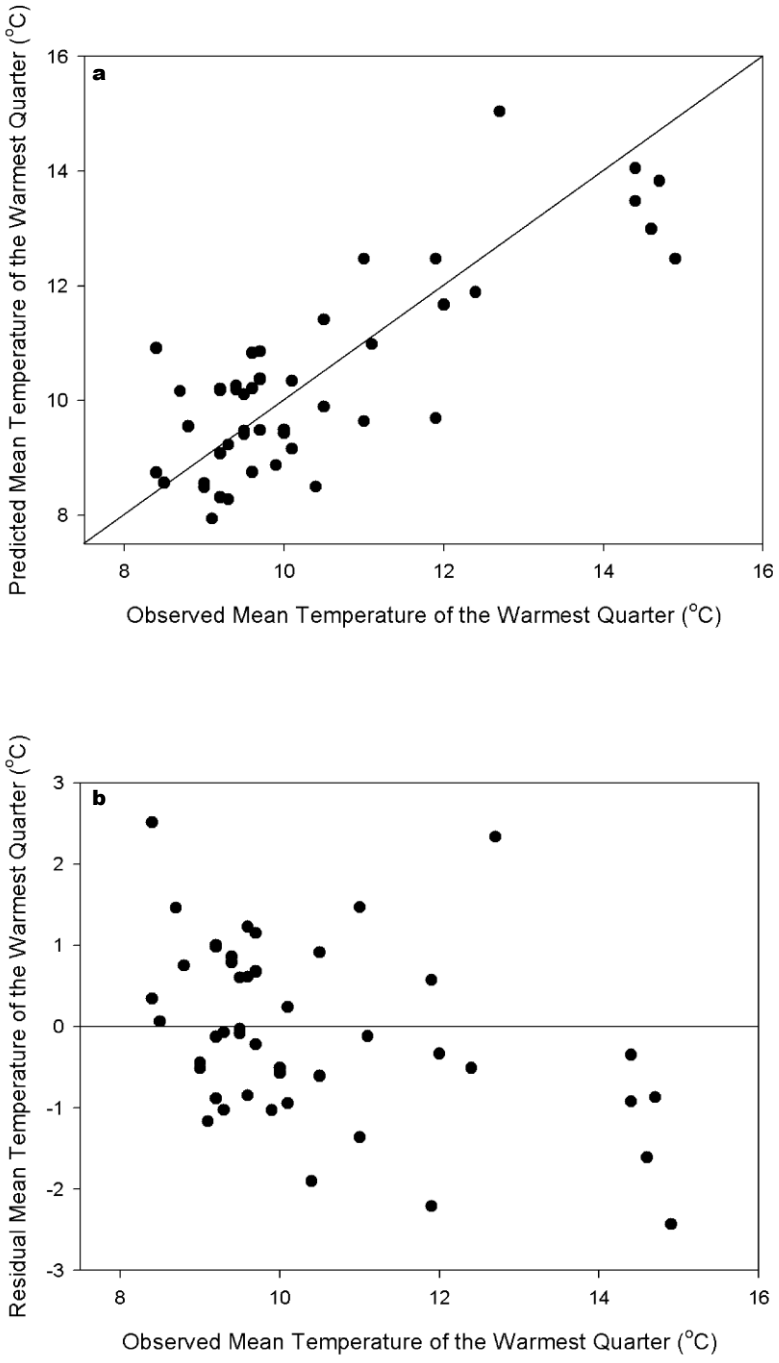

Figure 2.5: Performance of second component WA-PLS model.

Table 2.1: Environmental variables of the 54 lakes sampled for the Tasmanian training set.

#	Lake	SOUTH metric	EAST metric	ELEV m	pH	TWARM °C	RAD MJ/m^2	Mg mg/L	PRECIP mm	SiO_2 mg/L	DEPTH m	CON µS/cm	LOI %	TURB mg/L
1	Lake Mallanna	42.02	145.28	9.4	4.4	14.9	11.9	2.66	1534	5.1	3.70	159	28.5	1.7
2	Lake Strahan	42.15	145.27	22.2	5.5	14.7	11.9	7.00	1528	2.5	0.55	347	5.0	0.7
3	Lake Ashwood	42.10	145.29	39.7	5.8	14.6	11.8	3.17	1573	0.2	0.13	158	34.5	0.9
4	Lake Bellinger	42.11	145.31	70.6	4.8	14.4	11.6	3.44	1711	6.0	1.48	197	41.0	1.6
5	Lake Garcia	42.10	145.31	88.3	5.0	14.4	11.5	2.37	1750	1.1	8.00	138	56.6	0.9
6	Cumberland Lake	41.90	145.21	411.4	4.9	12.7	10.6	1.07	2638	2.8	1.35	62	37.5	1.7
7	Lake Selina	41.88	145.61	520.0	5.7	12.4	10.5	0.61	2818	0.2	9.17	33	24.8	0.9
8	Basin Lake	41.98	145.55	576.7	4.7	12.0	10.2	0.65	3170	0.5	1.90	45	50.6	0.6
9	Little Basin Lake*	41.98	145.56	599.0	4.6	11.9	10.2	0.71	3219	0.3	2.90	47	38.4	0.9
10	Lake Herbert	41.75	145.64	618.7	4.8	11.9	10.9	0.63	2378	0.5	5.35	39	31.0	0.7
11	Michael Tarn	41.95	145.64	751.5	5.2	11.1	10.4	0.49	2935	0.4	5.10	30	34.7	1.0
12	Lake A*	41.95	145.64	764.7	5.9	11.0	10.5	0.54	2899	0.2	2.80	32	21.8	1.2
13	Les Tarn*	41.94	145.64	765.5	4.5	11.0	10.4	0.88	2904	2.1	1.97	53	39.7	1.8
14	Lake 50*	43.02	146.41	862.4	4.6	10.0	10.7	0.34	2158	0.2	1.90	28	35.5	0.5
15	Lake Cygnus	43.13	146.23	873.4	4.9	9.7	10.3	0.51	2457	0.1	8.30	34	5.0	0.4
16	Lake Fortuna	43.13	146.24	880.1	4.7	9.7	10.3	0.48	2462	0.1	9.12	33	12.8	0.5
17	Lake Rodway	41.69	145.96	916.2	5.8	10.5	11.0	0.36	2463	1.1	35.2	23	35.4	0.6
18	Lake Osborne	43.22	146.76	919.5	6.9	9.5	11.0	0.91	1775	3.1	8.90	32	29.4	0.3
19	Lake Lilla	41.65	145.96	928.0	5.0	10.5	10.9	0.38	2577	0.9	13.10	21	33.1	0.8
20	Flynns Tarn	41.69	145.96	936.0	6.2	10.4	10.9	0.54	2482	1.2	0.58	20	18.6	0.7
21	Platypus Tarn	42.67	146.59	953.8	6.7	10.0	11.5	0.83	1586	4.3	10.32	25	30.1	0.4
22	Ladies Tarn	43.24	146.77	971.0	6.5	9.2	11.0	0.88	1808	3.1	8.80	25	40.1	0.3
23	Lake Esperance	43.23	146.77	976.0	6.4	9.1	11.0	0.60	1811	2.0	19.2	27	33.6	0.3
24	Lake Nicholls	42.67	146.65	981.4	6.5	9.9	11.7	0.49	1479	4.7	11.2	22	32.0	0.5
25	Twilight Tarn	42.65	146.57	999.1	6.1	9.7	11.4	0.57	1663	1.6	0.74	19	41.6	0.7
26	Wombat Pool	41.65	145.95	1001	4.6	10.1	11.0	0.32	2499	0.4	2.15	27	38.6	1.0
27	Lake Hanson	41.66	145.97	1002	4.8	10.1	11.0	0.27	2466	0.8	10.4	20	39.5	1.0
28	Lake Rayner	42.66	146.65	1020	6.8	9.6	11.6	0.57	1523	5.9	0.94	27	23.7	0.4
29	Lake Dobson	42.68	146.59	1027	7.0	9.5	11.4	1.60	1651	7.3	4.47	39	21.7	0.4
30	Eagle Tarn	42.68	146.59	1040	6.5	9.5	11.3	2.09	1729	3.2	0.19	54	29.4	2.0
31	Andrew Tarn*	41.74	145.94	1066	5.2	9.7	10.9	0.33	2472	0.1	0.95	22	10.1	2.8
32	Lake Holmes	41.74	145.95	1076	5.0	9.6	11.0	0.38	2441	0.1	0.95	23	16.1	1.8
33	Twisted Lakes	41.67	145.97	1123	5.5	9.4	11.1	0.34	2391	0.5	2.25	17	32.0	0.9
34	Lake Loane	41.79	146.26	1126	6.5	9.6	11.8	0.44	1700	1.4	1.80	18	29.2	0.8
35	Lake Newdegate	42.66	146.56	1144	6.5	8.8	10.8	0.66	2121	2.2	2.90	20	27.3	0.4
36	Central Plateau 2*	41.87	146.41	1184	6.3	9.4	12.9	0.42	1080	0.2	3.30	20	29.4	0.5
37	Solomons Jewels 2	41.80	146.27	1189	6.4	9.2	11.9	0.31	1675	0.2	2.90	19	29.8	0.7
38	Central Plateau 1*	41.87	146.41	1193	6.6	9.3	13.0	0.63	1043	0.3	0.46	24	44.2	1.6
39	Terry Tarn	41.88	146.40	1193	6.4	9.3	12.9	0.38	1094	0.1	1.61	21	39.5	0.5
40	Solomons Jewels 1	41.80	146.27	1199	6.1	9.2	11.9	0.32	1678	0.5	2.35	16	36.0	0.9
41	Heather Tarn*	41.80	146.28	1201	6.1	9.2	11.9	0.37	1678	0.2	0.37	20	25.3	2.6
42	Johnston Tarn	42.67	146.57	1210	6.7	8.4	10.6	0.70	2441	2.7	9.03	21	21.7	0.9
43	MacKenzie Tarn	42.67	146.57	1210	6.5	8.5	10.6	0.63	2407	2.8	10.15	18	28.9	0.1
44	Robert Tarn	42.68	146.57	1214	6.4	8.4	10.6	0.58	2458	2.7	1.10	21	35.2	0.5
45	Lake Wilks	41.67	145.96	1254	6.1	8.7	11.1	0.55	2367	1.8	8.12	19	30.4	0.5
46	Lake Youl	41.59	147.69	1302	6.7	9.0	12.4	0.45	1456	0.5	0.71	16	14.9	0.4
47	Youls Tarn	41.59	147.69	1306	6.4	9.0	12.4	0.52	1464	0.4	0.30	18	10.9	0.7
48	Lake Chisholm	41.13	145.06	149.3	4.9	14.5	12.4	4.00	1497	3.5	10.07	117	44.3	0.9
49	Duckhole Lake	43.36	146.87	150.4	4.1	13.7	11.7	1.08	1346	3.5	3.10	80	44.0	0.8
50	Lake Baker	41.59	147.72	1357	6.5	8.7	12.4	0.52	1498	1.8	0.40	19	-	3.1
51	Lake Baker 2*	41.59	147.72	1359	6.2	8.7	12.4	0.28	1499	1.0	1.25	14	-	0.7
52	Menamatta Tarns 1	41.54	147.63	1446	6.2	8.2	12.3	0.52	1549	0.2	0.16	23	-	2.3
53	Menamatta Tarns 2	41.54	147.63	1447	6.0	8.2	12.3	0.50	1549	0.4	0.09	22	-	0.6
54	Menamatta Tarns 3	41.54	147.63	1451	5.9	8.1	12.3	0.46	1551	0.2	0.10	26	28.7	10.1

Only the first 47 lakes were used in the final model. The lakes are ordered based on increasing elevation. Abbreviations of environmental parameters are mentioned in the text. Latitude (SOUTH), longitude (EAST), and elevation (ELEV) were measured using a Garmin® global positioning system. As these variables only affect midge distributions indirectly (i.e., through temperature, precipitation, soil fertility, etc.), they were removed from analyses.
* Lake names created by the authors.

Table 2.2: Taxa enumerated in this study.

#	Taxon Name	Occurrence	Hill's N2	Max	Mean	WA-PLS β	pH	TWARM	RAD	Mg	PRECIP	SiO_2	DEPTH
1	Pentaneurini Genus E	51.1	14.4	9.5	1.7	12.7							
2	*Larsia* Fittkau	72.3	19.1	13.8	2.5	11.4	x		X		X		
3	*Paramerina* Fittkau	40.4	10.9	5.5	0.7	8.1							
4	*Telmatopelopia* Fittkau	21.3	7.2	8.1	0.9	6.3			x				x
5	Pentaneurini undifferentiated	76.6	17.7	14.7	2.0	9.6			X		X		
6	Macropelopini type 1 Unofficial morphotype	19.1	7.5	2.4	0.2	8.5						x	
7	*Procladius* Skuse	76.6	24.8	10.2	2.3	12.3		x	X	X	x		
8	Macropelopini undifferentiated	61.7	20.1	6.1	1.3	11.6	x						
9	Genus Australia	6.4	2.5	3.0	0.1	10.0	x	x	x			X	
10	*Botryocladius* Cranston & Edward	68.1	14.6	12.6	1.8	6.5		X		X	x		
11	*Cricotopus* 'parbicintus'	48.9	9.8	13.3	1.4	7.7	X				x		
12	*Echinocladius* Cranston	61.7	13.6	27.9	3.0	7.3			x	X			
13	*Gymnometriocnemus* type 1 Unofficial morphotype	27.7	8.5	3.6	0.3	11.5							
14	Orthoclad type 1 Unofficial morphotype	14.9	5.5	2.3	0.2	12.3						X	
15	Orthoclad type 2 Unofficial morphotype	10.6	4.1	2.6	0.2	5.1	x	x	X	x	X	x	
16	Orthoclad type 3 Unofficial morphotype	48.9	15.8	3.6	0.6	11.2	x		X			x	
17	Orthoclad type 4 Unofficial morphotype	17.0	6.4	3.7	0.4	4.7	X	X	x	X	x	X	x
18	*Parakiefferiella* type 1 Unofficial morphotype	63.8	11.4	55.5	7.1	7.5	x	X			x		
19	*Parakiefferiella* type 2 Unofficial morphotype	29.8	5.8	33.0	2.5	12.7	x	X	X		X	X	
20	*Parakiefferiella* type 3 Unofficial morphotype	19.1	4.3	5.5	0.4	5.6	x		X				
21	*Parakiefferiella* type 4 Unofficial morphotype	6.4	2.3	16.4	0.6	8.4	x	X		X		x	
22	*Paralimnophyes* type 1 Unofficial morphotype	83.0	18.9	44.6	7.1	9.4	X	X	X	X	X	x	
23	*Paralimnophyes* type 2 Unofficial morphotype	25.5	4.3	12.9	0.7	6.0		x					
24	*Paralimnophyes* type 3 Unofficial morphotype	34.0	12.1	2.3	0.4	11.3							
25	'SO1'	6.4	2.8	4.2	0.2	3.2	X	X	X	x	X	X	
26	*Stictocladius* Edwards	14.9	4.2	3.9	0.2	8.0			X			X	
27	*Chironomus* Meigen	76.6	15.7	31.6	6.1	8.5					x		x
28	*Cladopelma* Kieffer	31.9	6.0	8.5	0.7	11.8	x					x	
29	*Cladotanytarsus* Kieffer	19.1	4.4	25.8	1.4	7.9	X	X	X		X		
30	*Cryptochironomus* Kieffer	27.7	10.1	2.3	0.3	12.2							
31	*Dicrotendipes* Kieffer	21.3	3.5	14.7	0.6	11.7	x			x	x		
32	*Kiefferulus martini* Freeman	6.4	2.4	6.2	0.2	31.4	X	X		X		X	
33	*Parachironomus* Lenz	46.8	16.6	3.2	0.7	15.8	X	X					
34	*Polypedilum vespertinus* Skuse	44.7	7.9	34.0	2.8	6.5	X			x			
35	*Polypedilum watsoni* Freeman	38.3	11.3	8.1	1.3	9.3	x		X		X		
36	*Polypedilum* type 1 Unofficial morphotype	27.7	10.7	2.6	0.3	10.9	X		X		X		
37	*Riethia* Kieffer	87.2	23.0	21.6	5.6	9.4		X		x			x
38	*Stempellina* Thienemann & Bause	53.2	12.0	57.8	8.4	17.0	X	X		x	x		x
39	*Tanytarsus* nr. *chinyensis*	31.9	7.0	15.1	1.0	21.0	X	X					
40	*Tanytarsus* type 1 Unofficial morphotype	61.7	14.0	37.2	6.8	11.9	X						
41	*Tanytarsus* type 2 Unofficial morphotype	46.8	12.3	20.3	3.1	13.2				X		X	x
42	*Tanytarsus* type 3 Unofficial morphotype	25.5	6.0	22.8	2.0	6.4			X		X		X
43	*Tanytarsus* type 4 Unofficial morphotype	12.8	1.7	37.8	1.1	1.7		X		x			
44	*Tanytarsus* type 5 Unofficial morphotype	8.5	3.2	2.0	0.1	16.7	x					X	
45	Tanytarsini undifferentiated	100.0	26.0	66.2	16.6	10.0	X	x				x	
46	*Parochlus* Enderlein	29.8	9.0	4.7	0.5	7.9			X		X	x	x
47	Ceratopogonidae type 1 Unofficial morphotype	34.0	10.7	3.9	0.5	6.3						x	
48	Ceratopogonidae type 2 Unofficial morphotype	12.8	4.8	3.6	0.3	27.3	x	X		X			
49	*Chaoborus* Unofficial morphotype	29.8	7.9	7.0	0.7	21.6	X	X		X			X

Occurrence is a percentage out of the 47 lakes comprising the final transfer function whereas the WA-PLS β coefficient is from the jack-knifed 2nd component model. Generalized linear modelling was used to determine significant relationships between taxa and environmental parameters.
x=significant at P≤0.05.
X=significant at P≤0.01.

Table 2.3: Partial CCAs of the seven significant environmental variables.

Environmental Variable	Covariable(s)	λ_1	λ_1/λ_2	P	% variance
pH	None	0.203	1.010	0.001	11.6
	TWARM	0.152	0.879	0.001	9.6
	TWARM, RAD	0.099	0.589	0.001	6.8
	TWARM, RAD, Mg	0.057	0.365	0.010	4.3
	TWARM, RAD, Mg, PRECIP	0.060	0.395	0.009	4.7
	TWARM, RAD, Mg, PRECIP, SiO_2	0.055	0.369	0.013	4.5
	TWARM, RAD, Mg, PRECIP, SiO_2, DEPTH	0.056	0.378	0.011	4.8
TWARM	None	0.161	0.668	0.001	9.2
	pH	0.110	0.636	0.001	7.1
	pH, RAD	0.099	0.589	0.001	6.8
	pH, RAD, Mg	0.095	0.609	0.001	6.9
	pH, RAD, Mg, PRECIP	0.085	0.559	0.001	6.5
	pH, RAD, Mg, PRECIP, SiO_2	0.085	0.570	0.001	6.8
	pH, RAD, Mg, PRECIP, SiO_2, DEPTH	0.086	0.581	0.001	7.2
RAD	None	0.137	0.576	0.001	7.8
	pH	0.091	0.508	0.001	5.9
	pH, TWARM	0.080	0.476	0.001	5.6
	pH, TWARM, Mg	0.079	0.506	0.001	5.8
	pH, TWARM, Mg, PRECIP	0.084	0.553	0.001	6.5
	pH, TWARM, Mg, PRECIP, SiO_2	0.085	0.570	0.001	6.8
	pH, TWARM, Mg, PRECIP, SiO_2, DEPTH	0.071	0.480	0.001	5.9
Mg	None	0.080	0.296	0.006	4.6
	pH	0.079	0.397	0.002	5.1
	pH, TWARM	0.078	0.500	0.002	5.4
	pH, TWARM, RAD	0.076	0.487	0.001	5.6
	pH, TWARM, RAD, PRECIP	0.063	0.414	0.004	4.9
	pH, TWARM, RAD, PRECIP, SiO_2	0.055	0.369	0.007	4.5
	pH, TWARM, RAD, PRECIP, SiO_2, DEPTH	0.046	0.311	0.032	4.0
PRECIP	None	0.129	0.592	0.001	7.3
	pH	0.060	0.311	0.017	3.9
	pH, TWARM	0.052	0.301	0.029	3.6
	pH, TWARM, RAD	0.073	0.468	0.001	5.3
	pH, TWARM, RAD, Mg	0.060	0.395	0.004	4.7
	pH, TWARM, RAD, Mg, SiO_2	0.062	0.416	0.002	5.1
	pH, TWARM, RAD, Mg, SiO_2, DEPTH	0.057	0.385	0.003	4.8
SiO_2	None	0.100	0.417	0.001	5.7
	pH	0.071	0.353	0.003	4.6
	pH, TWARM	0.077	0.458	0.001	5.4
	pH, TWARM, RAD	0.069	0.416	0.001	5.1
	pH, TWARM, RAD, Mg	0.055	0.357	0.005	4.3
	pH, TWARM, RAD, Mg, PRECIP	0.057	0.383	0.004	4.7
	pH, TWARM, RAD, Mg, PRECIP, DEPTH	0.053	0.358	0.011	4.6
DEPTH	None	0.089	0.335	0.001	5.1
	pH	0.085	0.455	0.001	5.5
	pH, TWARM	0.073	0.422	0.001	5.1
	pH, TWARM, RAD	0.056	0.335	0.010	4.1
	pH, TWARM, RAD, Mg,	0.056	0.360	0.005	4.4
	pH, TWARM, RAD, Mg, PRECIP	0.050	0.446	0.016	4.1
	pH, TWARM, RAD, Mg, PRECIP, SiO_2	0.046	0.311	0.025	4.0

Table 2.4: CCA summary with canonical coefficients, their associated t-values, and interset correlations.

	Axis 1	Axis 2	Axis 3	Axis 4
Eigenvalue	0.242	0.147	0.081	0.061
Cum % var. spp.	13.8	22.2	26.9	30.3
Cum % var. spp.-env. relation	38.2	61.4	74.2	83.9
Regression/canonical coefficients				
pH	0.308	0.490	-0.064	-0.512
TWARM	-0.676	0.873	-0.317	-0.568
RAD	0.677	1.164	1.194	-0.984
Mg	-0.392	0.125	0.323	-0.713
PRECIP	0.365	0.988	0.944	-1.479
SiO_2	0.241	0.000	-0.313	-0.948
DEPTH	-0.114	-0.330	0.193	-0.235
t-values of regression coefficients				
pH	3.076 *	3.105 *	-0.331	-2.177 *
TWARM	-6.295 *	5.139 *	-1.518	-2.248 *
RAD	4.045 *	4.404 *	3.672 *	-2.502 *
Mg	-3.782 *	0.760	1.604	-2.926 *
PRECIP	2.231 *	3.818 *	2.967 *	-3.841 *
SiO_2	3.236 *	0.004	-2.168 *	-5.424 *
DEPTH	-1.788	-3.284 *	1.563	-1.572
Interset correlations				
pH	0.852	-0.015	-0.003	-0.047
TWARM	-0.575	0.523	-0.403	-0.026
RAD	0.527	0.487	0.229	0.166
Mg	-0.080	-0.228	0.733	-0.091
PRECIP	-0.595	-0.281	0.011	-0.254
SiO_2	0.392	-0.072	-0.574	-0.407
DEPTH	-0.211	-0.522	0.046	-0.348

* Significant at $P \leq 0.05$
Cum % var. spp. = Cumulative percent variance of species data
Cum % var. spp.-env. relation = Cumulative percent variance of species-environment relation

Table 2.5: Performance of PLS and WA-PLS models for reconstructing TWARM.

Model		Apparent				Jack-knifed				
		r^2	Ave Bias	Max Bias	RMSE	r^2	Ave Bias	Max Bias	RMSEP	Reduced (%)
PLS	Component 1	0.62	$1.51x10^{-15}$	2.03	1.09	0.47	$1.45x10^{-3}$	2.66	1.29	
	Component 2	0.77	$1.47x10^{-15}$	0.86	0.84	0.56	$-1.40x10^{-}$	1.63	1.18	8.7
	Component 3	0.84	$1.32x10^{-15}$	0.66	0.72	0.58	$5.06x10^{-4}$	1.52	1.15	2.6
	Component 4	0.87	$1.40x10^{-15}$	0.58	0.64	0.59	$8.93x10^{-3}$	1.46	1.15	-0.4
	Component 5	0.89	$1.32x10^{-15}$	0.50	0.59	0.56	$8.98x10^{-3}$	1.44	1.20	-4.0
WA-PLS	Component 1	0.78	$1.70x10^{-2}$	1.16	0.82	0.66	$3.92x10^{-3}$	1.92	1.02	
	Component 2	**0.87**	**$3.17x10^{-3}$**	**1.29**	**0.64**	**0.72**	**$-5.38x10^{-}$**	**1.35**	**0.94**	**8.4**
	Component 3	0.90	$-1.27x10^{-4}$	0.62	0.57	0.69	$9.42x10^{-3}$	1.21	0.99	-4.3
	Component 4	0.92	$8.34x10^{-3}$	0.47	0.49	0.65	$5.09x10^{-2}$	1.24	1.07	-9.7
	Component 5	0.93	$-4.09x10^{-4}$	0.36	0.45	0.60	$5.00x10^{-2}$	1.36	1.16	-7.7

Emboldened row indicates the model of choice.

Chapter 3 A test of Tyler's Line - response of chironomids to a pH gradient in Tasmania and their potential as a proxy to infer past changes in pH

Citation for published manuscript: Rees, A.B.H., Cwynar, L.C., 2010. A test of Tyler's Line - response of chironomids to a pH gradient in Tasmania and their potential as a proxy to infer past changes in pH. Freshwater Biology 55, 2521-2540.

Abstract

Tyler's Line delimits two distinct limnological provinces that reflect differences in climate, geology, and vegetation in Tasmania. Lakes west of Tyler's Line are typically acidic and dystrophic with relatively shallow euphotic zones, whereas eastern lakes are circumneutral and oligotrophic or ultra-oligotrophic, allowing deeper penetration of light. Consequently, Tyler's Line defines a boundary where species assemblages change over a relatively short distance. A survey of 48 Tasmanian lakes was undertaken to identify indicator taxa of the two limnological provinces and breakpoints along the pH gradient where shifts in taxa occur. Chironomidae (Diptera) were used because they are ideal candidates for lake classification. Three independent methods (geographical position, piecewise linear regression, two-way indicator species analysis) verified that chironomids accurately reflect the environmental variables defining Tyler's Line at lake and catchment scales. Chironomid genera are often speciose, and members of the same genus can have markedly different responses to a given environmental variable. Although the types of taxa changed along the pH gradient, richness did not. This finding contrasts with many studies from the Northern Hemisphere but accords with other studies from Australia. Finally, we developed models of pH using both partial least squares and weighted averaging partial least squares. These models can be used to understand past natural variability of pH in Tasmania and to test hypotheses regarding the timing, magnitude, and source of contamination in impacted aquatic ecosystems.

Keywords: Chironomid, Inference model, Lake classification, pH, Tasmania

Introduction

Tasmania has more than 4,000 lakes and tarns, mostly of glacial origin. Limnologically, Tasmania is bisected by a corridor that runs north-west by south-east, aslant the 146th meridian, called Tyler's Line. Named in honour of Peter Tyler, Tasmania's first resident phycologist and limnologist, the term was coined by Shiel et al. (1989) to describe the eastern boundary of a rotifer species assemblage in western Tasmania.

Lakes west of Tyler's Line are typically acidic and coloured by humic derivatives. In these dystrophic systems, euphotic depths are usually less than 2 m, with red wavelengths penetrating furthest. Lakes east of Tyler's Line are typically more alkaline and oligotrophic or ultra-oligotrophic. These systems generally have clear water and euphotic depths of 10 m or more, with blue-green wavelengths penetrating furthest (Tyler, 1992).

Tyler's Line integrates geological, climatic, edaphic, and vegetational change (Fig. 3.1). Western Tasmania is characterized by quartz rocks that are slow to weather, producing shallow, infertile, and acidic soils. East of Tyler's Line, landscapes have been extensively modified by doleritic intrusions. These basalts readily weather, producing soils generally rich in clay and more fertile than those in the west (Jackson, 2005). The discontinuity in geology coincides with a marked decrease in rainfall from west to east coasts resulting from orographic lift of the prevailing Westerlies. The compositions of several terrestrial and aquatic faunal groups coincide with these boundaries (Mesibov, 1994).

Chironomids are the most widely distributed and typically the most abundant macroinvertebrate in freshwater systems and are important components of food webs (Armitage et al., 1995). With short generation times and winged adults, chironomids are useful proxies that integrate climatic, hydrological, and geological information (Nyman and Korhola, 2005) and have proven to be reliable candidates for lake classification (Thienemann, 1922; Nyman and Korhola, 2005; Bitušík et al., 2006) and water quality monitoring (Sæther, 1979; Rosenberg, 1992; Marziali et al., 2009). Chironomid communities respond both directly (Bell, 1970; Havas, 1981; St. Louis, 1993) and indirectly (Mackay and Kersey, 1985; Økland and Økland, 1986; Appelberg et al., 1993) to lake water pH and can therefore be expected to respond to Tyler's Line. The objectives of this study were twofold. The first was to test the hypothesis that the taxonomic composition of chironomid (larval) communities changes across Tyler's Line and to identify critical breakpoints across the pH gradient where shifts in taxa occur. The second objective was to create an inference model that can be used to both model past changes in pH and interpret the impact of modern, anthropological factors on these aquatic systems.

Materials and methods

Environmental data collection

Lake water chemistry was measured in 54 Tasmanian lakes during January and February of 2006 and 2007 (Table 3.1; Fig. 3.1). A 250-mL plastic bottle was filled from approximately 0.5 m below the water surface and kept cool until analysis of concentrations of Na, K, Ca, Mg, Fe, Mn, Zn, Cl, SiO_2, SO_4, HCO_3, total organic carbon (TOC), turbidity (TURB), conductivity (CON), alkalinity (ALK), and pH. A further 125-

mL glass bottle was filled with filtered lake water to which 1 mL of 30% H_2SO_4 was added, and the bottle was kept cool until analysis of dissolved total Kjeldahl nitrogen (dissolved TKN) and dissolved total phosphorus (dissolved TP). All analyses were conducted at the Research and Productivity Council in Fredericton, New Brunswick, Canada using standard procedures (Standards Council of Canada, Ottawa, Canada).

Climate variables were obtained with BIOCLIM (Houlder et al., 2003), which combines data from meteorological stations having adequate records (minimum of 30 years) and a digital elevation model to generate point values for a specific longitude, latitude, and elevation. We used the program to estimate mean temperature of the warmest quarter (TWARM), annual precipitation (PRECIP), and annual radiation (RAD). Lake perimeter (PERIM) and surface area (AREA), catchment area (CATCH), vegetation and geology, catchment area to lake area ratio (CATCH : LAKE), and shoreline development (SHORE) were obtained from shapefiles provided by TASMAP©, State of Tasmania. CATCH was acquired with the Watershed tool in the Spatial Analyst Tools toolbox of ArcMap 9.2 (ESRI, Redlands, CA, U.S.A.). Catchment vegetation and geology are expressed as percentages of major units comprising CATCH. SHORE was determined as the ratio of the length of the shore line to the circumference of a circle with an area equal to that of the lake. This parameter is a rough estimate of the available littoral biotopes in relation to the volume of the lake (Wetzel, 2001). Water depth (DEPTH) was measured by sounding at the geographical centre of each lake until a maximum depth was found. Loss-on-ignition (LOI) was measured on 1 mL of wet sediment, dried at 100°C overnight and ashed in a furnace at 550°C for 4 h. The percent

of dry weight lost is a coarse indication of the organic content of the sediment (Dean, 1974).

Chironomid collection and processing

Lake sediment was collected, in duplicate, from the deepest part of each lake, using a mini-Glew corer (Glew, 1991). The variety and patchiness of freshwater biotopes makes sampling for living chironomid larvae tedious and time-consuming; it is more effective to take surface sediment samples from the deepest part of a lake and analyze subfossil chironomids. In shallow lakes, sediment samples collected from this area typically contain chironomid remains representative of the whole assemblage (Iovino, 1975; Walker et al., 1984; Heiri, 2004). The upper 1 and 2 cm of each duplicate were extruded on site, packaged in separate Whirl-Pak® sample bags (Nasco, Fort Atkinson, WI, USA), and kept cool until analysis.

In the laboratory, chironomid analysis followed the protocol of Walker et al. (1991). Lake sediment was volumetrically sampled, heated, deflocculated in 10% KOH, and then rinsed with distilled water on a sieve with 95 μm meshes. Aliquots of the residue were poured into a Bogorov tray and scanned under a dissecting microscope at 50x magnification. Chironomid head capsules and chaoborid mandibles were hand-picked using fine forceps. Head capsules were mounted on slides ventral side up and fixed with Entellan® (Merck, Darmstadt, Germany). Identification was conducted with a compound microscope at 400x magnification, following Wiederholm (1983), Oliver and Roussel (1983), Cranston (2000), and Brooks et al. (2007). If a specimen could only be identified to genus (i.e., because of an early instar or degraded head capsule), the

specimen was placed into an undifferentiated category. After species identification was complete, each undifferentiated category was divided among reliably identified morphotypes of respective genera proportional to each morphotype's abundance.

Data screening and transformations

A detrended correspondence analysis (DCA) of the species data and a principal components analysis (PCA) of the environmental data were performed to identify lakes with unusual chironomid assemblages and environmental parameters. Sites with sample scores lying outside one standard deviation of the means of the first two axes of both the DCA and PCA were considered for elimination. While Lake Fortuna, Central Plateau 1, Lake Youl, and Roberts Tarn failed the DCA and Lakes Strahan, Ashwood, and Chisholm failed the PCA, no lake failed both tests and all were retained in the analysis.

Rees et al. (2008) showed that a minimum count size of 50 head capsules captured, on average, 84.3% of actual taxonomic richness in Tasmanian lakes. This value was used as the minimum count size for chironomid remains. Menamatta Tarns 1 and 2 and Baker Lakes 1 and 2 were removed from modelling exercises because all had fewer than 10 head capsules after processing the sediment.

The difference between observed and predicted pH, generated by partial least squares (PLS) and weighted averaging partial least squares (WA-PLS) models (see Model development section), was also used to identify outlying sites. The differences for Wombat Pool and Duckhole Lake were large and, consequently, these sites were eliminated from analyses.

Prior to statistical analyses, chironomid distributional data were transformed into percent abundance and rare taxa, here defined as occurring in only one lake and/or having a maximum abundance less than 2%, were removed. Environmental data were assessed for normality using the Kolmogorov-Smirnov normality test and measures of skewness and kurtosis (Zar, 1999) and transformed where necessary. Pearson's correlation tests and a series of canonical correspondence analyses (CCAs) were used to assess the collinearity of environmental variables. Variables with the highest variance inflation factor (VIF) were sequentially removed until all VIFs were less than 20 (ter Braak and Šmilauer, 2002).

Statistical analysis

Ordinations were run in CANOCO version 4.5 (ter Braak and Šmilauer, 2002) with chironomid abundance data square root-transformed and the effects of rare taxa downweighted. CCA, with forward selection and Monte Carlo permutation testing (999 unrestricted permutations), were used to select the minimum number of variables explaining the largest amount of variation in the species data. A series of partial CCAs (pCCAs) was run to assess the robustness of the significant environmental variables with and without the remaining environmental variables included as covariables. The relationship between significant environmental variables and ordination axes was assessed with canonical coefficients, their associated t-values, and interset correlations. Catchment vegetation and geology data were highly skewed, so these variables were included in ordinations passively. Only major vegetational and geological units with interset correlation values greater than 0.4 are shown in ordination plots.

Piecewise linear regression (PLR) was used to identify faunal breaks in chironomid abundance data along the pH gradient. Our methods largely follow those outlined by Heegaard et al. (2006). A principal coordinate analysis (PCoA), run with the PrCoord application of CANOCO, was used to estimate species turnover (i.e., beta-diversity). Beta-diversity (β), the difference in species composition between two habitats, is defined here as the distance between two points in ordinal space. We used the chord distance metric, as recommended for abundance data (Overpeck et al., 1985; Wahl, 2004). The site scores of the first four PCoA axes were used to calculate beta-diversity with the following equation:

$$\beta = \sqrt{\sum_{j=1}^{4} (x_{ji} - x_{jk})^2}$$

where x_{ji} is the i^{th} site score of the j^{th} axis; *i* and *k* are neighbours along the pH gradient. The cumulative rate of species turnover was plotted as the response variable against pH.

The R software environment (R Development Core Team, 2009), with the strucchange library (Zeileis et al., 2003), was used to identify abrupt changes or breakpoints in cumulative β rate of change. The strucchange library uses a function that detects structural changes in regression models. The function detects potential breakpoints, or faunal breaks, where species turnover drastically changes along the gradient. After identifying the breakpoints, a full model was constructed with the spline library in R (R Development Core Team, 2009). The full model consisted of intervals between all breakpoints, each with unique cumulative β rates of change (i.e., slopes) and intercepts. Each breakpoint was removed, and the resulting model was compared against

the full model with an analysis of deviance. If a breakpoint was removed and did not produce a significantly different model from the full model, the breakpoint was eliminated from further analyses.

The average number of species constituting groups defined by PLR analysis depends on sampling effort. To compare species richness between these groups, we used rarefaction analysis to scale samples of varying size to the same count. All samples were scaled down to the minimum count size (77 head capsules), and rarefaction was performed with the program RAREPOLL (Birks and Line, 1992).

Two-Way Indicator Species Analysis (TWINSPAN) was used to group samples with similar community composition into a hierarchical structure of clusters. TWINSPAN is a semi-quantitative, divisive classification technique that is especially robust for noisy data sets (Gauch and Whittaker, 1981). We ran TWINSPAN in WinTWINS (Hill and Šmilauer, 2005) with pseudospecies cut levels set to 2, 5, 7, 12, and 20%; otherwise, default settings were used in the analysis. Any pseudotaxon occurring three times or more on one side of a division than on the other is considered a good indicator, while a pseudotaxon occurring twice as often on one side compared to the other is considered a preferential. McCune and Grace (2002) recommend using TWINSPAN only when a single underlying variable is structuring species distributions. In previous work on this data set, Rees et al. (2008) found that pH explained close to double the amount of variance in the species data compared to TWARM, the next most powerful explanatory variable.

A canonical variates analysis (CVA) was used to visually inspect whether lake classification was consistent between the three independent techniques: grouping lakes as

either geographically east or west of the 146th meridian, PLR analysis, and TWINSPAN. In CANOCO, a CVA is identical to a CCA, except a priori lake groupings (input as dummy variables) replace the species data (ter Braak and Šmilauer, 2002). If the chironomid larvae are responding to a strong pH gradient, then groupings defined by geography, PLR analysis, and TWINSPAN should cluster together. As with the CCAs, partial CVAs were run to assess the robustness of environmental variables explaining a significant portion of the variance in the groupings data.

Model development

Chironomid-based inference models were developed for pH using C2 version 1.5 (Juggins, 2007). A DCA was used to determine the response of chironomid taxa across the gradients captured by our sampling regime. The gradient length of DCA axis 1 was 2.675, indicating that either linear or unimodal methods could adequately model species response (Birks, 1998). Consequently, we constructed models using both PLS and WA-PLS techniques. We used leave-one-out cross-validation (1,000 cycles) because this technique is more robust than bootstrapping for data sets with fewer than 80 samples (Kim and Han, 1997). Criteria for the best model were a high jack-knifed coefficient of determination (r^2_{jack}) between observed and predicted pH values, low average ($AveBias_{jack}$) and maximum ($MaxBias_{jack}$) biases of jack-knifed predictions, and a low root mean square error of prediction (RMSEP). A reduction of at least 5% in the RMSEP was necessary to include more components in the final model (Birks, 1998).

Results

A PCA of the environmental variables revealed three distinct classes of Tasmanian lakes: coastal lakes, lakes west of Tyler's Line, and lakes east of Tyler's Line (Fig. 3.2a). Wombat Pool was the only western lake grouped with the eastern lakes, while Duckhole Lake was the only eastern lake that plots out between western and coastal lakes, confirming their status as outliers. One western lake (Lake Chisholm) grouped closely with the coastal lakes (Fig. 3.2a). Examination of major cations and anions indicates that the chemistry of coastal lakes and lakes west of Tyler's Line are closely related, resembling the ionic complexion of sea water (Fig. 3.2b,c). Lakes east of Tyler's Line had higher concentrations of Ca and HCO_3 (Fig. 3.2b,c).

CCA identified seven environmental variables that accounted for a significant percentage of the variance in chironomid abundance data (Fig. 3.3): pH (19.1%), TWARM (11.4%), Mg (9.6%), DEPTH (6.8%), PRECIP (5.5%), SiO_2 (5.3%), and Zn (4.6%). After running a series of pCCAs, Zn lost its explanatory power (Table 3.2). The first four axes of a reduced CCA (with the remaining six environmental variables) explained 26.4% of the variance in species data. Only pH and DEPTH were not significantly correlated with the first axis, while Mg, PRECIP, and SiO_2 were not significantly correlated with the second. In terms of interset correlations, pH was most strongly associated with the first axis and TWARM was most strongly associated with the second (Table 3.3).

The lakes west and east of Tyler's Line clearly separated to the right and left sides of the CCA plot (Fig. 3.3a). Western lakes are associated with higher TWARM values, receive more precipitation, and are more acidic than those to the east. The catchment

areas of these lakes were associated with two types of vegetational groups: 1) saltmarshes and wetlands and 2) scrub, heathland, and coastal vegetation and two major geological units: 1) coastal dunes and 2) the Tyennan group and correlates (sedimentary siliclastics). Lakes east of Tyler's Line are more alkaline, receive less precipitation, and are associated with cooler temperatures. The vegetation of eastern catchment areas was characterized by 1) dry *Eucalyptus* forests and woodlands and 2) highland treeless vegetation, while the geology of these systems consisted largely of Tasmanian dolerite (Fig. 3.3b). For simplicity, only the species scores of indicator and preferential taxa detected by TWINSPAN are shown in the CCA (Fig. 3.3c).

PLR analysis revealed breakpoints at pH values of 5.0 and 5.8 (Fig. 3.4a); both values retained their significance after an analysis of deviance. These breakpoints correspond to a group of acidic lakes with pH values ranging between 4.4 and 5.0 (PLR 1), a group of circumneutral lakes with pH values between 5.9 and 7.0 (PLR 3), and a group of transitional lakes characterized by pH values between 5.1 and 5.8 (PLR 2). The rate of cumulative β diversity change (i.e., species turnover) per unit pH was 19.1, 5.1, and 18.5 for PLR groups 1, 2, and 3, respectively, while the average rarefied taxon richness was 14, 14, and 12 for those same groups.

The first level of the TWINSPAN division resulted in two groups, TWIN 1 and TWIN 2, consisting of 25 and 23 lakes, respectively (Fig. 3.4b). In general, lakes from TWIN 1 had lower pH and Ca values and higher PRECIP and TWARM values than those of TWIN 2 (Fig. 3.5). Indicator taxa of TWIN 1 were *Tanytarsus* morphotype 1, *Paralimnophyes* morphotype 1, *Stempellina*, and *Parakiefferiella* morphotype 2. Preferential taxa of TWIN 1 included Pentaneurini Genus E, *Tanytarsus* nr. *chinyensis*,

Chaoborus, and *Riethia* (Table 3.4; Fig 3.4c). Indicator taxa of TWIN 2 were *Tanytarsus* morphotypes 2 and 3, while preferential taxa included *Larsia*, *Paramerina*, *Cricotopus* 'parbicintus', *Parakiefferiella* morphotype 1, *Cladotanytarsus*, and *Procladius* (Table 3.4; Fig. 3.4c).

Since several *Tanytarsus* species are either indicators or preferentials of a TWINSPAN division, it is worth elaborating on the defining features of these morphotypes. *Tanytarsus* morphotype 1 possesses a spur on the antennal pedestal, simple labral setae S1, and a pale median complex with a central tooth accompanied by two smaller teeth on either side (Fig. 3.6a). *Tanytarsus* nr. *chinyensis* is characterized by a long spur on the antennal pedestal, a simple median tooth, and branched labral setae S1 (Fig. 3.6b). *Tanytarsus* morphotype 2 has blunt antennal pedestals, a notched median tooth, and simple labral setae S1 (Fig. 3.6c). Finally, *Tanytarsus* morphotype 3 has a spur on the antennal pedestal, a notched median tooth, and branched labral setae S1 (Fig. 3.6d). Although the labral setae S1 usually do not preserve on fossil specimens, the feature confirms that these taxa belong to different morphotypes. The presence or absence of a spur, in conjunction with the nature of the median tooth, is typically enough to establish a reliable identification. All four *Tanytarsus* morphotypes possess mandibles with an apical tooth, three inner teeth, and a dorsal tooth.

CVA was used to both visually compare lake classification based on geography, PLR analysis, and TWINSPAN as well as identify the environmental variables that best discriminate between these groups (Fig. 3.7). The CVA detected seven variables that accounted for a significant portion of the variance in the groupings data: pH (62.2%), SO_4 (5.8%), Ca (7.8%), TWARM (5.3%), SiO_2 (3.3%), PRECIP (4.3%), and Mg (2.8%). A

series of partial CVAs was used to test the robustness of these environmental variables and, in this case, only pH retained its significance (Table 3.5). The first four axes of the reduced CVA (including only pH) account for 98.2% of variance in the groupings data. Lake water pH was significantly correlated to the first axis, as reflected by the interset correlation (Table 3.6). Lakes west of Tyler's Line plot out on the right half of the CVA with PLR 1 and TWIN 1. This group is characterized by low pH values. Lakes east of Tyler's Line plot out on the left of the ordination with PLR 3 and TWIN 2. This group has higher pH values, and catchment areas are associated with dry *Eucalyptus* forests and dolerite. PLR 2 is intermediate in pH between the western and eastern groups (Fig. 3.7).

Model development

We constructed both PLS and WA-PLS models (Fig. 3.8). Both the second component PLS and first component WA-PLS models perform very similarly, with the PLS model only slightly outperforming the WA-PLS model (Table 3.7). Beta (β) coefficients from the PLS and WA-PLS models can be used to reconstruct pH estimates using fossil chironomids (Table 3.4).

Discussion

Gibbs (1970) concluded that three major mechanisms control the chemistry of surface waters throughout the world: atmospheric precipitation, geochemical processes, and evaporation-crystallisation, the last typically associated with arid regions. Our PCA of environmental variables agrees with Tyler's (1992) suggestion that Tasmania has three lake districts: lakes west of Tyler's Line, lakes east of Tyler's Line, and coastal lakes. However, inspection of the major cations and anions reveals that coastal lakes and lakes

west of Tyler's Line are both strongly influenced by atmospheric precipitation, having ionic complexions with a clear marine influence. Lakes east of Tyler's Line had higher concentrations of Ca and HCO_3, suggesting a stronger influence from geochemical processes, such as the weathering of underlying basement rock. CCA, PLR analysis, and TWINSPAN did not detect a group of coastal lakes, indicating that, in terms of chironomid response to physicochemical variables, coastal lakes can be lumped with lakes west of Tyler's Line.

The CCA sample scores showed a clear west-east dichotomy. The higher TWARM values of western lakes probably reflect elevation; lakes west of Tyler's Line were, on average, closer to sea-level than lakes east of Tyler's Line and had a larger range of elevations. It is interesting to note that lakes west of Tyler's Line were more dispersed along CCA axis 2 than the eastern lakes. As TWARM was most associated with the second axis, this pattern may reflect the range in elevation of western lakes compared to their eastern counterparts. However, the spread of western lakes along CCA axis 2 could also reflect catchment geology.

Lakes west of Tyler's Line were characterized by high percentages of two major geological groupings: coastal dunes and the Tyennan group and correlates, while lakes east of Tyler's Line were generally situated on a single geological unit (dolerite). Lakes west of Tyler's Line ranged in pH from 4.4 to 5.0, while lakes east of Tyler's Line ranged from 5.9 to 7.0. The presence of a transitional group, ranging in pH from 5.1 to 5.8, supports the notion that lakes west and east of Tyler's Line are separated by a corridor rather than an abrupt discontinuity (Tyler, 1992; Vyverman et al., 1996). Further divisions of TWINSPAN could not accurately reflect this transitional group, suggesting

that communities in this pH range do not possess unique indicator taxa. This group also has the lowest rate of change in terms of cumulative β diversity, indicating that chironomid communities of PLR 2 are relatively uniform throughout their pH range. A decrease in species richness typically occurs when pH drops below 5 (Mossberg, 1979; Mossberg and Nyberg, 1979; Schindler and Turner, 1982; Økland and Økland, 1986). Many studies demonstrate a decrease in chironomid species richness, and an increase in the abundance of relatively few, tolerant taxa, coincident with acidification (Henrikson, et al., 1982; Armitage and Blackburn, 1985; Leuven et al., 1987; Bitušík et al., 2006). However, the average rarefied taxon richness for PLR groups 1, 2, and 3 was 14, 14, and 12, respectively, suggesting that Tasmanian chironomid communities do not decrease in richness at low pH. Studies from mine drainage sites in Australia suggest that the response of macroinvertebrate communities in southern waters may be different from those in northern, temperate regions (Faith et al., 1991; Smith and Cranston, 1995; Cranston et al., 1997). Cranston et al. (1997) studied the response of chironomid communities in Rockhole Mine Creek, a small stream in the Northern Territory of Australia that receives acid water drainage, rich in heavy metals, that originates from an abandoned uranium mine. Species richness was higher in sites receiving the acid water effluent. The authors suggested that higher species richness at low pH, contrasting with many studies from temperate regions in the Northern Hemisphere, may result from the large pool of tropical taxa that have adapted to naturally occurring acidic conditions. During glacial episodes, an isthmus would have formed between mainland Australia and Tasmania, allowing for the migration of plants and animals (Blom, 1988; Jackson, 2005).

This could have been a potential route of colonization for the suite of acid-adapted taxa from mainland Australia and Southeast Asia into Tasmania.

Lakes west of Tyler's Line were characterized by *Tanytarsus* morphotype 1, *Paralimnophyes* morphotype 1, *Stempellina*, and *Parakiefferiella* morphotype 2. The majority of these genera are eurytopic, occurring in regions that range from temperate to warm conditions (Wiederholm, 1983; Brooks et al., 2007). Many studies indicate that members of the Tanytarsini suffer more from acidification than other subfamilies of the Chironomidae (Wiederholm and Eriksson, 1977; Mossberg and Nyberg, 1979; Raddum and Sæther, 1981). However, in Rockhole Mine Creek, the majority of *Tanytarsus* species showed a preference for the acidified effluent entering the stream. In some sites in northern Europe, the relative numbers of Tanytarsini did not change to any great extent with respect to acidification and some typically oligotrophic species were actually favoured by low pH (Brodin, 1990; Brodin and Gransberg, 1993). In Tasmania, *Tanytarsus* morphotype 1 and *Stempellina* are both indicators of acidic conditions, while *Tanytarsus* nr. *chinyensis* is a preferential.

Insects with a tolerance of low pH can increase in abundance in acidified lakes because of reduced fish predation. Secondary consumers, such as odonate, chaoborid, and tanypod larvae, become top predators (Eriksson et al., 1980; Mossberg and Nyberg, 1979; Økland and Økland, 1986; Appelberg et al., 1993). Although there are no data on fish populations in our survey, *Chaoborus* is a preferential with respect to acidic conditions, possibly indicating reduced fish predation.

The Tanytarsini indicative of lakes east of Tyler's Line are typically associated with warm, productive lakes, while *Parakiefferiella* and *Larsia* are common in locations

ranging from temperate to cool conditions. *Cricotopus* is eurytopic and usually associated with macrophytes or algae (Wiederholm, 1983; Brooks et al., 2007). Both *Paramerina* and *Procladius* are eurythermic and prefer the substrata of standing or slowly flowing waterbodies (Wiederholm, 1983). Here, *Tanytarsus* and *Cladotanytarsus* were indicators of circumneutral pH, but both genera contain morphotypes that can tolerate acidic conditions (Brooks et al., 2007). It is important to recognize that many chironomid genera are speciose and that species within the same genus may have markedly different responses to pH (Armitage and Blackburn, 1985; St. Louis, 1993; de Bisthoven et al., 2005). In our data set, both *Tanytarsus* and *Parakiefferiella* possess morphotypes indicative of acidic and circumneutral conditions.

Drivers of pH change in Tasmania

Because Tasmania receives minimal atmospheric pollution and has a variety of lakes that range in pH from acidic to circumneutral, it is an ideal region to study the effects of acidity on chironomid communities. Our results indicate that chironomids are ideal candidates for lake classification schemes and that, in Tasmania, chironomids integrate information across different spatial scales. We have shown, through three independent methods (geography, PLR analysis, TWINSPAN), that chironomid distributions accurately respond to Tyler's Line, a boundary that reflects geological, climatic, vegetational, and chemical changes over a relatively short distance.

Lakes east of Tyler's Line are circumneutral and associated with intrusions of dolerite, an igneous rock that weathers relatively quickly, releasing magnesium, sodium, and calcium. Consequently, the catchment areas of these lakes have a strong buffering

capacity, as reflected in the pH of the lake water. The comparatively rich soils and reduced precipitation support dry *Eucalyptus* forests and woodlands. On the other hand, lakes in western Tasmania are situated on shallow soils atop basement rock that is slow to weather. Precipitation is comparatively higher than in the east and the surrounding vegetation, broadly speaking, consists of moorland and rainforest. Consequently, surface run-off is rich in humic acids, derived from leaf litter, and enters western lakes unbuffered. All of these factors are reflected by the ordinations, PLR analysis, and TWINSPAN of the chironomid species data.

Model development and the "Paleo approach"

This survey of chironomid taxa provides a baseline for relatively undisturbed, pristine, Tasmanian lakes and taxon inventories described here and elsewhere (Rees et al., 2008) could be compared to those collected from polluted sites. Unfortunately, because our methods use the head capsule alone to identify specimens, taxonomic resolution is limited to either genus or species morphotype levels. Nevertheless, there are advantages to the approach of analyzing subfossil chironomids from surface sediment (a paleo approach). Since sediment samples from the centre of a lake are typically representative of the whole chironomid community, sampling strategies are straightforward and cost effective. Further, because chironomid head capsules preserve in lake sediments, it is possible to reconstruct pH estimates from fossil communities using inference models.

Ours are among the few models developed to estimate pH from chironomid remains (see Ruse and Brooks, 2010). These inference models could be used

quantitatively to estimate changes in pH over a variety of temporal and spatial scales in south-eastern Australia. For example, the evolution of Tyler's Line may be determined by analyzing the long-term records from several sites on either side of the line. Has Tyler's Line evolved since the end of the last Ice Age or is it a consistent feature of the landscape throughout a glacial/interglacial cycle? Results could be used to help understand the natural variability of pH in Tasmanian lakes. In terms of environmental monitoring, these models could be used to extend the historical record of recently impacted lakes to test hypotheses about the cause, timing, and magnitude of contamination.

Acknowledgments

We thank Rob Wiltshire and Marian McGowen for hosting us during our field work, Greg Jordan for input into site selection, the Department of Primary Industries, Water and Environment (DPIWE) for permission to sample, TASMAP© for providing map data, Einar Heegaard for statistical advice, Dr. Robert Mesibov for reading an earlier draft, Peter Cranston, whose review improved the quality of our work, and the comments of an anonymous reviewer. This project was funded by a Natural Sciences and Engineering Research Council (NSERC) grant to L.C. Cwynar and a NSERC postgraduate scholarship to A.B.H. Rees.

References

Appelberg, M., Henrikson, B.-I., Henrikson, L., Svedäng, M., 1993. Biotic interactions within the littoral community of Swedish forest lakes during acidification. Ambios 5, 290-297.

Armitage, P.D., Blackburn, J.H., 1985. Chironomidae in Pennine stream system receiving drainage and organic enrichment. Hydrobiologia 121, 165-172.

Armitage, P., Cranston, P.S., Pinder, L.C.V., 1995. The Chironomidae: The Biology and Ecology of Non-Biting Midges. Chapman and Hall, London.

Bell, H.L., 1970. Effects of pH on the life cycle of the midge *Tanytarsus dissimilis*. Canadian Entomologist 102, 636-639.

Birks, H.J.B., 1998. Numerical tools in paleolimnology - Progress, potentialities, and problems. Journal of Paleolimnology 20, 307-332.

Birks, H.J.B., Line, J.M., 1992. The use of rarefaction analysis for estimating palynological richness from Quaternary pollen-analytical data. Holocene 2, 1-10.

Bitušík, P., Svitok, M., Kološta, P., Hubková, M., 2006. Classification of the Tatra Mountain lakes (Slovakia) using chironomids (Diptera, Chironomidae). Biologia 61 (Supplement 18), 191-201.

Blom, W.M., 1988. Late Quaternary sediments and sea-levels in Bass basin, southeastern Australia - a preliminary report. Search 19, 94-96.

Brodin, Y.-W., 1990. Midge fauna development in acidified lakes in northern Europe. Philosophical Transactions of the Royal Society of London 327, 295-298.

Brodin, Y.-W., Gransberg, M., 1993. Responses of insects, especially Chironomidae (Diptera), and mites to 130 years of acidification in a Scottish lake. Hydrobiologia 250, 201-212.

Brooks, S.J., Langdon, P.G., Heiri, O., 2007. Using and Identifying Chironomid Larvae in Palaeoecology. QRA Technical Guide no. 10. Quaternary Research Association, London, UK.

Cranston, P.S., 2000. Electronic guide to the Chironomidae of Australia. URL http://www.science.uts.edu.au/sasb/chiropage/.

Cranston, P.S., Cooper, P.D., Hardwick, R.A., Humphrey, C.L., Dostine, P.L., 1997. Tropical acid streams - the chironomid (Diptera) response in northern Australia. Freshwater Biology 37, 473-483.

de Bisthoven, L.J., Gerhardt, A., Soares, A.M.V.M., 2005. Chironomidae larvae as bioindicators of an acid mine drainage in Portugal. Hydrobiologia 532, 181-191.

Dean Jr., W.E., 1974. Determination of carbonate and organic matter in calcareous sediments and sedimentary rocks by loss on ignition: comparison with other methods. Journal of Sedimentary Petrology 44, 242-248.

Eriksson, M.O.G., Henrikson, L., Nilsson, B.-I., Nyman, G., Oscarson, H.G., Stenson, A.E., 1980. Predator-prey relations important for the biotic changes in acidified lakes. Ambios 9, 248-249.

Faith, D.P., Humphrey, C.L., Dostine, P.L., 1991. Statistical power and BACI design in biological monitoring: comparative evaluation of measures of community dissimilarity based on benthic macroinvertebrate communities in Rockhole Mine Creek, Northern Territory, Australia. Australian Journal of Marine and Freshwater Research 42, 589-602.

Gauch, H.G., Whittaker, R.H., 1981. Hierarchical classification of community data. Journal of Ecology 69, 537-557.

Gibbs, R.J., 1970. Mechanisms controlling world water chemistry. Science 170, 1088-1090.

Glew, J., 1991. Miniature gravity corer for recovering short sediment cores. Journal of Paleolimnology 5, 285-287.

Havas, M., 1981. Physiological response of aquatic animals to low pH. In: Singer, R. (Ed.), Effects of Acid Precipitation on Benthos: Proceedings of a Symposium. Colgate University, Hamilton, NY, pp. 49-65.

Heegaard, E., Lotter, A.F., Birks, H.J.B., 2006. Aquatic biota and the detection of climate change: are there consistent aquatic ecotones? Journal of Paleolimnology 35, 507-518.

Heiri, O., 2004. Within-lake variability of subfossil chironomid assemblages in shallow Norwegian lakes. Journal of Paleolimnology 32, 67-84.

Henrikson, L., Olofsson, J.B., Oscarson, H.G., 1982. The impact of acidification on Chironomidae (Diptera) as indicated by subfossil stratification. Hydrobiologia 86, 223-229.

Hill, M.O., Šmilauer, P., 2005. TWINSPAN for Windows Version 2.3. Hydrology & University of South Bohemia, Huntingdon & České Budějovice.

Houlder, D., Hutchinson, M., Nix, H.A., McMahon, J., 2003. ANUCLIM User's Guide. Centre for Resource and Environmental Studies, Australian National University, Canberra, Australia.

Iovino, A.J., 1975. Extant chironomid larval populations and the representativeness and nature of their remains in Lake Sediments. PhD Thesis, Indiana University.

Jackson, W.D., 2005. The Tasmanian environment. In: Reid, J.B., Hill, R.S., Brown, M.J., Hovenden, M.J. (Eds.), Vegetation of Tasmania. Australian Biological Resources Study, Tasmania, Australia, pp. 11-34.

Juggins, S., 2007. C2 Version 1.5 User Guide. Software for Ecological and Palaeoecological Data Analysis and Visualisation. Newcastle University, Newcastle upon Tyne, UK.

Kim, N., Han, J.K., 1997. Assessing the integrity of cross-validation: a case for small sample-based research. Department of Marketing, Hong Kong University of Science and Technology, Hong Kong, Working Paper Series no. MKTG 97.096.

Leuven, R.S.E.W., van der Velden, J.A., Vanhemelrijk, J.A.M., van der Velde, G., 1987. Impact of acidification on chironomid communities in poorly buffered waters in the Netherlands. Entomologica Scandinavica Supplement 29, 269-280.

Mackay, R.J., Kersey, K.E., 1985. A preliminary study of aquatic insect communities and leaf decomposition in acid streams near Dorset, Ontario. Hydrobiologia 122, 3-11.

Marziali, L., Armanini, D.G., Cazzola, M., Erba, S., Toppi, E., Buffagni, A., Rossaro, B., 2010. Responses of chironomid larvae (Insecta, Diptera) to ecological quality in Mediterranean river mesohabitats (South Italy). River Research and Application 26, 1036-1051.

McCune, B., Grace, J.B., 2002. Analysis of Ecological Communities. MjM Software Design, Oregon.

Mesibov, R., 1994. Faunal breaks in Tasmania and their significance for invertebrate conservation. Memoirs of the Queensland Museum 36, 133-136.

Mossberg, P., 1979. Benthos of oligotrophic and acid lakes. Information from the Institute of Freshwater Research, Drottningholm 11, 1-40.

Mossberg, P., Nyberg, P., 1979. Bottom fauna of small acid forest lakes. Report - Institute of Freshwater Research, Drottningholm 58, 77-87.

Nyman, M.T., Korhola, A., 2005. Chironomid-based classification of lakes in western Finnish Lapland. Boreal Environment Research 10, 239-254.

Økland, J., Økland, K.A., 1986. The effects of acid deposition on benthic animals in lakes and streams. Experimentia 42, 471-486.

Oliver, D.R., Roussel, M.E., 1983. The Insects and Arachnids of Canada, Part 11: The Genera of Larval Midges of Canada, Diptera: Chironomidae. Research Branch, Agriculture Canada, Ottawa.

Overpeck, J.T., Webb, T., Prentice, I.C., 1985. Quantitative interpretation of fossil pollen spectra-dissimilarity coefficients and the method of modern analogs. Quaternary Research 23, 87-108.

R Development Core Team, 2009. R: A Language and Environment for Statistical Computing. R Foundation for Statistical Computing, Vienna, Austria. ISBN 3-900051- 07-0, URL http://www.R-project.org.

Raddum, G.R., Sæther, O.A., 1981. Chironomid communities in Norwegian lakes with different degrees of acidification. Verhandlungen Der Internationalen Vereinigung Für Theoretische Und Angewandte Limnologie 21, 399-405.

Rees, A.B.H., Cwynar, L.C., Cranston, P.S., 2008. Midges (Chironomidae, Ceratopogonidae, Chaoboridae) as a temperature proxy: a training set from Tasmania, Australia. Journal of Paleolimnology 40, 1159-1178.

Rosenberg, D.M., 1992. Freshwater biomonitoring and Chironomidae. Netherlands Journal of Aquatic Ecology 26, 101-122.

Ruse, L.P., Brooks, S.J., 2010. Lake reference state deduced from chironomid pupal skin data. In: Ferrington, L.C.J. (Ed.), Proceedings of the XV International Symposium

on Chironomidae. Chironomidae Research Group, Saint Paul, Minnesota, pp. 140-155.

Sæther, O.A., 1979. Chironomid communities as water quality indicators. Holarctic Ecology 2, 65-74.

Schindler, D.W., Turner, M.A., 1989. Biological, chemical and physiological responses of lakes to experimental acidification. Water, Air, and Soil Pollution 18, 259-271.

Shiel, R.J., Koste, W., Tan, L.W., 1989. Tasmania revisited: rotifer communities and habitat heterogeneity. Hydrobiologia 186/187, 239-245.

Smith, M., Cranston, P.S., 1995. "Recovery" of an acid mine-waste impacted tropical stream - the chironomid story. In: Cranston, P.S. (Ed.), Chironomids: From Genes to Ecosystems. CSIRO, Melbourne, pp. 161-173.

St. Louis, V.L., 1993. Element concentrations in chironomids and their abundance in the littoral zone of acidified lakes in Northwestern Ontario. Canadian Journal of Fisheries and Aquatic Sciences 50, 953-963.

ter Braak, C.J.F., Šmilauer, P., 2002. CANOCO Version 4.5. Biometris-Plant Research International, Wageningen.

Thienemann, A., 1922. Die beiden Chironomus-arten der Thiefenfauna der norddeutschen Seen. Ein Hydrobiologisches Problem. Archiv Für Hydrobiologie 13, 609-646.

Tyler, P.A., 1992. A lakeland from the dreamtime: the second founder's lecture. British Phycological Journal 27, 353-368.

Vyverman, W., Vyverman, R., Rajendran, V.S., Tyler, P., 1996. Distribution of benthic diatom assemblages in Tasmanian highland lakes and their possible use as

indicators of environmental changes. Canadian Journal of Fisheries and Aquatic Sciences 53, 493-508.

Wahl, E.R., 2004. A general framework for determining cut-off values to select pollen analogs with dissimilarity metrics in the modern analog technique. Review of Palaeobotany and Palynology 128, 263-280.

Walker, I.R., Fernando, C.H., Paterson, C.G., 1984. The chironomid fauna of four shallow, humic lakes and their representation by subfossil assemblages in the surficial sediments. Hydrobiologia 112, 61-67.

Walker, I.R., Smol, J.P., Engstrom, D.R., Birks, H.J.B., 1991. An assessment of Chironomidae as quantitative indicators of past climatic change. Canadian Journal of Fisheries and Aquatic Sciences 48, 975-987.

Wetzel, R.G., 2001. Limnology. Academic Press, London, UK.

Wiederholm, T., 1983. Chironomidae of the Holarctic Region. Keys and Diagnoses. Part 1. Larvae. Entomologica Scandinavica Supplement 19.

Wiederholm, T., Eriksson, L., 1977. Benthos of an acidic lake. Oikos 29, 261-267.

Zar, J.H., 1999. Biostatistical Analysis. Prentice Hall, Upper Saddle River, New Jersey.

Zeileis, A., Kleiber, C., Kraemer, W., Hornik, K., 2003. Testing and dating of structural changes in practice. Computational Statistics & Data Analysis 44, 109-123.

Figure 3.1: Map of Tasmania, Australia, with the 48 lakes retained in this study. Solid, dotted, and dashed lines demark the approximate congruence of climatic, geological, and vegetational change aslant the 146th meridian, while diamonds, squares, and circles represent coastal lakes, lakes west of Tyler's Line, and lakes east of Tyler's Line, respectively. Due to the rain-shadow effect in eastern Tasmania, the majority of eastern lakes lay near Tyler's Line. Map data provided by TASMAP©, State of Tasmania.

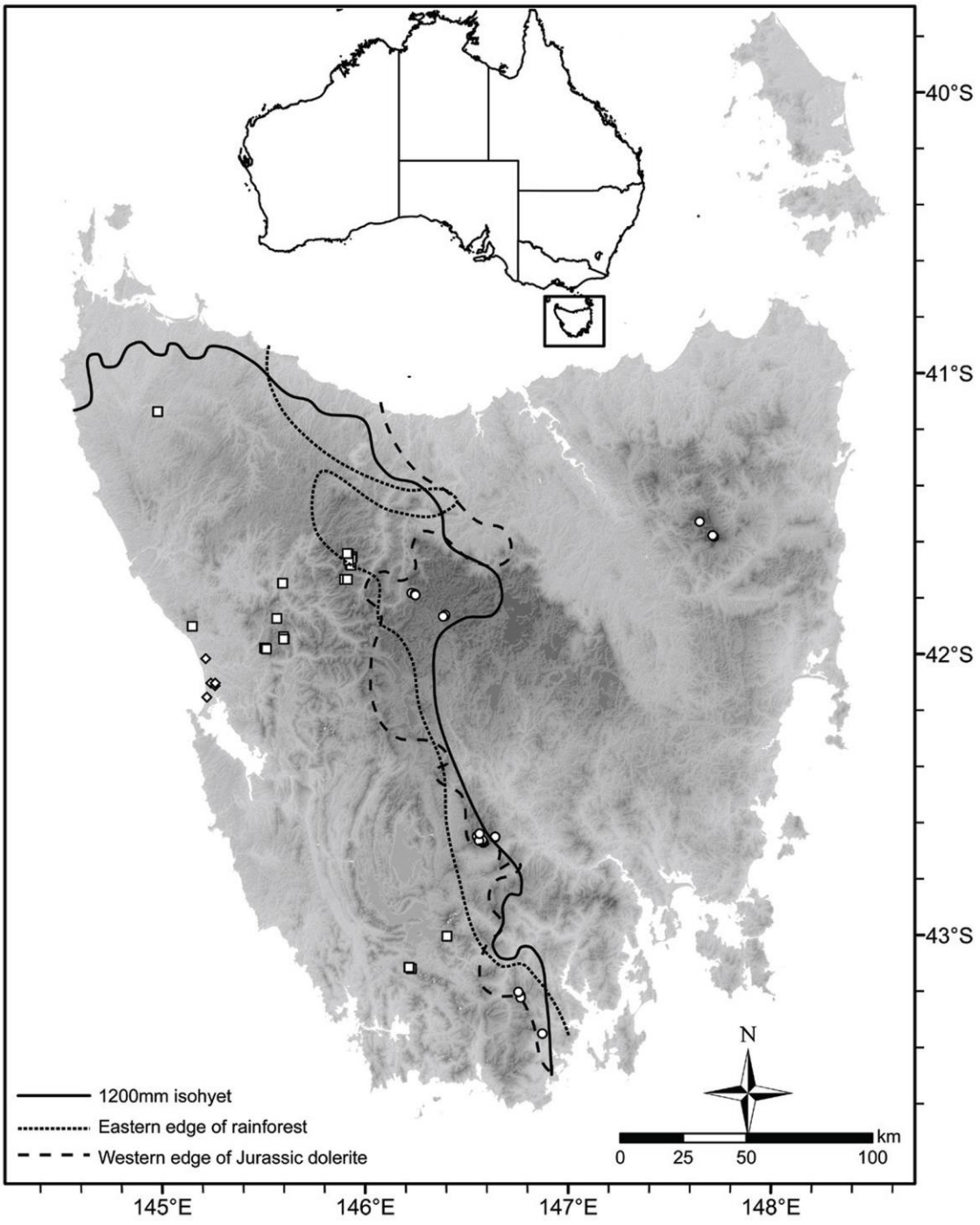

Figure 3.1: Map of Tasmania, Australia with features denoting Tyler's Line.

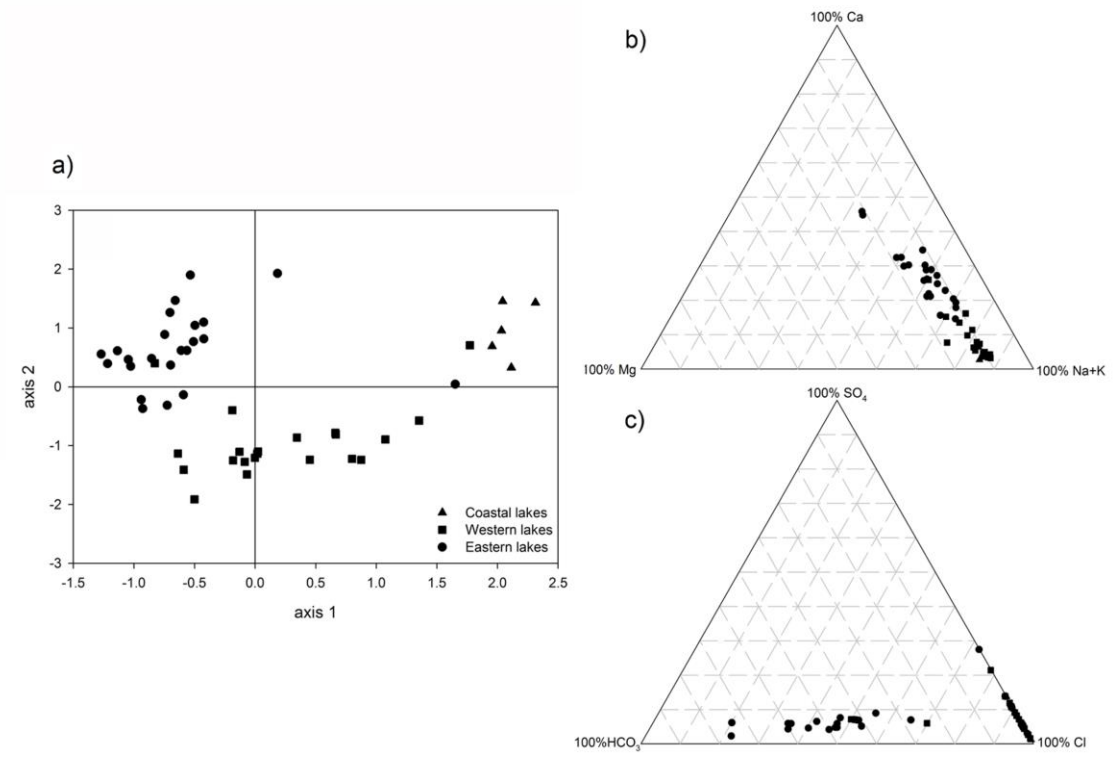

Figure 3.2: Summary of lake categories based on environmental variables.

a) Principal components analysis of the environmental variables reflecting the three lake districts of Tasmania. Ternary plots of b) major cations and c) anions indicate that western lakes are similar to coastal lakes in terms of ionic complexion.

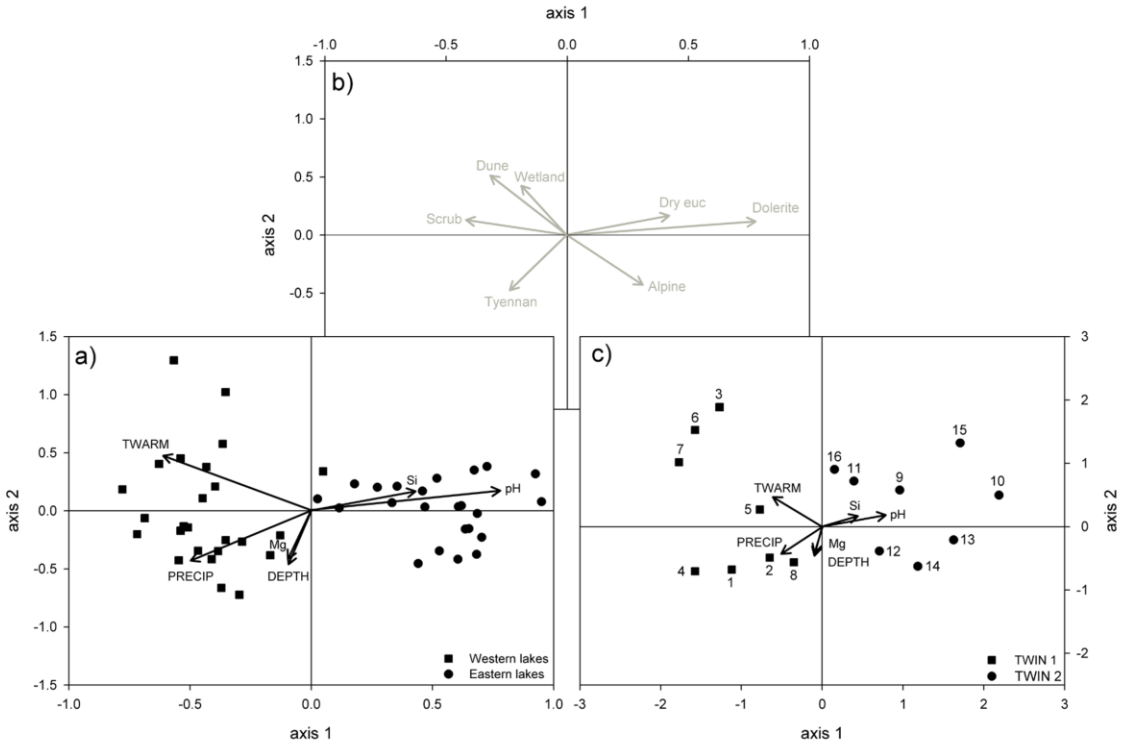

Figure 3.3: Canonical correspondence analyses (CCAs) of the 48 Tasmanian lakes with the six significant environmental variables.

a) Sample scores and c) species scores. Only indicator and preferential taxa identified by TWINSPAN are included in the biplot of species scores: numbers correspond to the taxon inventory in Table 3.4. b) Catchment geology and vegetation were included in the ordinations passively. Only variables with an interset correlation greater than 0.4 for either axis 1 or 2 of the CCA are shown.

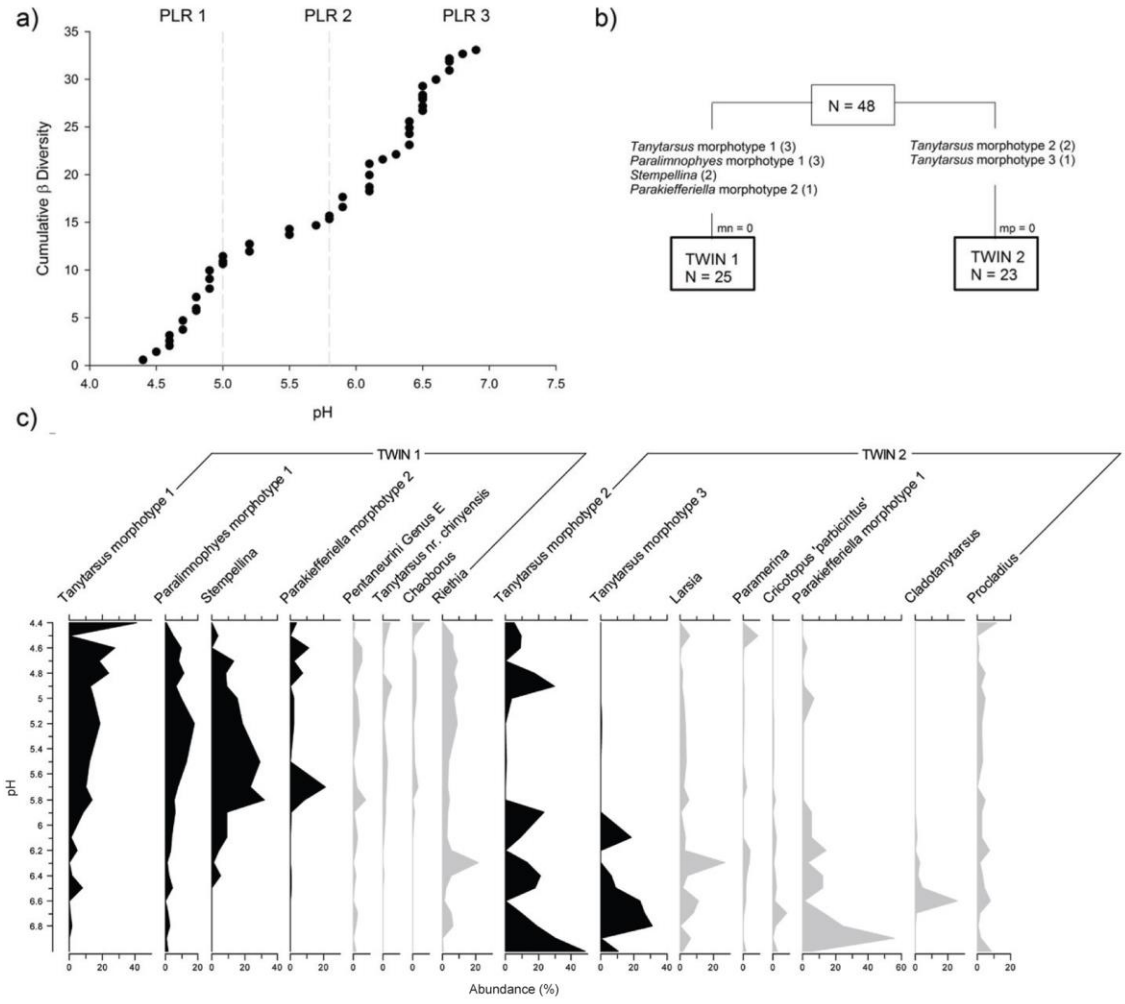

Figure 3.4: Summary of PLR and TWINSPAN groupings.

a) Breakpoints identified by piecewise linear regression analysis and b) the classification of 48 Tasmanian lakes using TWINSPAN. In the TWINSPAN dendrogram, the indicator species relative abundance levels are expressed on an ordinal scale in parentheses (1 = 2-4.9%; 2 = 5-6.9%; 3 = 7-11.9%). There were no misclassified negatives (mn) or misclassified positives (mp). c) A chironomid percent diagram of the indicator (black) and preferential (grey) taxa identified by TWINSPAN reflects shifts in major taxa along the pH gradient.

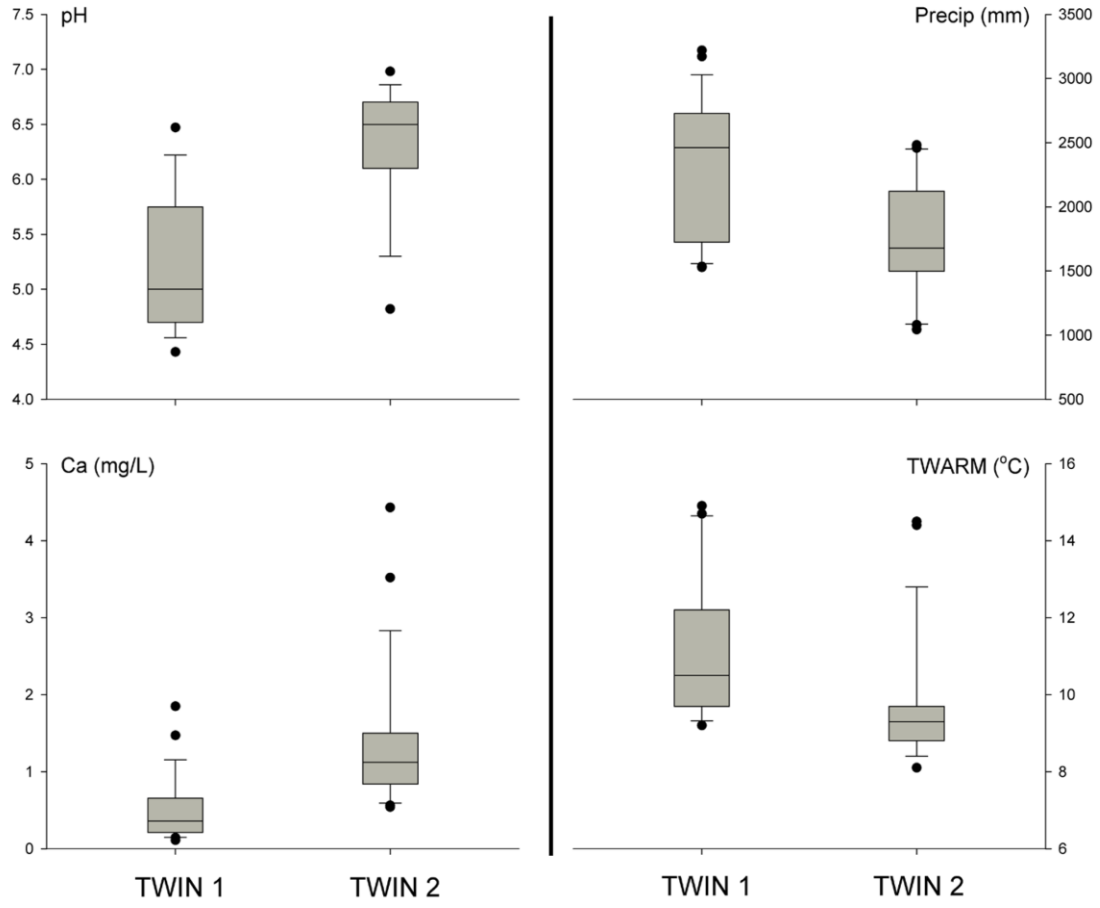

Figure 3.5: Summary box-plot diagram of major environmental variables.

These variables discriminate between lakes classified by TWINSPAN. Box lengths represent the interquartile range, while the solid line through the box represents the median. Dots represent sites below and above the 5th and 95th percentiles.

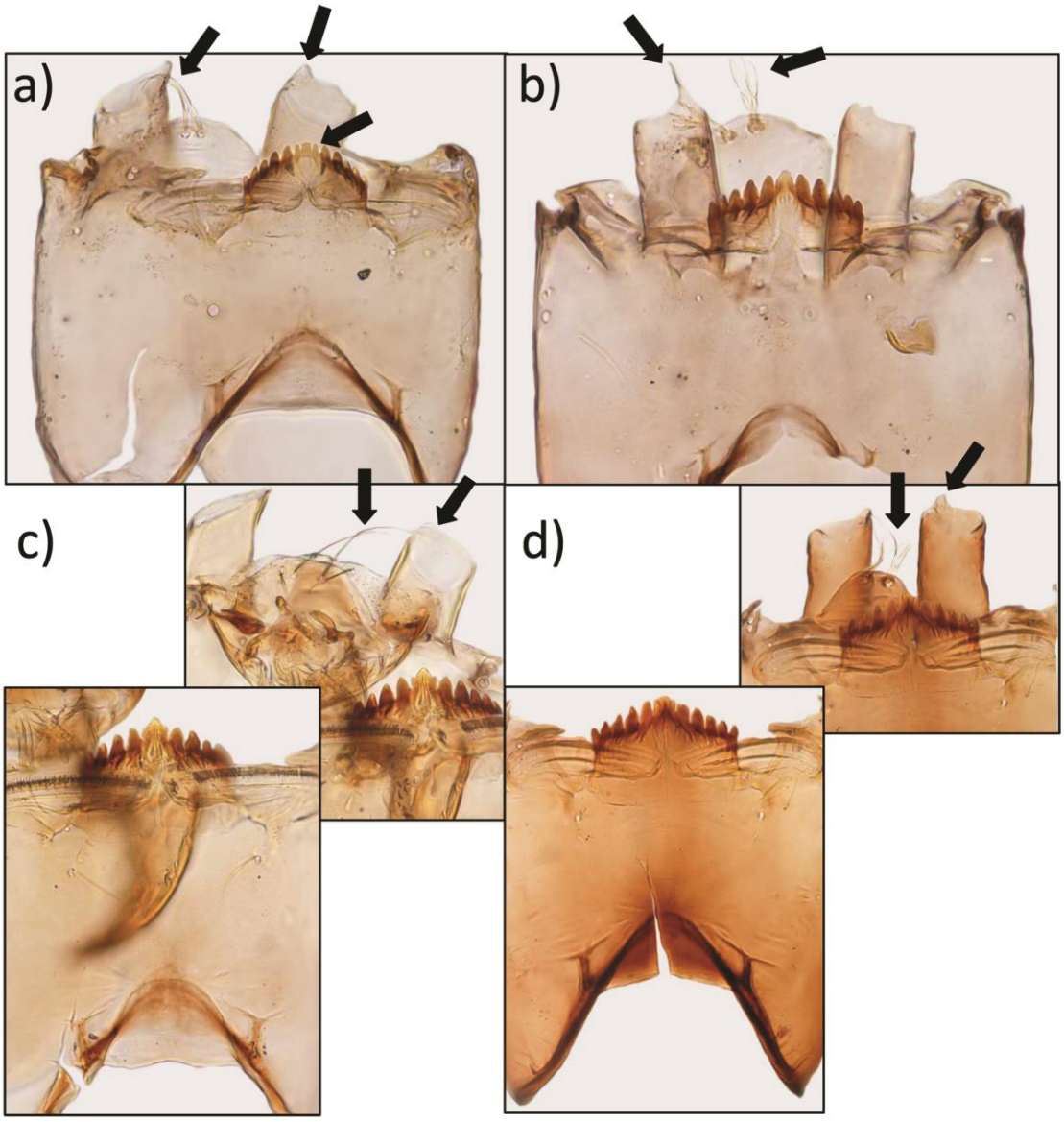

Figure 3.6: Images of *Tanytarsus* morphotypes.

a) *Tanytarsus* morphotype 1, b) *Tanytarsus* nr. *chinyensis*, c) *Tanytarsus* morphotype 2, and d) *Tanytarsus* morphotype 3. Black arrows highlight features mentioned in the text.

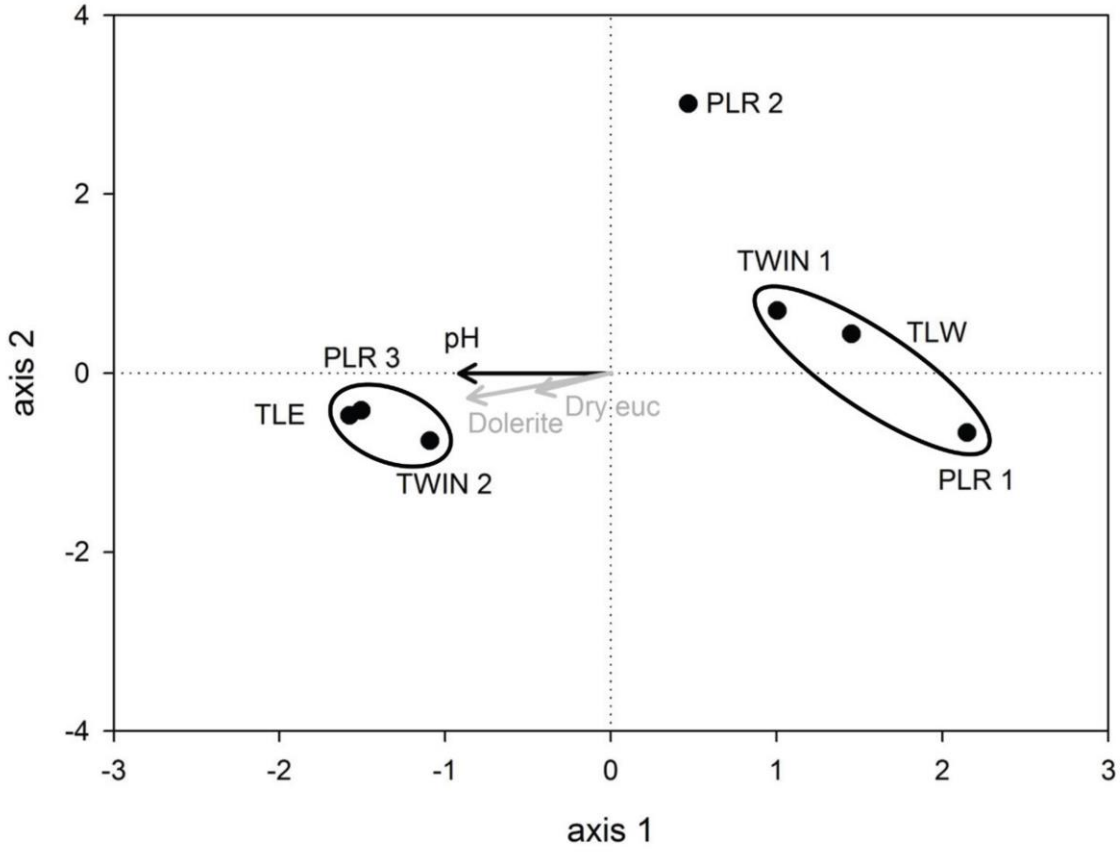

Figure 3.7: Canonical variates analysis (CVA) summarizing the relationship between three independent classification schemes.

The classification of Tasmanian lakes includes: geographical position, piecewise linear regression (PLR) analysis, and TWINSPAN. Lakes geographically west of the 146th meridian (TLW) plot out with TWIN 1 and PLR 1, while lakes geographically east of the 146th meridian (TLE) are associated with TWIN 2 and PLR 3. A transitional group of lakes ranging in pH between 5.1 and 5.8 is not accurately reflected by further TWINSPAN divisions.

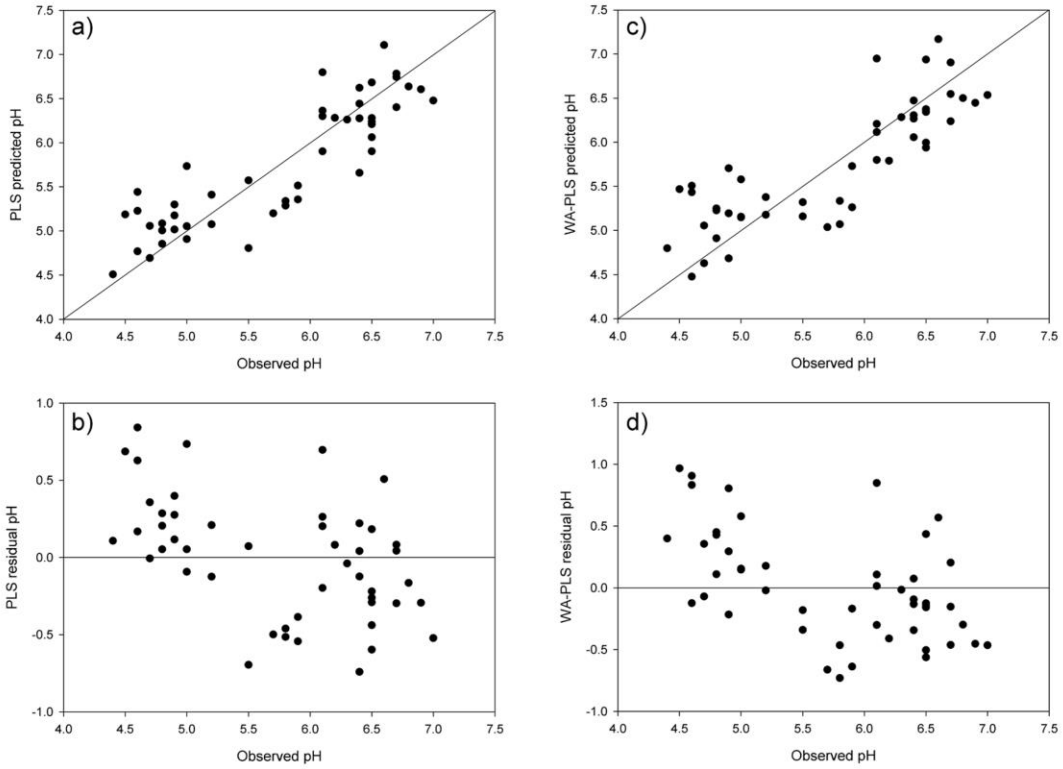

Figure 3.8: Model performance.

Performance of the second component partial least squares (a, b) and first component weighted averaging partial least squares (c, d) models where a) and c) illustrate predicted pH versus observed pH and b) and d) illustrate the residuals of predicted pH versus observed pH.

Table 3.1: Summary statistics of environmental variables for our 54 study lakes in Tasmania.

	West of Tyler's Line (n=24)				East of Tyler's Line (n=24)				Geological Descriptions
	Min	Max	Mean	Median	Min	Max	Mean	Median	
LONG (°E)	145.1	146.4	145.7	145.6	146.3	147.7	146.7	146.6	
LAT (°S)	-43.1	-41.1	-42	-41.9	-43.2	-41.5	-42.3	-42.7	
ELEV (m a.s.l.)	9.4	1123	642	764.7	919.5	1451	1128.6	1184	
LOI (%)	5	56.6	30.6	34.5	14.9	44.2	30.5	29.4	
DEPTH (m)	0.1	35.2	5.6	2.8	0.1	19.2	4.8	2.9	
PERIM (m)	240.7	5375	1199.1	877.1	98.2	1613.3	762.6	726.2	
AREA (ha)	0.3	22.8	5.7	3.3	0	10.5	2.8	2.6	
SHORE	1.1	3.2	1.6	1.5	1.1	2.4	1.4	1.3	
CATCH (ha)	0.4	496	100.5	28.2	0	786.1	60.6	17.7	
CATCH:LAKE	1	460.2	31.9	8.2	1	75	12.2	8.7	
TWARM (°C)	9.4	14.9	11.7	11	8.1	10	9.2	9.2	
PRECIP (mm)	1497	3219	2376.9	2463	1043	2458	1729.3	1678	
RAD (MJ m^{-2})	10.2	12.4	11	10.9	10.6	13	11.6	11.5	
pH	4.4	6.2	5.1	4.9	5.9	7	6.5	6.5	
Na (mg L^{-1})	2	46.1	9.1	4.2	1.7	3.5	2.3	2.2	
K (mg L^{-1})	0.2	1.7	0.4	0.3	0.1	0.3	0.2	0.2	
Ca (mg L^{-1})	0.1	1.9	0.6	0.4	0.5	4.4	1.3	1	
Mg (mg L^{-1})	0.3	7	1.3	0.5	0.3	2.1	0.7	0.6	
Fe (mg L^{-1})	0	1	0.3	0.2	0	0.4	0.1	0.1	
Mn (mg L^{-1})	0	0.1	0	0	0	0	0	0	
Cu (mg L^{-1})	0	0	0	0	0	0	0	0	
Zn (mg L^{-1})	0	0.1	0	0	0	0.1	0	0	
Dissolved TKN (mg L^{-1})	0.2	1.2	0.5	0.6	0.2	1	0.4	0.5	
Cl (mg L^{-1})	3.1	98	18.7	8.6	2.9	6.6	4.1	4	
SO_4 (mg L^{-1})	0.5	12.5	1.6	0.5	0.5	2.5	0.6	0.5	
Dissolved TP (mg L^{-1})	0	0	0	0	0	0	0	0	
SiO_2 (mg L^{-1})	0.1	6.1	1.3	0.6	0.2	7.4	2.3	2.1	
TOC (mg L^{-1})	3.6	36	9.6	7.5	1.5	6.7	3.2	3	
TURB (NTU)	0.5	2.8	1.1	0.9	0.1	10.2	1.1	0.5	
CON (µS cm^{-1})	17	347	69	32.7	15.8	53.7	23.8	20.9	
Agricu, Urban and Exotic Vegetation (%)	0	38.1	3	0	0	1.6	0.1	0	
Dry Eucalypt Forest and Woodland (%)	0	38.9	2.6	0	0	66.2	22.5	10.8	
Highland Treeless Vegetation (%)	0	68.2	9.1	0	0	100	26.9	16.1	
Moorland, Sedgeland, Rushland and Peatland (%)	0	73.1	16.4	0.5	0	10.1	0.9	0	
Native Grassland (%)	0	0	0	0	0	41.1	3.4	0	
Non-Eucalypt Forest and Woodland (%)	0	94.5	7.2	0	0	0	0	0	
Other Natural Environments (%)	0	99.4	21.6	12.8	0	86.7	20.3	7.9	
Rainforest and Related Scrub (%)	0	100	22.1	2.8	0	82.6	21.8	3.3	
Saltmarsh and Wetland (%)	0	3.3	0.2	0	0	0	0	0	
Scrub, Heathland and Coastal Vegetation (%)	0	78.9	12.2	0	0	16.5	0.9	0	
Wet Eucalypt Forest and Woodland (%)	0	85.5	5.7	0	0	26.3	3.3	0	
Togari Group and Correlates (%)	0	100	8	0	0	0	0	0	sedimentary carbonate, sedimentary siliclastic, igneous mafic extrusive
Heemskirk (red) Granite (%)	0	100	4	0	0	0	0	0	igneous felsic intrusive
Coastal Dunes (%)	0	100	19.7	0	0	0	0	0	regolith
Glacial Sediments (%)	0	100	17.3	0	0	12.7	0.6	0	regolith
Denison Group and Correlates (%)	0	100	8.3	0	0	0	0	0	sedimentary siliclastic
Felsic to Intermediate Volcanics (%)	0	100	11.3	0	0	0	0	0	igneous felsic-intermediate volcanic, sedimentary siliclastic
Tyennan Group and Correlates (%)	0	100	30.1	0	0	87.3	3.8	0	sedimentary siliclastic
Lower Parmeener Supergroup (%)	0	26.6	1.1	0	0	0	0	0	argillaceous detrital sediment, sedimentary siliclastic
Tasmanian Dolerite (%)	0	0	0	0	0	100	89.8	100	igneous mafic intrusive
Colluvium (%)	0	0	0	0	0	100	5.9	0	regolith
Rarefied Taxa	7	20	14	14	5	18	12	12	
Head capsule concentration (hc mL^{-1})	3.7	152	37	19.2	1.7	64.3	15.6	9.3	

Table 3.2: Partial CCAs of the seven significant environmental variables.

Environmental Variable	Covariable (s)	λ_1	λ_1/λ_2	P ($\leq$0.05)	% of Total Variance
pH	None	0.218	0.901	0.001	9.9
	TWARM	0.160	0.681	0.001	8.0
	TWARM, Mg	0.116	0.523	0.001	6.3
	TWARM, Mg, DEPTH	0.112	0.528	0.001	6.3
	TWARM, Mg, DEPTH, PRECIP	0.081	0.382	0.002	4.8
	TWARM, Mg, DEPTH, PRECIP, SiO_2	0.074	0.351	0.006	4.6
	TWARM, Mg, DEPTH, PRECIP, SiO_2, Zn	0.077	4.808	0.004	4.9
TWARM	None	0.188	0.633	0.001	8.5
	pH	0.130	0.553	0.001	6.6
	pH, Mg	0.135	0.608	0.001	7.2
	pH, Mg, DEPTH	0.134	0.632	0.001	7.4
	pH, Mg, DEPTH, PRECIP	0.138	0.651	0.001	7.9
	pH, Mg, DEPTH, PRECIP, SiO_2	0.136	0.645	0.001	8.1
	pH, Mg, DEPTH, PRECIP, SiO_2, Zn	0.137	0.659	0.001	8.5
Mg	None	0.105	0.312	0.005	4.8
	pH	0.104	0.432	0.001	5.2
	pH, TWARM	0.109	0.491	0.001	5.9
	pH, TWARM, DEPTH	0.110	0.519	0.001	6.2
	pH, TWARM, DEPTH, PRECIP	0.115	0.542	0.001	6.7
	pH, TWARM, DEPTH, PRECIP, SiO_2	0.078	0.370	0.004	4.8
	pH, TWARM, DEPTH, PRECIP, SiO_2, Zn	0.081	0.389	0.004	5.2
DEPTH	None	0.086	0.257	0.013	3.9
	pH	0.083	0.343	0.005	4.2
	pH, TWARM	0.078	0.336	0.010	4.2
	pH, TWARM, Mg	0.078	0.368	0.006	4.5
	pH, TWARM, Mg, PRECIP	0.073	0.344	0.008	4.4
	pH, TWARM, Mg, PRECIP, SiO_2	0.064	0.303	0.025	4.0
	pH, TWARM, Mg, PRECIP, SiO_2, Zn	0.063	0.303	0.020	4.1
PRECIP	None	0.141	0.496	0.001	6.4
	pH	0.074	0.306	0.018	3.7
	pH, TWARM	0.064	0.276	0.041	3.5
	pH, TWARM, Mg	0.068	0.311	0.017	3.9
	pH, TWARM, Mg, DEPTH	0.063	0.297	0.027	3.8
	pH, TWARM, Mg, DEPTH, SiO_2	0.063	0.299	0.025	3.9
	pH, TWARM, Mg, DEPTH, SiO_2, Zn	0.061	0.293	0.030	4.0
SiO_2	None	0.130	0.428	0.002	5.9
	pH	0.097	0.404	0.001	4.9
	pH, TWARM	0.102	0.443	0.001	5.5
	pH, TWARM, Mg	0.070	0.321	0.017	4.0
	pH, TWARM, Mg, DEPTH	0.060	0.284	0.042	3.6
	pH, TWARM, Mg, DEPTH, PRECIP	0.060	0.284	0.037	3.7
	pH, TWARM, Mg, DEPTH, PRECIP, Zn	0.066	0.317	0.017	4.3
Zn	None	0.048	0.142	**0.392**	2.2

pCCA runs were conducted with and without the effects of the remaining environmental variables partialled out. The eigenvalue of the first CCA axis (λ1), the ratio of the eigenvalues for axes 1 and 2 (λ1/λ2), the statistical significance (P), and the percentage of variance of the species data are shown. All of the variables, except Zn, retained their significance. The emboldened value indicates P > 0.05.

Table 3.3: CCA summary with canonical coefficients, their associated t-values, and interset correlations.

	Axis 1		Axis 2		Axis 3		Axis 4		
Eigenvalue	0.269		0.140		0.100		0.071		
sum of all eigenvalues									2.204
sum of all canonical eigenvalues									0.658
Cumulative percentage variance									
of species data	12.2		18.6		23.1		26.4		
of species-environment relation	40.9		62.3		77.4		88.3		
Regression/canonical coefficients									
pH	0.074		0.275		-0.204		-0.281		
TWARM	-0.425		0.413		-0.128		-0.297		
Mg	-0.192		0.093		-0.251		-0.313		
Depth	-0.041		-0.176		0.072		-0.030		
PRECIP	-0.144		-0.050		0.001		-0.178		
SiO_2	0.145		0.012		0.151		-0.196		
t-values of regression coefficients									
pH	1.136		3.859	*	-3.025	*	-4.442	*	
TWARM	-6.325	*	5.609	*	-1.822		-4.540	*	
Mg	-3.084	*	1.369		-3.882	*	-5.165	*	
Depth	-1.016		-3.991	*	1.708		-0.760		
PRECIP	-3.046	*	-0.957		0.027		-3.851	*	
SiO_2	2.885	*	0.221		2.885	*	-3.993	*	
Interset correlation									
pH	0.780		0.179		-0.201		-0.193		
TWARM	-0.609		0.468		0.369		0.011		
Mg	-0.098		-0.419		-0.616		-0.142		
Depth	-0.096		-0.466		0.227		-0.319		
PRECIP	-0.497		-0.431		0.129		-0.188		
SiO_2	0.428		0.165		0.561		-0.335		

Asterisks indicate statistically significant t-values.

Table 3.4: Indicator and preferential taxa identified by TWINSPAN.

	Name	Occurrence (% of lakes)	Hill's N2	Max (%)	Mean (%)	Median (%)	PLS β coefficient	WA-PLS β coefficient
1	*Tanytarsus* type 1 Unofficial morphotype	58.3	18.3	41.2	10.4	3.5	-0.0984	4.3
2	*Paralimnophyes* type 1 Unofficial morphotype	81.3	21.5	27.4	6.1	3.0	-0.0369	5.0
3	*Stempellina* Thienemann & Bause	52.1	12.0	57.8	8.2	0.5	-0.0253	4.9
4	*Parakiefferiella* type 2 Unofficial morphotype	29.2	5.7	33.5	2.4	0.0	-0.0099	4.2
5	Pentaneurini Genus E	50.0	14.4	12.5	2.0	0.4	-0.0067	5.2
6	*Tanytarsus* nr. *chinyensis*	31.3	7.0	15.1	1.0	0.0	-0.0295	4.3
7	*Chaoborus* Unofficial morphotype	29.2	8.4	7.0	0.8	0.0	-0.0569	3.5
8	*Riethia* Kieffer	85.4	22.1	21.6	5.2	3.6	-0.0283	5.3
9	*Tanytarsus* type 2 Unofficial morphotype	50.0	14.5	81.1	12.8	0.8	-0.0202	6.4
10	*Tanytarsus* type 3 Unofficial morphotype	25.0	6.0	74.6	6.2	0.0	0.0898	8.2
11	*Larsia* Fittkau	70.8	16.1	26.7	3.4	1.9	0.0339	6.4
12	*Paramerina* Fittkau	39.6	11.0	8.8	1.0	0.0	0.0019	6.3
13	*Cricotopus* 'parbicintus'	47.9	9.8	13.3	1.4	0.0	0.0604	7.6
14	*Parakiefferiella* type 1 Unofficial morphotype	62.5	11.3	55.5	6.9	0.7	0.1267	7.2
15	*Cladotanytarsus* Kieffer	18.8	4.4	25.7	1.4	0.0	0.0528	8.0
16	*Procladius* Skuse	75.0	24.2	13.0	3.3	2.3	0.0176	6.0

Numbers correspond with labels from Fig. 3.3c. Occurrence is a percentage of the 48 lakes included in this study, Hill's N2 is a diversity index, and the PLS and WA-PLS β coefficients are values used by inference models to reconstruct pH estimates from fossil chironomids. For a complete taxon inventory, see Rees et al. (2008).

Table 3.5: Partial CVAs with the significant environmental variables alone and with the effects of the remaining variables partialled out.

Environmental Variable	Covariable (s)	λ_1	λ_1/λ_2	P (≤0.05)	% of Total Variance
pH	None	0.672	1.552	0.001	50.4
	SO_4	0.647	1.716	0.001	52.0
	SO_4, Ca	0.265	0.815	0.001	33.3
	SO_4, Ca, TWARM	0.088	0.309	0.001	15.6
	SO_4, Ca, TWARM, SiO_2	0.092	0.362	0.001	17.4
	SO_4, Ca, TWARM, SiO_2, PRECIP	0.097	0.451	0.001	19.8
	SO_4, Ca, TWARM, SiO_2, PRECIP, Mg	0.081	0.438	0.001	18.3
SO_4	None	0.088	0.112	0.021	6.6
	pH	0.063	0.167	0.029	9.6
	pH, Ca	0.101	0.311	0.007	16.0
	pH, Ca, TWARM	0.042	0.147	0.043	8.1
	pH, Ca, TWARM, SiO_2	0.025	0.098	**0.093**	5.5
Ca	None	0.355	0.671	0.001	26.6
	pH	0.030	0.070	**0.116**	4.5
TWARM	None	0.335	0.638	0.001	25.1
	pH	0.041	0.101	**0.053**	6.2
SiO_2	None	0.134	0.185	0.005	10.1
	pH	0.051	0.129	0.031	7.7
	pH, SO_4	0.061	0.188	0.010	10.2
	pH, SO4, Ca	0.021	0.068	**0.172**	4.0
PRECIP	None	0.257	0.439	0.001	19.3
	pH	0.026	0.063	**0.158**	3.9
Mg	None	0.019	0.023	**0.512**	1.5

The eigenvalue of the first CVA axis (λ1), the ratio of the eigenvalues for axes 1 and 2 (λ1/λ2), the statistical significance (P), and the percentage of variance of the species data are shown. Only pH retained its significance. Emboldened values indicate P > 0.05.

Table 3.6: CVA summary with canonical coefficient, the associated t-value, and interset correlation.

	Axis 1		Axis 2	Axis 3	Axis 4	
Eigenvalue	0.672		0.433	0.149	0.056	
sum of all eigenvalues						1.333
sum of all canonical eigenvalues						0.672
Cumulative percentage variance						
of species data	50.4		82.9	94.1	98.2	
of species-environment relation	100.0		0	0	0	
Regression/canonical coefficients						
pH	-1.745		0	0	0	
t-values of regression coefficients						
pH	-15.657	*	0	0	0	
Interset correlation						
pH	-0.918		0	0	0	

Asterisks indicate statistically significant t-values.

Table 3.7: PLS and WA-PLS models for reconstructing pH.

Model		Apparent				Jack-knifed				Reduction (%)
		r^2	Ave Bias	Max Bias	RMSE	r^2	Ave Bias	Max Bias	RMSEP	
PLS	Component 1	0.63	-1.18×10^{-15}	0.71	0.48	0.53	4.11×10^{-03}	0.84	0.55	
	Component 2	**0.76**	**-1.15×10^{-15}**	**0.49**	**0.39**	**0.60**	**8.91×10^{-04}**	**0.72**	**0.51**	**7.5**
	Component 3	0.82	-1.13×10^{-15}	0.38	0.33	0.58	-8.00×10^{-03}	0.71	0.52	-3.2
	Component 4	0.87	-1.15×10^{-15}	0.25	0.29	0.55	-2.59×10^{-03}	0.65	0.55	-4.6
	Component 5	0.91	-1.15×10^{-15}	0.24	0.24	0.54	7.62×10^{-03}	0.63	0.56	-3.3
WA-PLS	**Component 1**	**0.70**	**-1.26×10^{-2}**	**0.60**	**0.44**	**0.60**	**-1.43×10^{-02}**	**0.74**	**0.51**	
	Component 2	0.81	-4.80×10^{-4}	0.48	0.34	0.58	-1.07×10^{-02}	0.73	0.52	-3.0
	Component 3	0.86	-1.60×10^{-2}	0.25	0.30	0.53	-3.02×10^{-02}	0.69	0.57	-8.1
	Component 4	0.89	-8.30×10^{-3}	0.23	0.27	0.48	-4.07×10^{-02}	0.72	0.61	-8.6
	Component 5	0.91	-8.79×10^{-3}	0.26	0.23	0.44	-4.75×10^{-02}	0.80	0.66	-7.3

Apparent models were evaluated with leave-one-out, cross-validation (i.e., jack-knifing). Criteria for the best models were a low r^2_{jack}, $AveBias_{jack}$, $MaxBias_{jack}$, and the fewest components to reduce the RMSEP by at least 5%. Emboldened rows indicate models of choice.

Chapter 4 Evidence for early postglacial warming in Mount Field National Park, Tasmania

Citation for published manuscript: Rees, A.B.H., Cwynar, L.C., 2010. Evidence for early postglacial warming in Mount Field National Park, Tasmania. Quaternary Science Reviews 29, 443-454.

Abstract

Situated between the Western Pacific Warm Pool to the north and Antarctica to the south, Tasmania is an ideal location to study both postglacial and Holocene paleoclimates. Few well-dated, quantitative temperature reconstructions exist for the region so that important questions about the occurrence and magnitude of events, such as the Antarctic Cold Reversal and Younger Dryas, in Tasmania remain unanswered. Here, we provide chironomid-based reconstructions of temperature of the warmest quarter (TWARM) for two small subalpine lakes: Eagle and Platypus Tarns, Mount Field National Park. Shortly after deglaciation, TWARM reached modern values by approximately 15 cal ka BP and remained high until 13 cal ka BP after which temperatures began to steadily cool, reaching a minimum by 11.1-10 cal ka BP. These results are consistent with sea surface temperature (SST) reconstructions and cosmogenic dates from south of Tasmania, but are in stark contrast to temperature inferences drawn from vegetation reconstructions based on pollen data that indicate cool initial temperatures followed by a broad warm period between 11.6-6.8 cal ka BP (10-6 ^{14}C ka BP). The chironomid record broadly matches the summer insolation curve whereas the vegetation record and associated climate inferences mirror winter insolation. The Antarctic Cold Reversal and Younger Dryas cold events are not evident in the chironomid-inferred temperatures, but the Antarctic Cold Reversal is evident in the loss-on-ignition curves.

Keywords: Midges, Tasmania, Paleoclimate, Antarctic Cold Reversal, Insolation, Late Pleistocene, Holocene

Introduction

The late Pleistocene/early Holocene transition marked a switch between two drastically different modes of climate and the consequent rearrangement of major biomes. During the Last Glacial Maximum (LGM) in Tasmania, annual temperatures were 8°C cooler than modern, assuming a 50% reduction in precipitation (Galloway, 1986); ice covered roughly 1,000 km^2 of the island (Colhoun and Shulmeister, 2006); and the Australasian continental shelf was exposed, creating a temporary land bridge that connected Tasmania to mainland Australia, providing an opportunity for floral and faunal exchange.

The late Pleistocene/early Holocene transition was a period characterized by abrupt and extreme climate change. Traditionally, the stratigraphy of events during the transition from glacial to interglacial modes of climate from the Greenland Ice Core Project (GRIP) has been considered a good template of climate change, providing a helpful model for both testing hypotheses and interpreting the paleoclimates of other parts of the world (Turney et al., 2006). The strength of thermohaline circulation in the North Atlantic provided a mechanism for regionally synchronous, abrupt climate change (Broecker, 2003), supporting the rationale of comparing climate histories to the GRIP ice core template.

However, comparisons of Antarctic ice cores to Greenland records suggest a more complicated sequence of postglacial climate change. Some researchers have suggested that warm episodes in the south correspond to cooling in the north and that, rather than leading, the Northern Hemisphere responds to climate change initiated by its southern

counterpart (Morgan et al., 2002). The tendency of opposing interhemispheric climates has been termed the "bipolar seesaw" (Broecker, 1998) and meltwater pulses from Antarctic ice sheets have been suggested as a potential mechanism driving this relationship between hemispheres (Weaver et al., 2003). However, more detailed paleoclimate records encompassing the late Pleistocene/early Holocene transition are needed from the Southern Hemisphere in order to assess the magnitude, extent, and duration of climate events during deglaciation.

Tasmania, an island-state of Australia, is ideally located to study climate change during both the Lateglacial and Holocene. At 41-44°S, Tasmania is one of the few landmasses of the "Water Hemisphere" positioned within the critical latitudinal range for ice building during glacials and stadials. During the repeated periods of Quaternary glaciations, ice carved out significant parts of the Tasmanian landscape, generating countless cirque and valley lakes in western and central mountain ranges (Fig. 4.1). The lacustrine sediments of these lakes archive past climate change extending back to the time of ice retreat in Australia, 20-17 ka BP, as suggested by boulder exposure ages from terminal moraines (Barrows et al., 2002; Mackintosh et al., 2006) and, in regions that remained unglaciated during the last Ice Age, to at least the previous interglacial, 125 ka BP (Colhoun et al., 1999).

Tasmania is positioned between two important controls of synoptic-scale climate, the Western Pacific Warm Pool to the north and Antarctica to the south. Tasmania is also on the boundary of the Roaring Forties - strong, zonal Westerlies that deliver precipitation to the island year-round. Pollen records (ratio of herbs to woody taxa) from Lake Selina and Tullabardine Dam, western Tasmania, correlate with the Vostok ice core

record from Antarctica and deep sea core RC 11-120 from the south-western sub-polar Indian Ocean (Colhoun et al.,1999), suggesting that climates in Tasmania respond in concert with hemispheric climate change. As a result, Tasmanian lake sediment records have the potential to reveal large-scale changes in atmospheric and oceanic circulation characteristic of the late Pleistocene/early Holocene transition, such as the Antarctic Cold Reversal (ACR; EPICA Community Members, 2006) and Younger Dryas (YD; Alley, 2000).

Despite the suite of lakes generated during the last Ice Age, the sensitivity of Tasmania to large-scale climate change, and the development of sophisticated statistical techniques, few quantitative reconstructions exist for the region. Most of the previous studies from Tasmania focused on qualitative or semi-quantitative interpretations of pollen records (Macphail, 1979; Colhoun and van de Geer, 1986; Markgraf et al., 1986; van de Geer et al., 1989). The pollen records from sites predominantly located in western and south-central Tasmania generally indicate increasing temperature and precipitation between approximately 13.9 and 11.6 cal ka BP (12-10 ^{14}C ka BP). Between 11.6 and 6.8 cal ka BP (10 - 6 ^{14}C ka BP), temperatures and precipitation gradually reached a maximum with values slightly greater than modern. From 6.8 cal ka BP (6 ^{14}C ka BP) to present, the inferred climate cooled from the maximum of the early/mid-Holocene to its modern state (Macphail, 1979; Markgraf et al., 1986; Harrison, 1993).

Although these studies are valuable for interpreting temperature and precipitation change throughout the postglacial, they are limited by chronological control (i.e., sparse ^{14}C dating), lack of modern plant community analogues, ecological lags in response time, and the insensitivity of the local vegetation's response to environmental variations (Xia et

al., 2001). The modern distribution of vegetation in Tasmania is controlled to a certain extent by temperature, but also by other important environmental factors, such as soil characteristics, precipitation (particularly precipitation of the dry season), and fire (Jackson, 2005). These factors are active now and were certainly important during the development of vegetation in Tasmania after deglaciation. Fire, used by Aborigines to maintain non-climax vegetation since their arrival to the island at least by 40 cal ka BP (Cosgrove et al., 1990), may mimic the effects of climate deterioration by generating open-structured vegetation communities. All of these factors complicate the interpretation of pollen records and highlight the importance of multiple lines of evidence when trying to understand the paleoclimate of Tasmania.

Importantly, cosmogenic dates from Tasmanian boulders (Barrow et al., 2002; Mackintosh et al., 2006) and sea surface temperatures (SST) from adjacent ocean waters (Sikes et al., 2009) indicate that temperatures were warm shortly after the LGM, starkly contrasting the pollen records. Therefore, we developed independent reconstructions of temperature from two sites in Mount Field National Park, Tasmania; we created the reconstructions with the Tasmanian, chironomid-based transfer function for temperature of the warmest quarter (TWARM; Rees et al., 2008). Chironomids (Diptera: Chironomidae) are often the most abundant aquatic invertebrate found in freshwater systems (Armitage et al., 1995). They have chitinous head capsules that can be preserved in lacustrine sediments and possess enough diagnostic features to be identified to genus and sometimes species levels. Furthermore, the distribution and abundance of chironomids in Tasmania are significantly related to temperature (Rees et al., 2008), and therefore can be used to quantitatively model past TWARM in the region. With our

reconstructions, we attempt to address the following paleoclimatic questions: 1) given the recent chironomid-based evidence for the ACR in New Zealand (Vandergoes et al., 2008), does the ACR also occur in Tasmania and, if so, what was the magnitude of temperature change associated with it; 2) does the chironomid-based reconstruction support warming shortly after the LGM, as indicated by the cosmogenic dates and SST, or warming at the onset of the Holocene, as suggested by the pollen records; and 3) when was the Holocene thermal maximum and how warm was it relative to modern temperature? These reconstructions are among the first in Tasmania to employ a calibration set and among the few quantitative reconstructions that exist for Australia, building on the sparse number of chironomid-based reconstructions for the Australasian region as a whole (e.g., Dimitriadis and Cranston, 2001; Woodward and Shulmeister, 2007; Vandergoes et al., 2008).

Study area

Mount Field is a plateau that lies to the west of the Derwent Graben in south-central Tasmania. The plateau is capped by a sill of Jurassic dolerite that was intruded by the Parmeener Supergroup of Carboniferous-Triassic mudstone, sandstone, and glacigenic sedimentary rocks (Brown et al., 1989; Kiernan et al., 2001). At peak ice development during the last glacial, ice persisted in Mount Field as cirque and valley glaciers (Colhoun, 2004).

Vegetation communities found in the lower areas of Mount Field include tall open and closed forests dominated by *Eucalyptus* and *Acacia* species. Closed forests with canopies dominated by *Nothofagus cunninghamii*, *Atherosperma moschatum*,

Phyllocladus aspleniifolius, and often emergent *Eucalyptus* prevail between roughly 600 and 900 m a.s.l. Subalpine environments above 900 m a.s.l. include open forest dominated by *Eucalyptus* and an understory of sclerophyllous shrubs to the west, shrubland and grasses to the east (*Eucalyptus* woodland with a shrub understory occurs at both Eagle and Platypus Tarns), and *Gymnoschoenus sedgeland* centrally. Alpine vegetation found atop the mountains and plateaux of Mount Field is characterized by open and closed heath communities, herbfield, sedgeland, moor, and bogs (Macphail, 1979).

Eagle Tarn (42°40.794 S, 146°35.481 E) is a small cirque pond at 1040 m a.s.l. with a surface area of 0.9 ha, impounded by a moraine located below Mount Mawson (Fig. 4.1). It is shallow, with a maximum depth of 0.19 m at the time of coring. Because of its shallow nature, and that people visiting Mount Field National Park have swum in the tarn, ice skaters have fallen through, and the middle of the tarn has been cored on at least three separate occasions (Eric Colhoun, personal communication), the upper 40 cm of sediment may have been disturbed. We nevertheless decided to core Eagle Tarn because it is a classic site frequently referred to in the Tasmanian paleoclimate literature. No permanent streams flow into or out of the tarn. Annual precipitation for the site is 1729 mm, as estimated by BIOCLIM (software that estimates climate parameters); the software combines data from meteorological stations and a digital elevation model to generate point values for specific climate parameters (Houlder et al., 2003). Similarly, mean annual temperature, mean TWARM, and mean temperature of the coldest quarter for Eagle Tarn are 5.4, 9.5, and 1.6°C, respectively.

Platypus Tarn (42°40.402 S, 146°35.210 E), another small cirque lake, is at 941 m a.s.l. with a surface area of 2.0 ha, located about 700 m north of Eagle Tarn. Its basin was created by a valley glacier that deposited a moraine, damming Platypus Tarn and Lake Seal, a larger lake to the north-west (Fig. 4.1). The tarn is roughly 14.5 m deep with inflowing and outflowing streams. It receives an estimated 1586 mm of annual precipitation, slightly less than Eagle Tarn. Mean annual temperature, mean TWARM, and mean temperature of the coldest quarter are 5.9, 10, and 2.1°C, respectively.

Methods

Eagle and Platypus Tarns were cored during the austral summer month of January, 2007. A plastic tube, fitted with a piston and attached to coring rods, was used to collect the uppermost, flocculent sediment (Wright, 1991). The remainder of the sediment was collected with a modified Livingstone piston corer (Wright et al., 1984). Two overlapping cores were taken from the geographical centre of each tarn. Each drive was wrapped in plastic film and aluminum foil after extrusion and, after transport to the lab, the cores were stored in a cold room at 4°C.

Fourteen terrestrial plant macrofossil samples were recovered for AMS ^{14}C dating, six from Platypus Tarn and eight from Eagle Tarn (Table 4.1). Sediment was sieved through a two-tiered system with 1 mm and 0.5 mm meshes on the upper and lower sieves, respectively. Macrofossils were dried at 90°C overnight and wrapped in aluminum foil before being submitted to the UCI Keck Carbon Cycle AMS Program at the University of California, Irvine. Since the majority of work from Tasmania is reported in radiocarbon years, we included the radiocarbon ages from the original

publications in brackets after the calibrated ages. We used IntCal04 to calibrate radiocarbon ages from previously published work and this study (Reimer et al., 2004). Both radiocarbon and calibrated ages for this study are based on point-to-point age-depth models constructed for both tarns (Fig. 4.2).

Overlapping cores were used to obtain radiocarbon datable material for Platypus Tarn. The macrofossils taken from 51.1 to 54.1 cm were retrieved from the first core; otherwise, the remaining material was taken from the second. Based on loss-on-ignition (LOI) profiles, 13.1 cm were added to depths from the first core to match the second (Fig. 4.3). Evidence from the LOI profiles of the two cores and the internal consistency of the radiocarbon dates from the age-depth model of Platypus Tarn indicate that the depth addition was appropriate (Figs. 4.2 and 4.3). The second core from Eagle Tarn was continuous from the surface sample to the base of the core and therefore was the only one used to collect radiocarbon datable material.

Subsamples were collected for chironomid analysis every 10 cm except at points of interest, where sampling resolution was increased to every 5 cm. As with the radiocarbon sampling, the first core of Platypus Tarn was used to fill in the gap between the surface sample (0-41 cm) and the second core (75-305 cm). The second core was used for the rest of the chironomid subsamples as it was longer than the first by 39 cm. The 13.1 cm addition was also applied to chironomid samples taken from the first core. Samples for LOI (0.5 mL) were taken every 5 cm, dried overnight at 100°C and ashed in a furnace for 4 h at 550°C. The percent of dry weight lost is a coarse indication of the organic content of the sediment (Dean, 1974).

Chironomid analysis followed the standard laboratory techniques outlined by Walker et al. (1991). These include deflocculating 2.0 mL (on average) of sediment with warm, 5% KOH followed by washing with distilled water on a sieve with 95 μm meshes. Aliquots of the residue were poured into a Bogorov tray and examined at 50x magnification under a dissecting scope. Chironomid head capsules were picked out using fine forceps and placed ventral-side up on a cover slip to facilitate identification. Slides were fixed using Entellan® (Merck, Darmstadt, Germany) and identification was conducted with a compound microscope at 400x magnification following Wiederholm (1983), Oliver and Roussel (1983), Cranston (2000), and Brooks et al. (2007).

The Tasmanian calibration model of midge-inferred mean TWARM (Rees et al., 2008) was applied to the chironomid abundance data from both sites. The model was made using the unimodal technique of weighted averaging partial least squares (ter Braak and Juggins, 1993) and has a jack-knifed coefficient of determination (r^2_{jack}) of 0.72 and a root mean square error of prediction (RMSEP) of 0.94°C. The model was run in C2, v1.5 (Juggins, 2007) where percent values of fossil taxa were square root-transformed to stabilize the variance. Psimpoll was used to zone the chironomid percent diagram using optimal-splitting by information content (Bennett, 2005).

Several reconstruction diagnostics were used to evaluate the reliability of the chironomid-inferred temperatures (outlined in Birks, 1995). Goodness of fit (Birks et al., 1990) was assessed by passively fitting fossil samples to an ordination axis derived from the modern training set constrained to TWARM. The quality of that fit was evaluated by comparing the squared residual distance of the modern samples from the constrained axis to the distance of the fossil samples. Fossil samples were considered to have a "poor" or

"very poor" fit if they were greater than the 90th and 95th percentiles of the modern squared residual distances, respectively. The abundance of rare taxa constituting fossil assemblages was also calculated. Rare taxa were defined here as having a Hill's N2 (Hill, 1973) of 5 or less in the modern training set. Optima of taxa with $N2 \leq 5$ are likely to be poorly estimated as these taxa are rare in the modern data (Brooks and Birks, 2001). Finally, the modern analogue technique (Birks et al., 1990) was used to determine the degree of dissimilarity between fossil and modern assemblages. Fossil samples had "good" or "close" modern analogues as defined by the 2nd and 5th percentiles of all chi-square distances in the modern data.

Results

Sediment lithology and chronology

Roughly 4.4 m and 3 m of sediment were recovered from Eagle and Platypus Tarns, respectively (Table 4.2). The most noticeable stratigraphical features of both cores are the distinct light grey mud layers, between 195 and 160 cm (~6.6-5.4 cal ka BP) in Eagle Tarn and between 275 and 249 cm (~19.1-15.8 cal ka BP) and again between 240 and 225 cm (~14.6-12.7 cal ka BP) in Platypus Tarn. A wet mount of material taken from these layers and examined at 400x magnification under a compound microscope revealed the sediment to consist largely of diatom frustules with little organic material. These layers represent hiatuses in the chironomid records, although sediment deposition is continuous.

The LOI profiles for both sites show similar trends (Figs. 4.4a,b and 4.5e,g). In each case, organic content increases until about 11 cal ka BP. The increasing trend is

punctuated by a slight decrease in organic content followed by a constant value lasting from roughly 14.8 to 12.8 cal ka BP in both tarns. Organic content slightly decreases in Eagle Tarn from approximately 11 to 6.6 cal ka BP whereas it remains more or less constant in Platypus Tarn during the same interval. Between 6.6 and 5.8 cal ka BP, organic content drops dramatically in Eagle Tarn, coinciding with the diatomaceous sediment layer (Table 4.2). Afterwards, peak organic content is reached by 5.1 cal ka BP in Eagle Tarn. Organic content generally decreases from 5.1 to 2.1 cal ka BP in Eagle Tarn and from 6.6 to 2.4 cal ka BP in Platypus Tarn. Both tarns show a slight increasing trend from 2.1 cal ka BP to modern.

The chronologies from both tarns indicate linear, uniform sediment deposition without any major dating reversals (Fig. 4.2). Based on the point-to-point age-depth models, sedimentation rate decreases toward the base of both cores. The minimum, maximum, and average number of years contained per centimetre of sediment are 21.9, 56.3, and 32.3 ^{14}C a/cm for Eagle Tarn and 33.2, 101.6, and 56.5 ^{14}C a/cm for Platypus Tarn. Ages beyond 15.1 and 15.6 cal ka BP at Eagle and Platypus Tarns, respectively, are based on an extrapolation of the sedimentation rate and, therefore, should not be over-interpreted.

Chironomid analysis and reconstruction

Altogether, 42 and 57 taxa were identified from 72 and 52 samples from Eagle and Platypus Tarns, respectively. A minimum of 50 head capsules is recommended to produce reliable temperature reconstructions (Heiri and Lotter, 2001; Quinlan and Smol, 2001); further, rarefaction of count sizes from Tasmanian surface sediments indicates that

count sizes of 50 head capsules captured, on average, 84.3% of the actual taxonomic richness (Rees et al., 2008). In this study, minimum, maximum, and average count sizes were 51.5, 392, and 119.

The chironomid record from Eagle Tarn contained two samples that were poorly fitted to temperature and 18 samples that were very poorly fitted (Fig. 4.6a). Of these samples, 17 had rare taxa with abundances summing to greater than 10% whereas another 16 samples with a good fit to temperature also had a high abundance of rare taxa. All of the fossil samples from Platypus Tarn had a very good fit to temperature though 17 samples had rare taxa with abundances summing to greater than 10% (Fig. 4.6b). In the majority of cases where rare taxa constituted a major component of the sample, *Tanytarsus* morphotype 4, with a Hill's N2 of 1.7 (Rees et al., 2008), was present in high abundance. In the modern training set, this taxon is largely found in a few sites on the Central Plateau, a high elevation plateau in central Tasmania (Fig. 4.1). Not surprisingly, *Tanytarsus* morphotype 4 also has the lowest WA-PLS β coefficient used to reconstruct temperature (Rees et al., 2008). Consequently, cooling in the records from Eagle and Platypus Tarns driven by a high abundance of this taxon should be interpreted with caution.

Only five samples from Eagle Tarn and nine samples from Platypus Tarn had a close analogue to a lake from the modern training set. Six samples from Eagle Tarn and one sample from Platypus Tarn had a good analogue (Fig. 4.6a,b). This is somewhat surprising given that there is generally a good fit to temperature at both tarns and, in the majority of cases, fossil samples consist of taxa well represented in the training set. Nevertheless, WA-PLS performs relatively well in no analogue situations (Birks, 1998)

and, consequently, the temperature reconstructions are considered reliable, except possibly when there is a cooling driven by *Tanytarsus* morphotype 4.

Although the temperature reconstructions from Eagle and Platypus Tarns share similar trends, important differences are readily apparent. First, the amplitude of temperature change at Eagle Tarn, the shallower and higher elevation of the two tarns, is much larger than at Platypus. Second, temperature change at Platypus Tarn leads Eagle Tarn, creating offsets in zonation by up to 1.2 cal ka.

Zonation of the fossil taxa by optimal-splitting by information content yielded four zones for each tarn. These zones broadly correspond with the Lateglacial (>12.7 cal ka BP), early Holocene (12.7-9.3 cal ka BP), mid-Holocene (9.3-4.9 cal ka BP), and late Holocene (<4.9 cal ka BP). In the following sections of the results, temperature preferences for taxa described as either warm- or cold-adapted are defined by Rees et al. (2008).

Lateglacial (>12.7 cal ka BP)

The Lateglacial assemblage at Eagle Tarn is dominated by warm-adapted taxa, including *Tanytarsus* morphotype 2, *Procladius*, *Larsia*, and undifferentiated *Tanytarsus* species. Some intermediate and cold-adapted taxa appear in the record, for instance *Paramerina*, *Echinocladius*, and *Tanytarsus* morphotype 3 (Fig. 4.4a). Temperature is more or less constant during this phase, reconstructing above modern at 10.2°C on average (Fig. 4.5f).

At Platypus Tarn (Fig. 4.4b), the chironomid record is interrupted by two hiatuses during the Lateglacial period. When present, chironomid assemblages are dominated by

Chironomus and warm-adapted taxa such as *Tanytarsus* morphotype 2, undifferentiated *Tanytarsus* species, and *Larsia*. *Parachironomus*, a warm indicator, is also present, one of only two times the taxon occurs throughout the record. Temperature is increasing during this phase, reaching a maximum of 10°C by 14.6 cal ka BP, before being interrupted by a second hiatus in the chironomid record (Fig. 4.5h).

Early Holocene (12.7-9.3 cal ka BP)

Cold-adapted taxa begin to appear at the beginning and throughout the early Holocene at Eagle Tarn. *Tanytarsus* morphotype 4, *Paralimnophyes* morphotype 2, and *Telmatopelopia*, all cold-adapted taxa, appear for the first time in the record. Another cold-adapted taxon, *Polypedilum vespertinus*, reaches its maximum abundance during this phase (Fig. 4.4a). Temperature trends downward from the maximum of the last phase, reaching a minimum of 8.0°C around 10 cal ka BP (Fig. 4.5f). After this minimum, temperature rises abruptly. Taxa generating this trend include *Tanytarsus* morphotype 2, *Procladius*, and the undifferentiated *Tanytarsus* species. *Stempellina* and Genus E, two warm-adapted taxa, also appear for the first time in the record (Fig. 4.4a). Temperature increases to a maximum of 10.6°C around 9.3 cal ka BP (Fig. 4.5h). Temperature is trending downward at the end of the early Holocene, with the phase ending at roughly 9 cal ka BP.

When the chironomid record resumes at Platypus Tarn, cold-adapted taxa, including *Tanytarsus* morphotype 4, *Paralimnophyes* morphotype 2, *Telmatopelopia*, *Tanytarsus* morphotype 3, *Botryocladius*, and *Polypedilum vespertinus* are all abundant (Fig. 4.4b). Temperature reaches a minimum of 8.2°C by 11.1 cal ka BP (Fig. 4.5h).

However, like Eagle Tarn, this cold period is followed by rapid warming, reflected by an increase of undifferentiated *Tanytarsus* species, *Larsia*, Genus E, *Tanytarsus* morphotype 2, and *Stempellina* (Fig. 4.4b). Temperature reaches a maximum of 9.5°C at 9.8 cal ka BP, followed by a cooling trend. The early Holocene phase ends at Platypus Tarn by roughly 9.7 cal ka BP (Fig. 4.5h).

Mid-Holocene (9.3-4.9 cal ka BP)

The mid-Holocene phase begins with an increase in the abundance of cold-adapted *Tanytarsus* morphotype 4 at Eagle Tarn. Warm-adapted taxa like *Procladius*, Genus E, and *Tanytarsus* morphotype 2 disappear from the record at this point (Fig. 4.4a). Temperatures reach a minimum of 7.3°C by 8.7 cal ka BP (Fig. 4.5f). The rest of the phase is typified by warming, punctuated by a chironomid hiatus from 6.6 to 5.4 cal ka BP. After the hiatus, the warming trend resumes. All of the warm-adapted taxa increase in abundance, producing a mid-Holocene thermal maximum of 11.0°C by 4.6 cal ka BP at Eagle Tarn (Fig. 4.5f).

At Platypus Tarn, this phase also begins with cold-adapted taxa, including *Tanytarsus* morphotype 4, *Paralimnophyes* morphotype 2, *Telmatopelopia*, *Tanytarsus* morphotype 3, and *Polypedilum vespertinus* present in abundance (Fig. 4.4b). Temperature reaches a minimum of 8.2°C by 9.5 cal ka BP (Fig. 4.5h). Like Eagle Tarn, the rest of the mid-Holocene is typified by a warming trend; however, unlike Eagle Tarn, there is no hiatus in the chironomid record. All of the warm-adapted taxa are present during the mid-Holocene whereas cold-adapted taxa decrease in abundance.

Parachironomus also occurs at this point in the record (Fig. 4.4b). A mid-Holocene thermal maximum of 10.1°C is reached by 6.7 cal ka BP (Fig. 4.5h).

Late Holocene (<4.9 cal ka BP)

After the mid-Holocene thermal maximum, cold-adapted taxa begin to dominate the late Holocene assemblage at Eagle Tarn. *Tanytarsus* morphotype 4, *Paralimnophyes* morphotype 2, and *Tanytarsus* morphotype 3 are present, with *Telmatopelopia* reaching its maximum abundance (Fig. 4.4a). Temperatures reach a minimum of 7.5°C by around 700 cal a BP (Fig. 4.5f). The general cooling trend is briefly interrupted between 4.0 and 2.4 cal ka BP by an increase in the abundance of warm-adapted taxa such as *Procladius* and *Tanytarsus* morphotype 2. *Larsia* reaches its maximum abundance at this point. After the temperature minimum at 700 cal a BP, warm-adapted taxa such as undifferentiated *Tanytarsus* species, *Cladopelma*, *Procladius*, and *Stempellina* increase in abundance whereas cold-adapted taxa, like *Tanytarsus* morphotype 4, *Paralimnophyes* morphotype 2, and *Telmatopelopia* decrease (Fig. 4.4a). Temperature is generally increasing over the last 700 cal a BP with the reconstruction over-estimating (though well within the error range of the model) modern temperature by 0.4°C at Eagle Tarn (Fig. 4.5f).

The late Holocene also begins with a cooling trend at Platypus Tarn. Cold-adapted taxa, including *Tanytarsus* morphotype 4, *Paralimnophyes* morphotype 2, *Telmatopelopia*, *Botryocladius*, and *Polypedilum vespertinus* are present in abundance (Fig. 4.4b). The cooling trend ends at 3.0 cal ka BP with a temperature of 8.5°C (Fig. 4.5h). Like Eagle Tarn, the trend is punctuated by a brief warm period between 3.5 and 3.4 cal ka BP with increases in the abundance of warm-adapted taxa like *Tanytarsus*

morphotype 2 and *Stempellina*. After 3.0 cal ka BP, temperature is generally increasing, driven by the presence of warm-adapted taxa like the undifferentiated *Tanytarsus* species, *Larsia*, *Procladius*, Orthoclad morphotype 1, Genus E, *Parakiefferiella* morphotype 2, *Tanytarsus* morphotype 2, and *Stempellina*, along with the decrease of cold-adapted taxa such as *Tanytarsus* morphotype 4 and *Botryocladius* (Fig. 4.4b). The model underestimates (though once again within the error of the training set) modern temperature at Platypus Tarn by 0.2°C (Fig. 4.5h).

Discussion

Insolation as a driver of climate in Tasmania

The Earth's energy budget, particularly the amount of insolation received at different latitudes, is an important component driving atmospheric and oceanic circulation. Equator-pole radiation gradients generate temperature gradients that define the strength and position of important components of the atmosphere (Dodson, 1997). Strong equator-pole radiation gradients force Subtropical Highs to lower latitudes, generating strong westerly air flow whereas weak equator-pole radiation gradients force Subtropical Highs to higher latitudes, having the opposite effect on the Westerlies (Young and Bradley, 1984).

The vegetation-inferred annual temperatures from Markgraf et al. (1986) mirror both winter insolation at 40°S and equator-pole maximum winter gradient strength (Fig. 4.5c,d). This suggests that the vegetation of Tasmania may be responding to an increased growing season due to greater winter insolation. The change in insolation is relatively small, at about 4% relative to modern, and it remains unclear if the vegetation is directly

responding to changing insolation or indirectly to changes in the climate system induced by changes in insolation.

The chironomid TWARM record broadly corresponds with summer insolation in that initial chironomid-inferred temperatures are high (close to or greater than modern) from 15 to 13 cal ka BP when summer insolation is relatively high, declines to minimum values between 10 and 8 cal ka BP when summer insolation is at a minimum, and increases toward the present as summer insolation increases (Fig. 4.5c,f,h). These broad trends are punctuated by smaller scale changes, such as the peaks in temperature at both tarns around 9.5 cal ka BP and the mid-Holocene thermal maximum, which indicate that other forcing factors are at play, such as El Niño/Southern Oscillation (ENSO), Antarctic sea ice extent, or variations in sea level.

The chironomid communities could be responding to peak summer temperatures early in the records from Eagle and Platypus Tarns whereas the vegetation could be responding to either low annual temperatures (as suggested by Markgraf et al., 1986) or low winter temperatures. The temperature threshold that the chironomid communities are responding to might be achieved long before the temperature threshold necessary for reforestation.

Evidence for the ACR and YD cold events in Tasmania

There is no previously published evidence supporting the existence of any major postglacial cold reversals such as the ACR or YD in Tasmania (Barrows et al., 2002; Colhoun, 2004). The chironomid-inferred temperatures presented here reconstruct modern values during the ACR at Eagle Tarn whereas the chironomid hiatus at Platypus

Tarn suggests that lake levels were low (this idea is elaborated upon in the following subsection). Across the Tasman Sea in New Zealand, chironomid-inferred temperatures between 14.2 and 14 cal ka BP were 1.5-2°C cooler. After a brief warming, cold conditions resumed for another 600-700 years with temperatures generally 2.0-2.9°C below modern (Vandergoes et al., 2008).

While there is no indication of cooling based on the chironomid-inferred temperatures in our records, organic content (LOI) from both tarns indicates the occurrence of the ACR and correlates with the deuterium content of EPICA Dome C (Fig. 4.5a,e,g). The establishment of warm temperatures at mid-latitude sites as shown by the chironomid records from Tasmania and marine records (Barrows et al., 2007b; Sikes et al., 2009) with associated cooling in Antarctica during the ACR would have increased the latitudinal temperature gradient. This would have resulted in Hadley cell intensification and ultimately the strengthening of the Westerlies that currently deliver precipitation to Tasmania year-round (Rind, 1998). Pepper et al. (2004) suggested that the ACR marked a period of increased zonal circulation in the Southern Ocean, supporting the idea of enhanced precipitation and glacial advance in New Zealand at this time. If this is the case for New Zealand, then it is likely that precipitation also increased in Tasmania during the ACR. At this point, vegetation had yet to become thoroughly established in the drainage area of either tarn. The decreasing trend in organic content at Mount Field, coinciding with the ACR, could reflect an increase in precipitation in the region and, consequently, an increase in the allochthonous, clastic input from the drainage area. The diatomaceous sediments at Platypus Tarn during this phase, however, indicate that evaporation, driven by warm temperatures, nevertheless exceeded the

increase in precipitation. This explanation corresponds well with the diatom data from Eagle Tarn that suggest seasonal moisture stress with associations characteristic of evaporation and chemical concentration co-occurring with associations characteristic of low conductivity, low pH, and oligotrophic conditions (Bradbury, 1986). Unfortunately, without any corroborating evidence, the LOI profile is difficult to interpret.

In terms of the YD, there is no evidence for cooling at our sites in either the LOI or chironomid-inferred temperature records. This finding is consistent with recent studies from New Zealand (Williams et al., 2005; Vandergoes et al., 2008) and the adjacent ocean (Barrows et al., 2007a), which also lack evidence for the YD.

Lateglacial (>12.7 cal ka BP)

One of the most noticeable features of our reconstructions is that temperatures reach high values shortly after glaciers receded from Mount Field. Ice retreated from the moraine impounding Eagle Tarn by at least 18.6±1.9 ka BP, as indicated by cosmogenic dating (Barrows et al., 2002). By 15.1 cal ka BP, when chironomid communities are established at both tarns, temperatures at Eagle Tarn were already above modern while temperatures at Platypus attained values close to modern. The radiocarbon dates constrain the start of warming, as indicated by the chironomid-inferred temperatures, to 15.9 cal ka BP at Platypus Tarn, culminating in maximum temperatures by 14.6 cal ka BP. At Eagle Tarn, temperatures were already above modern at the beginning of the record and continued to remain so until 10.8 cal ka BP.

Early warmth contrasts sharply with the pollen-based climate inferences from Markgraf et al. (1986) but is consistent with pollen records from Lake Selina (Colhoun et

al., 1999) and Tullabardine Dam (Colhoun and van de Geer, 1986; Colhoun, 2000), cosmogenic dates (Barrows et al., 2002; Mackintosh et al., 2006), and ocean core data from throughout the Australasian region. Evidence from foraminiferan-based sea surface temperature (SST) reconstructions, biogeochemical proxies (i.e., alkenone and Mg/Ca SST reconstructions), pollen data, and sediment analyses from ocean cores was compiled by Barrows et al. (2007b). These cores include SO136-GC3 (Barrows et al., 2007b), off the western coast of New Zealand's south island; DSDP 594 (Nelson et al., 1993) and MD97-2120 (Pahnke et al., 2003), to the east of New Zealand's south island; and MD88-770 (Bareille et al., 1994; Labeyrie et al., 1996), in the Indian Ocean. All of the records indicate rapid warming after the Last Glacial Maximum, with modern temperatures seen in all records by 15 cal ka BP. Further evidence from a foraminiferan-based SST reconstruction from ocean core RS147-GC07 (Fig. 4.5b), collected from the South Tasman Rise off the southern coast of Tasmania, reinforces an early postglacial warm period (Sikes et al., 2009).

Two chironomid hiatuses occur in the Platypus Tarn record during this interval, one from 19.1 to 15.8 cal ka BP and the other from 14.6 to 12.7 cal ka BP. A spatial and temporal analysis of lake level from 38 sites across Australia and Papua New Guinea reveals maximum aridity at 13.9 cal ka BP (12 ^{14}C ka BP) when the water level in nearly all of the lakes included (81%) was low (Harrison, 1993). Coinciding with this arid period at Eagle Tarn, diatom assemblages switch from taxa preferring open, clear water and neutral to slightly basic pH to benthic or epiphytic taxa that live in the photic zone, either on the bottom substrate or attached to macrophytes (Bradbury, 1986). This indicates that, at 13.9 cal ka BP (12 ^{14}C ka BP), Eagle Tarn switched from a larger and

deeper lake, to a shallow one. Among the benthic and epiphytic assemblages, coexistence of alkaliphilic associations preferring slightly saline, shallow water conditions and acidophilic associations, preferring dilute, oligotrophic, low pH conditions suggest seasonal moisture stress (Bradbury, 1986; Markgraf et al., 1986). Periodic drying and chemical concentration of the tarn along with seasonal input of fresh water could explain the coexistence of both alkaliphilic and acidophilic associations. This moisture stress must have affected Platypus Tarn as well. Shallow, well-oxygenated waters reduce the effectiveness of chitin preservation. Briggs et al. (1998) found that the 37.9% of the chitin of a weevil's (Order: Coleoptera, Superfamily: Curculionidae) cuticle was preserved in the anoxic facies of deeper water whereas less than 6% of the chitin was preserved in insects from sediments deposited in shallower water. Granted, their study considered specimens from the Pliocene, but it is plausible that the chitinized head capsules of the aquatic chironomid larvae did not preserve in Platypus Tarn during this warm period because of shallow, well-oxygenated water conditions.

Early Holocene (12.7-9.3 cal ka BP)

The chironomid temperature reconstructions are in stark contrast to the vegetation data during this phase (Fig. 4.5). After the initial warm period of the Lateglacial in both Eagle and Platypus Tarns, chironomid-inferred temperatures drop by 2.5°C and 1.8°C, reaching minima for the interval by 10 and 11.1 cal ka BP at Eagle and Platypus Tarns, respectively. This cooling is associated with increasing abundance of *Tanytarsus* morphotype 4 and therefore should be interpreted with caution. However, the presence of *Tanytarsus* morphotype 4 coincides with the presence of cold-adapted taxa that are well

represented in the modern training set (e.g., *Paralimnophyes* morphotype 2, *Telmatopelopia*, *Tanytarsus* morphotype 3, *Botryocladius*, *Polypedilum vespertinus*; Fig. 4.4a,b). Also, there is a good fit to temperature during this phase at both tarns (Fig. 4.6a,b).

Multiple pollen records indicate that, between 13.3 and 10.8 cal ka BP (11.5- 9.5 ^{14}C ka BP), subalpine sclerophyll shrubland and *Eucalyptus* woodland replaced non-arboreal taxa (Macphail, 1979; Colhoun, 1996). Macphail (1979) states that plant communities at high elevations dominated by shrubs and the upslope movement of *Eucalyptus* timberline indicate rapid warming during this interval and increased absolute rainfall. Markgraf et al. (1986) suggest that temperatures were initially cool (6°C mean annual temperature) during this phase; however, pollen-inferred temperatures begin to increase in the early Holocene and moisture stress, though present initially during this phase, becomes negligible by about 11.6 cal ka BP, coinciding with the increase in rainforest taxa (Bradbury, 1986; Markgraf et al.,1986). Markgraf et al. (1986) infer the interval between 11.6 and 8.9 cal ka BP (10-8 ^{14}C ka BP) to be the warmest on record, though not yet characterized by maximum precipitation, based on the rainforest taxa *N. cunninghamii* and *P. apetala* reaching their respective highest percentages.

The decreasing trend in chironomid-inferred temperatures from approximately 13.1 to 10 cal ka BP roughly corresponds with an increase in *Cyclotella arentii* between 11.9 and 10.8 cal ka BP (10.2-9.5 ^{14}C ka BP) at Eagle Tarn (Bradbury, 1986). *C. arentii* is an acidophilous diatom, common in nutrient poor, dystrophic lakes (Foged, 1972). Markgraf et al. (1986) interpret this increase, along with shifts in the vegetation, as potentially reflecting climates cooler and wetter than modern. A cooling trend is also

evidenced across the Tasman Sea in New Zealand. The PLS-based chironomid reconstruction for Boundary Stream Tarn indicates a 1°C decrease in temperature between roughly 13.1 and 11.5 cal ka BP (Vandergoes et al., 2008), broadly corresponding to our 13.1-10 cal ka BP interval.

These minima in the chironomid records are followed by sharp temperature increases reaching maximum values of 10.6°C by 9.3 cal ka BP at Eagle Tarn and 9.4°C by 9.8 cal ka BP at Platypus Tarn. While LOI remains constant during this temperature rise at Platypus Tarn, organic content at Eagle Tarn reaches a maximum corresponding with high temperatures. Other than the increase in *C. arentii* and the subtle evidence in the pollen record, this unstable period of cooling and subsequent warming is not corroborated by any other record from the region. It is important to test reconstructions with multiple lines of independent evidence. There is a need to develop non-pollen, paleotemperature reconstructions for the Holocene in Tasmania in order to fully understand drivers behind changes in climate and past vegetation communities.

Mid and late Holocene (9.3 cal ka BP to present)

The chironomid-based temperature records and LOI profiles reveal a mid-Holocene thermal maximum with maximum temperatures for the record of 11°C by 4.6 cal ka BP at Eagle Tarn and 10.1°C by 6.7 cal ka BP at Platypus Tarn. Organic content reaches maximum values of 34.2% by 5.1 cal ka BP and 39.0% by 6.5 cal ka BP at Eagle and Platypus Tarns, respectively. A layer of diatomaceous sediment occurs between 6.6 and 5.4 cal ka BP, this time at Eagle Tarn. Similar factors that generated this type of layer in Platypus Tarn early in the record come into play here. The interval was a warm period

and lake levels were low by 6.9 cal ka BP (6 ^{14}C ka BP) in Tasmania and north-eastern Queensland, with wetter conditions resuming by 4.5 cal ka BP (4 ^{14}C ka BP; Harrison, 1993). Macphail (1979) places the Holocene climate optimum somewhere between 8.9 and 5.7 cal ka BP (8.0-5.0 ^{14}C ka BP) based on maximum *Nothofagus* development occurring by 8.6 cal ka BP (7.8 ^{14}C ka BP). He further suggests that maximum postglacial warmth may have followed the precipitation maximum.

Chironomid-inferred temperatures generally decrease after the mid-Holocene thermal maximum with more distinct cooling phases between 2.3 and 0.5 cal ka BP at Eagle Tarn and between 3.9 and 3.0 cal ka BP at Platypus Tarn. This cooling is driven by high abundances of *Tanytarsus* morphotype 4 and generally corresponds to a very poor fit to temperature at Eagle Tarn (Fig. 4.6a,b). However, the increase in *Tanytarsus* morphotype 4 is consistent with both increases of cold-adapted taxa that are well represented in the training set (Fig. 4.4a,b) and the generally decreasing trend in organic content of lake sediment (LOI) after the mid-Holocene thermal maximum (Figs. 4.4a,b and 4.5e,g). The LOI at 2.1 cal ka BP at Eagle Tarn is comparable to values during the Lateglacial period (Fig. 4.4a). Geomorphic data from the Snowy Mountain area of south-eastern mainland Australia support this conclusion, showing a strong cooling event between 3.2 and 1.4 cal ka BP (3.0-1.5 ^{14}C ka BP; Costin, 1972).

After the temperature and precipitation optima of the mid-Holocene, essentially modern proportions of pollen taxa are recorded. Vegetation on Mount Field became more open-structured with *Eucalyptus* and sclerophyll shrubs replacing temperate, *N. cunninghamii*-dominated rainforests (Macphail, 1979; Markgraf et al., 1986). The

chironomid-inferred temperatures support Macphail's (1979) interpretation of climate deterioration as the likely cause of the rainforest replacement.

Conclusions

A key finding of this study is the seasonal contrast between the vegetation, whose response correlates with winter insolation and the maximum radiation gradient between the equator and pole, and the chironomid communities, which appear to broadly correlate with summer insolation.

There is mixed evidence for the ACR from both Eagle and Platypus Tarns. The chironomid records from both tarns indicate early warmth with TWARM values at modern during the ACR. The early warmth in the chironomid reconstructions supports the narrative from the cosmogenic dates and SST reconstructions from the region. However, the decrease in the organic content of the LOI profile from Eagle and Platypus Tarns corresponds with the timing of the ACR in the deuterium content of the EPICA Dome C ice core. There is no evidence of the YD cooling in Tasmania.

A mid-Holocene thermal maximum based on the chironomid record corresponds with the warming inferred from *N. cunninghamii*-dominated rainforest development at Mount Field. During this period, temperature was 1.5°C warmer than modern at Eagle Tarn and similar to modern at Platypus Tarn. The chironomid record provides evidence that the reversion to an open-structured landscape, characterized by sclerophyll scrub and *Eucalyptus*, was driven in part by cooling temperatures.

Acknowledgments

We would like to thank Rob Wiltshire and Marian McGowen for their incredible hospitality, along with Greg Jordan for logistical input; Eric Colhoun and G. Jordan for valuable comments on an early draft of this paper; the Department of Primary Industries, Water and Environment (DPIWE) for providing lake sampling permits; Fonya Irvine for field assistance; Joshua Kurek and Stefan Engels for statistical advice; TASMAP,© State of Tasmania, for providing map data; and two anonymous reviewers who provided helpful comments and insights. This project was supported by a Natural Sciences and Engineering Research Council of Canada (NSERC) Discovery Grant to L.C. Cwynar and an NSERC Postgraduate scholarship to A.B.H. Rees.

References

Alley, R.B., 2000. The Younger Dryas cold interval as viewed from central Greenland. Quaternary Science Reviews 19, 213-226.

Armitage, P., Cranston, P.S., Pinder, L.C.V., 1995. The Chironomidae: The Biology and Ecology of Non-Biting Midges. Chapman and Hall, London.

Bareille, G., Grousset, F.E., Labracherie, M., 1994. Origin of detrital fluxes in the southeast Indian Ocean during the last climatic cycles. Paleoceanography 9, 799-819.

Barrows, T.T., Stone, J.O., Fifield, L.K., Cresswell, R.G., 2002. The timing of the Last Glacial Maximum in Australia. Quaternary Science Reviews 21, 159-173.

Barrows, T.T., Lehman, S.J., Fifield, L.K., De Deckker, P., 2007a. Absence of cooling in New Zealand and the adjacent ocean during the Younger Dryas chronozone. Science 218, 86-89.

Barrows, T.T., Juggins, S., De Deckker, P., Calvo, E., Pelejero, C., 2007b. Long-term sea surface temperature and climate change in the Australian-New Zealand region. Paleoceanography 22. doi: 10.1029/2006PA001328.

Bennett, K.D., 2005. Documentation for Psimpoll 4.25 and Pscomb 1.03: C Programs for Plotting Pollen Diagrams and Analysing Pollen Data. Software Manual. Uppsala Universitet, Uppsala, Sweden.

Berger, A.L., 1978. Long-term variations of daily insolation and Quaternary climatic changes. Journal of Atmospheric Sciences 35, 2362-2367.

Birks, H.J.B., 1995. Quantitative palaeoenvironmental reconstructions. In: Maddy, D., Brew, J.J. (Eds.), Statistical Modeling of Quaternary Science Data. Quaternary Research Association, Cambridge, pp. 161-254.

Birks, H.J.B., 1998. Numerical tools in paleolimnology - Progress, potentialities, and problems. Journal of Paleolimnology 20, 307-332.

Birks, H.J.B., Line, J.M., Juggins, S., Stevenson, A.C., ter Braak, C.J.F., 1990. Diatoms and pH reconstruction. Philosophical Transactions of the Royal Society of London B 327, 263-278.

Bradbury, J.P., 1986. Late Pleistocene and Holocene paleolimnology of two mountain lakes in Western Tasmania. Palaios 1, 381-388.

Briggs, D.E.G., Stankiewicz, B.A., Meischner, D., Bierstedt, A., Evershed, R.P., 1998. Taphonomy of arthropod cuticles from Pliocene lake sediments, Willershausen, Germany. Palaios 13, 386-394.

Broecker, W.S., 1998. Paleocean circulation during the Last Deglaciation: a bipolar seesaw? Paleoceanography 13, 119-121.

Broecker, W.S., 2003. Does the trigger for abrupt climate change reside in the ocean or atmosphere? Science 300, 1519-1522.

Brooks, S.J., Birks, H.J.B., 2001. Chironomid-inferred air temperatures from Lateglacial and Holocene sites in north-west Europe: progress and problems. Quaternary Science Reviews 20, 1723-1741.

Brooks, S.J., Langdon, P.G., Heiri, O., 2007. Using and Identifying Chironomid Larvae in Palaeoecology. QRA Technical Guide no. 10. Quaternary Research Association, London, UK.

Brown, A.V., McClehaghan, M.P., Turner, N.J., Baillie, P.W., McClenaghan, J., Calver, C.R., 1989. Geological Atlas 1:50 000 Series, 73 (8112N) Huntley. Geological Survey of Tasmania Explanatory Report.

Colhoun, E.A., 1996. Application of Iversen's glacial-interglacial cycle to interpretation of the Late Last Glacial and Holocene vegetation history of western Tasmania. Quaternary Science Reviews 15, 557-580.

Colhoun, E.A., 2000. Vegetation and climate change during the Last Interglacial-Glacial cycle in western Tasmania, Australia. Palaeogeography, Palaeoclimatology, Palaeoecology 155, 195-209.

Colhoun, E.A., 2004. Quaternary glaciations of Tasmania and their ages. In: Ehlers, J., Gibbard, P.L. (Eds.), Quaternary Glaciations - Extent and Chronology, Part 3. Elsevier, Amsterdam, pp. 353-371.

Colhoun, E.A., van de Geer, G., 1986. Holocene to Middle Last Glaciation vegetation history at Tullabardine Dam, western Tasmania. Proceedings of the Royal Society of London B29, 177-207.

Colhoun, E.A., Shulmeister, J., 2006. Late Pleistocene of the south west Pacific region. In: Elias, S. (Ed.), Encyclopedia of Quaternary Science. Elsevier, pp. 1066-1075.

Colhoun, E.A., Pola, J.S., Barton, C.E., Heijnis, H., 1999. Late Pleistocene vegetation and climate history of Lake Selina, western Tasmania. Quaternary International 57/58, 5-23.

Cosgrove, R., Allen, J., Marshall, B., 1990. Palaeoecology and Pleistocene human occupation in south central Tasmania. Antiquity 64, 59-78.

Costin, A.B., 1972. Carbon-14 dates from the Snowy Mountains Area, southeastern Australia, and their interpretation. Quaternary Research 2, 579-590.

Cranston, P.S., 2000. Electronic guide to the Chironomidae of Australia. URL http://www.science.uts.edu.au/sasb/chiropage/.

Dean Jr., W.E., 1974. Determination of carbonate and organic matter in calcareous sediments and sedimentary rocks by loss on ignition: comparison with other methods. Journal of Sedimentary Petrology 44, 242-248.

Dimitriadis, S., Cranston, P.S., 2001. An Australian Holocene climate reconstruction using Chironomidae from a tropical volcanic maar lake. Palaeogeography, Palaeoclimatology, Palaeoecology 176, 109-131.

Dodson, J.R., 1997. Timing and response of vegetation change to Milankovitch forcing in temperate Australia and New Zealand. Global and Planetary Change 18, 161-174.

EPICA Community Members, 2006. One-to-one coupling of glacial climate variability in Greenland and Antarctica. Nature 444, 195-197.

Foged, N., 1972. Notes of diatoms V. *Cyclotella arentii* and *Nitzschia plana* var. *fennica* f. *ornate*. Svensk Botanisk Tidskrift 66, 437-441.

Galloway, R.W., 1986. Australian snow-fields past and present. In: Barlow, B.A. (Ed.), Flora and Fauna of Alpine Australasia: Ages and Origins. CSIRO, Melbourne, pp. 27-35.

Harrison, S.P., 1993. Late Quaternary lake-level changes and climates of Australia. Quaternary Science Reviews 12, 211-231.

Heiri, O., Lotter, A.F., 2001. Effect of low count sums on quantitative environmental reconstructions: an example using subfossil chironomids. Journal of Paleolimnology 26, 343-350.

Hill, M.O., 1973. Diversity and evenness: a unifying notation and its consequences. Ecology 54, 427-432.

Houlder, D., Hutchinson, M., Nix, H.A., McMahon, J., 2003. ANUCLIM User's Guide. Centre for Resource and Environmental Studies, Australian National University, Canberra, Australia.

Jackson, W.D., 2005. The Tasmanian environment. In: Reid, J.B., Hill, R.S., Brown, M.J., Hovenden, M.J. (Eds.), Vegetation of Tasmania. Australian Biological Resources Study, Tasmania, Australia, pp. 11-34.

Jouzel, J., 2004. EPICA Dome C Ice Cores Deuterium Data. NOAA/ NGDC Paleoclimatology Program, Boulder CO, USA, IGBP PAGES/World Data Center for Paleoclimatology Data Contribution Series No. 2004-038.

Juggins, S., 2007. C2 Version 1.5 User Guide. Software for Ecological and Palaeoecological Data Analysis and Visualisation. Newcastle University, Newcastle upon Tyne, UK.

Kiernan, K., Lauritzen, S.-E., Duhig, N., 2001. Glaciation and cave sediment aggradation around the margins of the Mt Field Plateau, Tasmania. Australian Journal of Earth Sciences 48, 251-263.

Labeyrie, L., Labracherie, M., Gorfti, N., Pichon, J.J., Vautravers, M., Arnold, E., Duprat, J., Caralp, M., Turon, J.L., 1996. Hydrographic changes of the Southern Ocean (southeast Indian sector) over the last 230 kyr. Paleoceanography 11, 57-76.

Mackintosh, A.N., Barrows, T.T., Colhoun, E.A., Fifield, L.K., 2006. Exposure dating and glacial reconstruction at Mt. Field, Tasmania, Australia, identifies MIS 3 and MIS 2 glacial advances and climatic variability. Journal of Quaternary Science 21, 363-376.

Macphail, M.K., 1979. Vegetation and climates in southern Tasmania since the Last Glaciation. Quaternary Research 11, 306-341.

Markgraf, V., Bradbury, J.P., Bubsy, J.R., 1986. Paleoclimates in southwestern Tasmania during the last 13,000 years. Palaios 1, 368-380.

Morgan, V., Delmotte, M., van Ommen, T., Jouzel, J., Chappellaz, J., Woon, S., Masson-Delmotte, V., Raynaud, D., 2002. Relative timing of deglacial climate events in Antarctica and Greenland. Science 297, 1862-1864.

Nelson, C.S., Cooke, P.J., Hendy, C.G., Cuthbertson, A.M., 1993. Oceanographic and climatic changes over the past 160,000 years at Deep Sea Drilling Project Site 594 off southwestern New Zealand, southwest Pacific Ocean. Paleoceanography 8, 435-458.

Oliver, D.R., Roussel, M.E., 1983. The Insects and Arachnids of Canada, Part 11: The Genera of Larval Midges of Canada, Diptera: Chironomidae. Research Branch, Agriculture Canada, Ottawa.

Pahnke, K., Zahn, R., Elderfield, H., Schulz, M., 2003. 340,000-year centennial-scale marine record of Southern Hemisphere climatic oscillation. Science 301, 948-952.

Pepper, A.C., Shulmeister, J., Nobes, D.C., Augustinus, P.A., 2004. Possible ENSO signals prior to the Last Glacial Maximum, during the last deglaciation and the early Holocene, from New Zealand. Geophysical Research Letters 31. doi: 10.1029/2004GL020236.

Quinlan, R., Smol, J.P., 2001. Setting minimum head capsule abundance and taxa deletion criteria in chironomid-based inference models. Journal of Paleolimnology 26, 327-342.

Rees, A.B.H., Cwynar, L.C., Cranston, P.S., 2008. Midges (Chironomidae, Ceratopogonidae, Chaoboridae) as a temperature proxy: a training set from Tasmania, Australia. Journal of Paleolimnology 40, 1159-1178.

Reimer, P.J., Baillie, M.G.L., Bard, E., Bayliss, A., Beck, J.W., Bertrand, C.J.H., Blackwell, P.G., Buck, C.E., Burr, G.S., Cutler, K.B., Damon, P.E., Edwards, R.L., Fairbanks, R.G., Friedrich, M., Guilderson, T.P., Hogg, A.G., Hughen, K.A., Kromer, B., McCormac, G., Manning, S., Bronk Ramsey, C., Reimer, R.W.,

Remmele, S., Southon, J.R., Stuiver, M., Talamo, S., Taylor, F.W., van der Plicht, J., Weyhenmeyer, C.E., 2004. IntCal04 terrestrial radiocarbon age calibration, 0-26 cal kyr BP. Radiocarbon 46, 1029-1058.

Rind, D., 1998. Latitudinal temperature gradients and climate change. Journal of Geophysical Research 103, 5943-5971.

Sikes, E.L., Howard, W.R., Samson, C.R., Mahan, T.S., Robertson, L.G., Volkman, J.K., 2009. Southern Ocean seasonal temperature and Subtropical Front movement on the South Tasman Rise in the late Quaternary. Paleoceanography 24, PA2201. doi: 10.1029/2008PA001659.

ter Braak, C.J.F., Juggins, S., 1993. Weighted averaging partial least squares regression (WA-PLS): an improved method for reconstructing environmental variables from species assemblages. Hydrobiologia 269/270, 485-502.

Turney, C.S.M., Kershaw, A.P., Lowe, J.J., van der Kaars, S., Johnston, R., Rule, S., Moss, P., Radke, L., Tibby, J., McGlone, M.S., Wilmshurst, J.M., Vandergoes, M.J., Fitzsimons, S.J., Bryant, C., James, S., Branch, N.P., Cowley, J., Kalin, R.M., Ogle, N., Jacobsen, G., Fifield, L.K., 2006. Climatic variability in the southwest Pacific during the Last Termination (20-10 kyr BP). Quaternary Science Reviews 25, 886-903.

van de Geer, G., Fitzsimons, S.J., Colhoun, E.A., 1989. Holocene to Middle Last Glaciation vegetation history at Newall Creek, western Tasmania. New Phytologist 111, 549-558.

Vandergoes, M.J., Dieffenbacher-Krall, A.C., Newnham, R.M., Denton, G.H., Blaauw, M., 2008. Cooling and changing seasonality in the Southern Alps, New Zealand during the Antarctic Cold Reversal. Quaternary Science Reviews 27, 589-601.

Walker, I.R., Smol, J.P., Engstrom, D.R., Birks, H.J.B., 1991. An assessment of Chironomidae as quantitative indicators of past climatic change. Canadian Journal of Fisheries and Aquatic Sciences 48, 975-987.

Weaver, A.J., Saenko, O.A., Clark, P.U., Mitrovica, J.X., 2003. Meltwater pulse 1A from Antarctica as a trigger of the Bølling-Allerød warm interval. Science 299, 1709-1713.

Wiederholm, T., 1983. Chironomidae of the Holarctic Region. Keys and Diagnoses. Part 1. Larvae. Entomologica Scandinavica Supplement 19.

Williams, P., King, D., Zhao, J., Collerson, K., 2005. Late Pleistocene to Holocene composite speleothem ^{18}O and ^{13}C chronologies from South Island, New Zealand - did a global Younger Dryas really exist? Earth and Planetary Science Letters 230, 301-317.

Woodward, C.A., Shulmeister, J., 2007. Chironomid-based reconstructions of summer air temperature from lake deposits in Lyndon Stream, New Zealand spanning the MIS 3/2 transition. Quaternary Science Reviews 26, 142-154.

Wright Jr., H.E., 1991. Coring tips. Journal of Paleolimnology 6, 37-49.

Wright Jr., H.E., Mann, D.H., Glaser, P.H., 1984. Piston corers for peat and lake sediments. Ecology 65, 657-659.

Xia, Q.K., Zhao, J.-X., Collerson, K.D., 2001. Early-Mid Holocene climatic variations in Tasmania, Australia: multi-proxy records in a stalagmite from Lynds Cave. Earth and Planetary Science Letters 194, 177-187.

Young, M., Bradley, R.S., 1984. Insolation gradients and the paleoclimatic record. In: Berger, A.L., Imbrie, J., Hays, J., Kukla, G., Saltzman, B. (Eds.), Milankovitch and Climate. Reidel, Dordrecht, Netherlands.

Figure 4.1: Location of study area in Mount Field National Park, Tasmania, Australia and other locations mentioned in the text: 1) Lake Selina, 2) Tullabardine Dam, 3) The Central Plateau, 4) Mount Field, and 5) Ben Lomond. Hobart, the capital of Tasmania and Launceston are the largest cities in Tasmania with approximately 42% and 21% of the population of the island, respectively (Census 2006, Australian Bureau of Statistics). Contour lines of the study area represent changes in elevation of 10 m. Map data provided by TASMAP, © State of Tasmania.

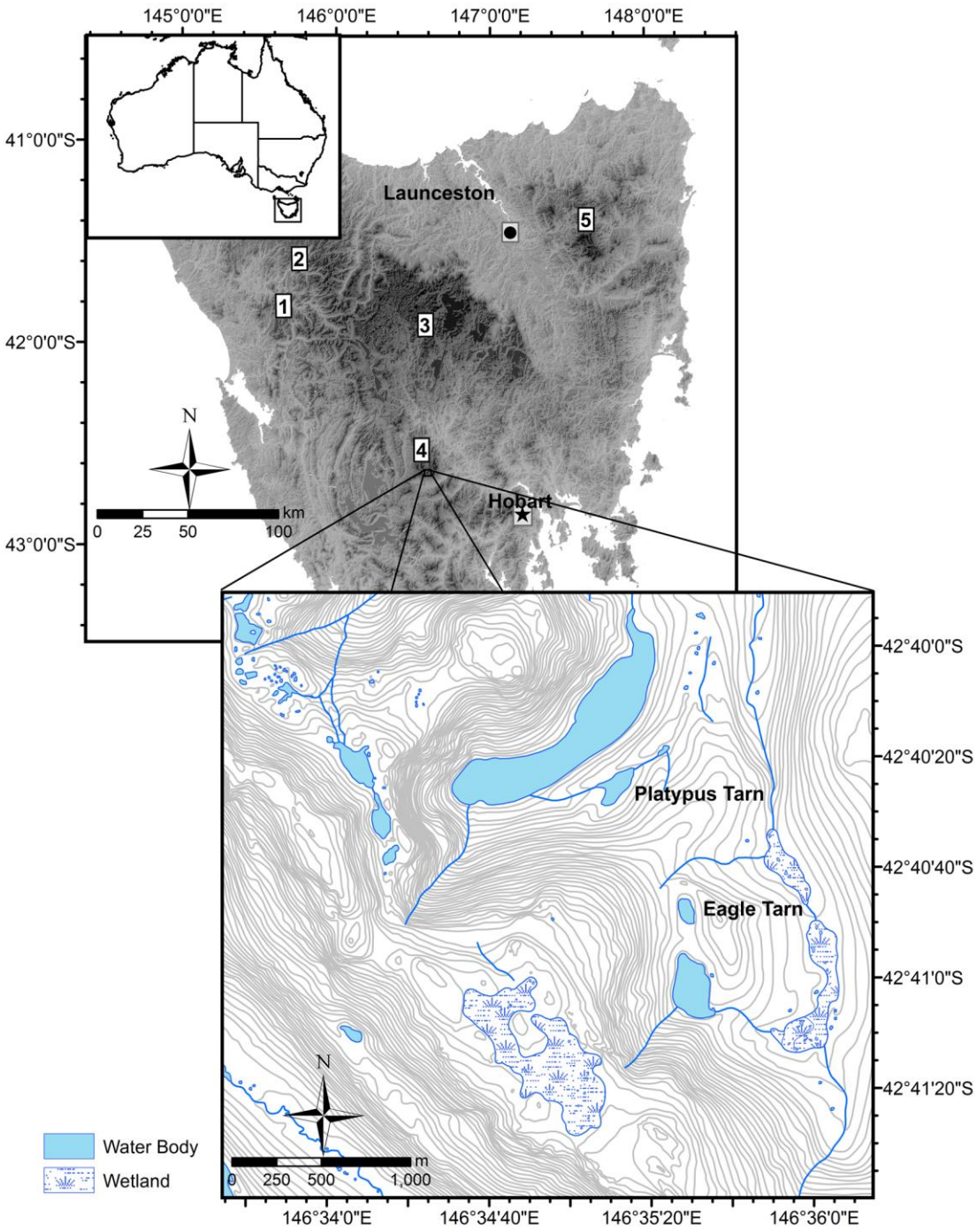

Figure 4.1: Location of study area in Mount Field National Park, Tasmania, Australia.

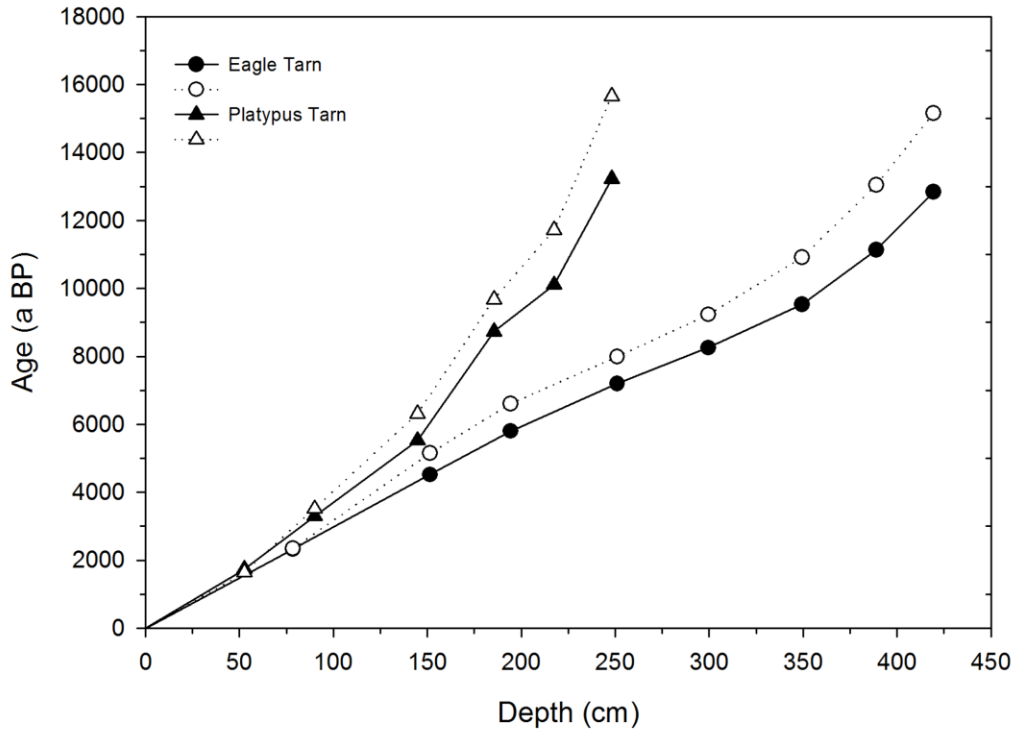

Figure 4.2: Radiocarbon and calibrated ages for Eagle and Platypus Tarns with respect to depth.

Closed shapes represent ^{14}C dates and open shapes represent ages calibrated using IntCal04 (Reimer et al., 2004). Ages for both tarns are based on point-to- point slopes. The first date from Platypus Tarn is based on material collected from the first core while the remaining points are based on material collected from the second core.

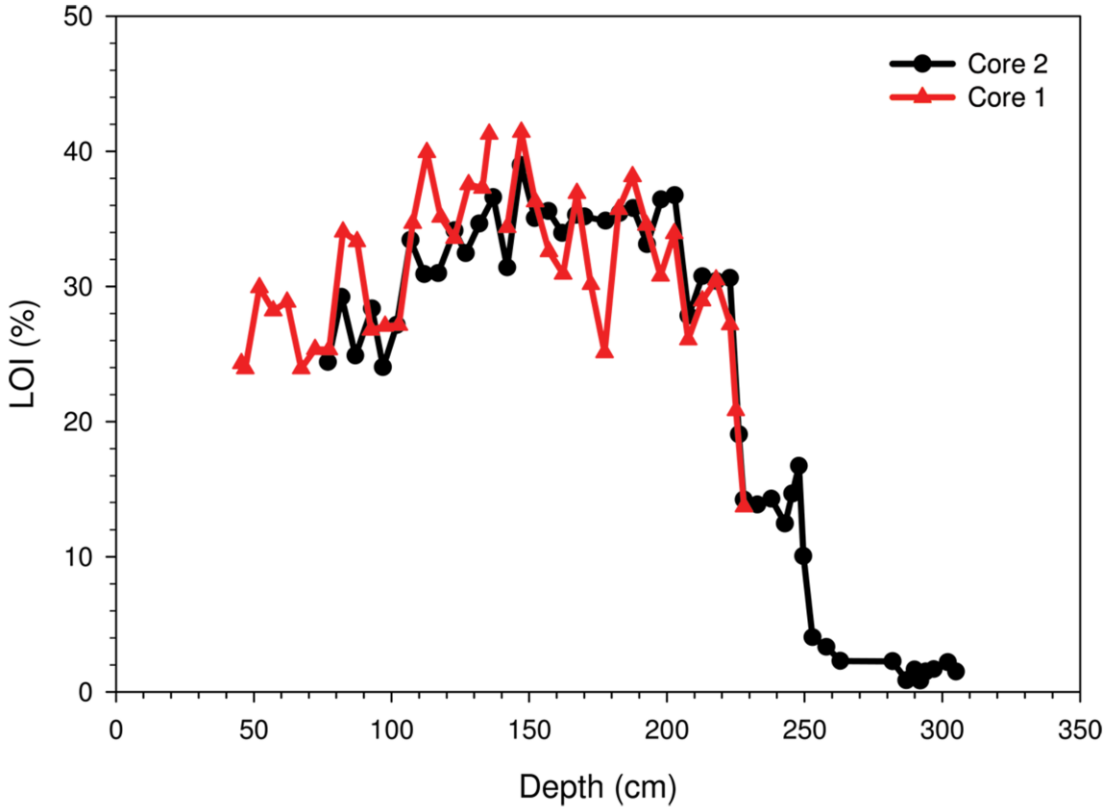

Figure 4.3: Loss-on-ignition profiles from cores 1 and 2 from Platypus Tarn.

To adjust for the offset, 13.1 cm was added to core 1 depths.

Figure 4.4: Chironomid percent diagram with chironomid concentrations and TWARM and LOI profiles of a) Eagle Tarn and b) Platypus Tarn. Only taxa present in high abundance are included in the diagram. Age in calibrated years is on the y-axis and the zones were created using optimal-splitting by information content. Taxa are arranged from lowest to highest β coefficient based on the calibration set produced by Rees et al. (2008). Grey areas represent diatomaceous sediment layers which reflect hiatuses in the chironomid records but not in sediment accumulation. Chironomid concentration is expressed as head capsules per cubic centimetre of wet sediment.

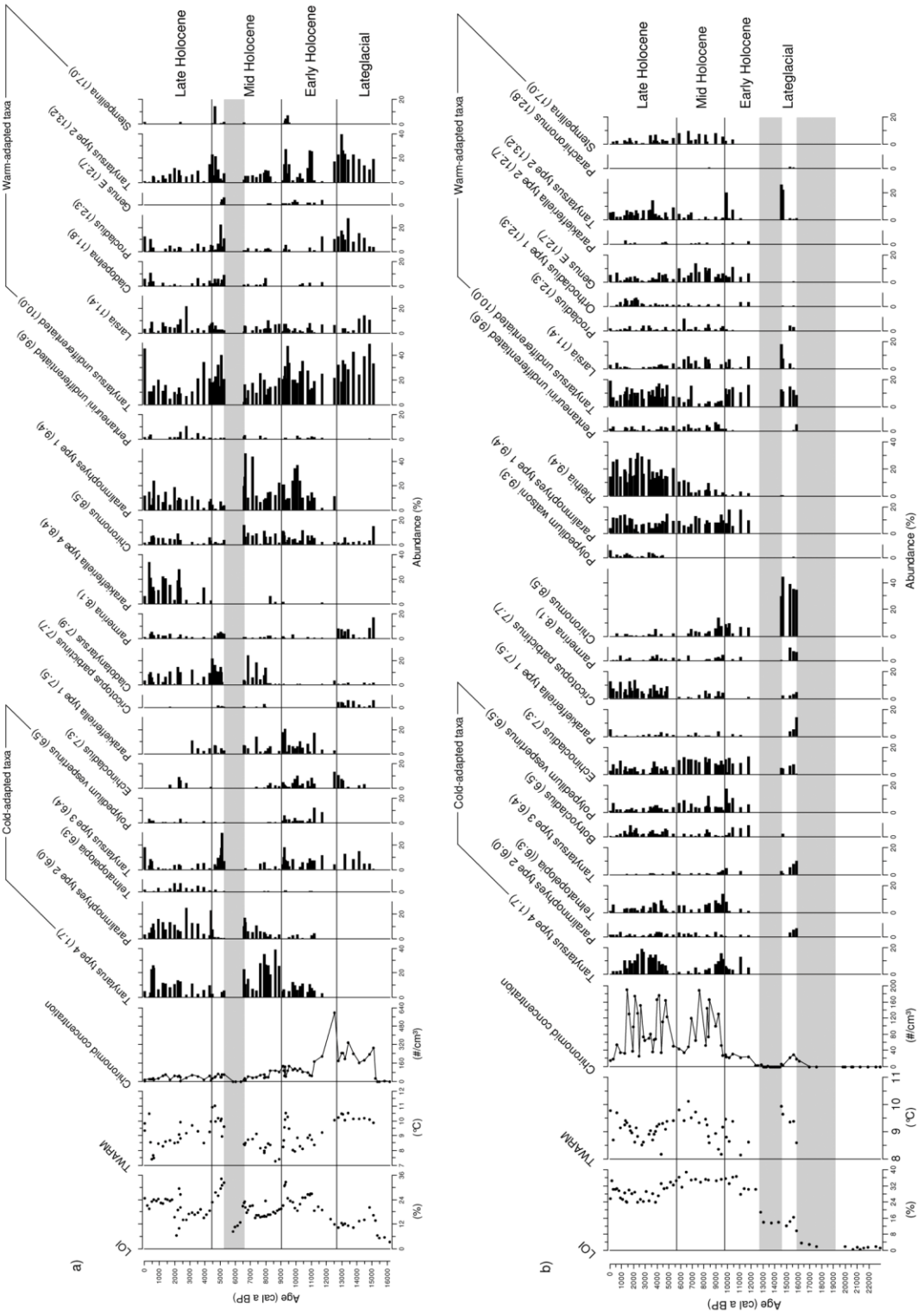

Figure 4.4: Chironomid percent diagram.

Figure 4.5: Summary figure including: a) the deuterium profile from the EPICA Dome C ice core from Antarctica, b) sea surface temperatures from ocean core GC07, c) percent difference between summer and winter insolation from modern at 40°S, and d) semi-quantitative temperatures from Markgraf et al. (1986) plotted as a grey bar chart with the difference between insolation at the equator versus insolation at 60°S (Berger, 1978) as a line graph. The figure also includes e) LOI and f) TWARM profiles from Eagle Tarn and the g) LOI and h) TWARM profiles from Platypus Tarn. Curves in the TWARM profiles were generated by LOESS smoothing; dashed lines represent present-day temperature values. Data for ocean core GC07 from Sikes et al. (2009) and data for EPICA Dome C from Jouzel (2004).

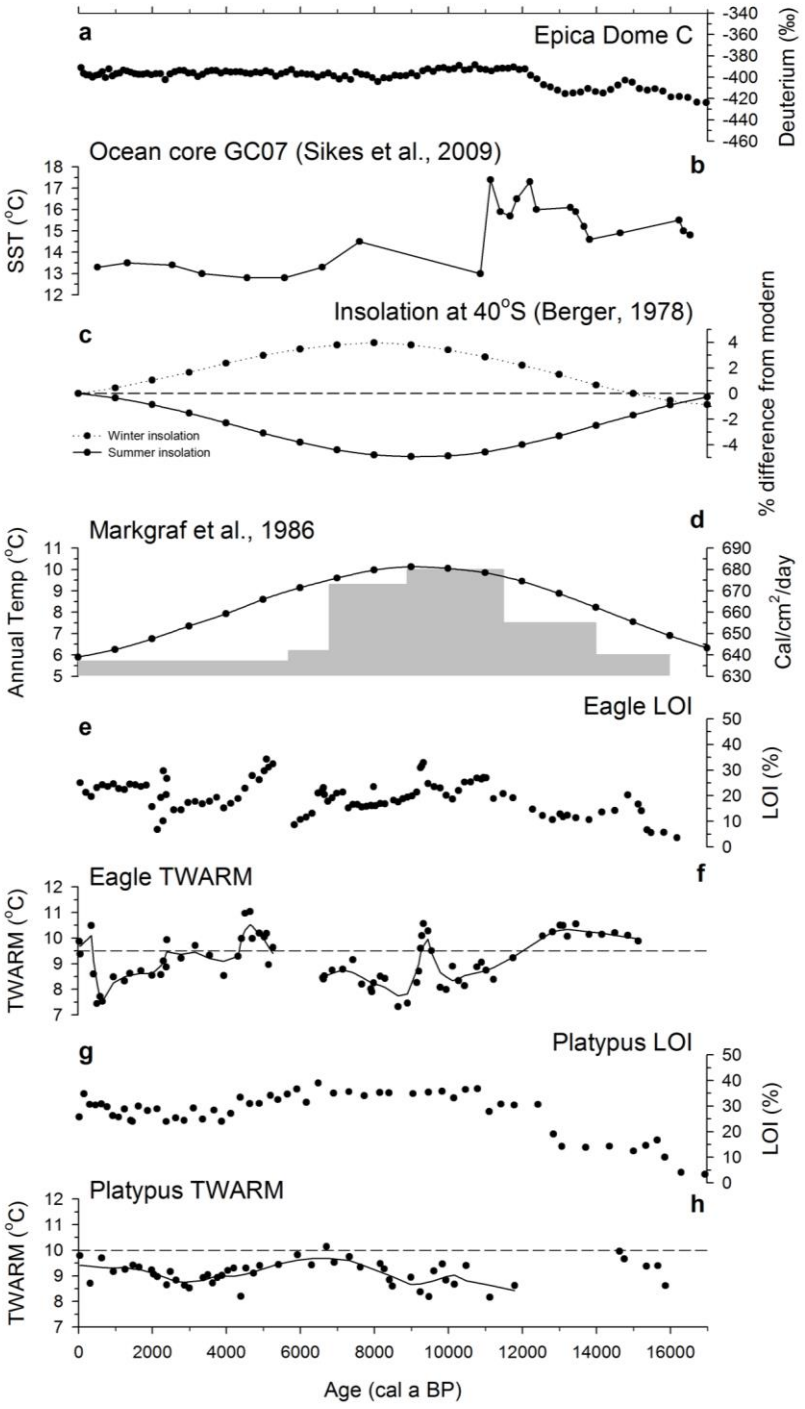

Figure 4.5: Summary figure.

Figure 4.6: Reconstruction diagnostics for a) Eagle and b) Platypus Tarns. The greyed areas from the TWARM reconstruction plots represent the RMSEP (0.94°C) from the modern training set (Rees et al., 2008) while the dashed lines represent LOESS smoothing of TWARM. The vertical lines from the fit to temperature plots represent the 90th and 95th percentiles of modern squared residual lengths beyond which fossil samples are considered to have either poor or very poor fits to TWARM, respectively. Closed circles represent fossil samples with well-represented taxa in the modern training set whereas open circles represent fossil samples with rare taxa ($N2 \leq 5$) summing to greater than 10% abundance. Likewise, closed circles in the non-analogues plots indicate fossil samples with either close or good modern analogues whereas open circles indicate fossil samples with no good modern analogues. The diagonally barred sections represent diatomaceous sediment layers, reflecting chironomid hiatuses.

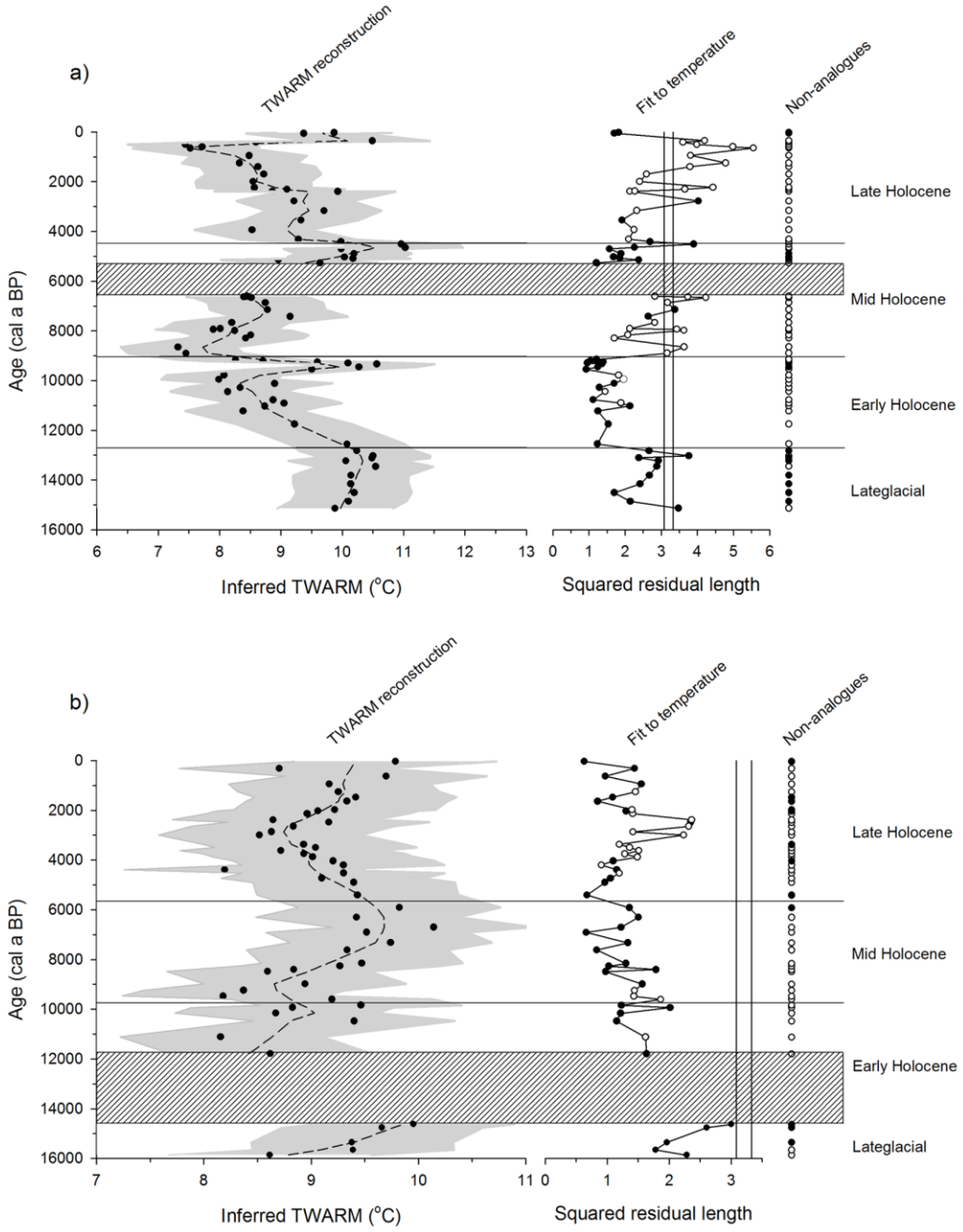

Figure 4.6: Reconstruction diagnostics.

Table 4.1: Radiometric dates from Eagle and Platypus Tarns, Mount Field National Park, Tasmania.

Site	Sample Depths (cm)	Sample Description	Weight (mg)	UCIAMS# (Lab code)	^{14}C Age	Calibrated Age
Eagle	417.3-421.3	Leaves	7.6	50165	12840±30	15160
	388.0-390.0	Leaves, twigs	7.3	50166	11135±25	13040
	348.5-350.4	Twigs, bark	24.2	50167	9530±20	10910
	297.6-301.4	Bark	12.1	50168	8255±25	9230
	250.0-252.0	Bark	48.6	50169	7195±20	7990
	193.8-194.8	Twigs	19.3	50170	5800±20	6600
	150.0-153.0	Twigs	18.2	50171	4520±20	5150
	77.0-80.0	Bark	39.2	50172	2325±20	2340
Platypus	246.0-250.0	Bark, leaves, twigs	12.6	50173	13220±30	15660
	216.9-219.9	Bark	18.0	50174	10110±60	11720
	183.9-186.9	Twigs, leaves	18.1	50175	8730±30	9680
	143.0-147.0	Leaves, bark	15.8	50176	5530±25	6320
	88.9-91.9	Bark	40.5	50177	3295±20	3520
	51.1-54.1	Leaves, twigs	8.5	50178	1745±20	1650

Samples were submitted to UCI Keck Carbon Cycle AMS Program at the University of California, Irvine, USA. Radiocarbon years were calibrated using 50% cumulative probability values from calibration curves generated by IntCal04 (Reimer et al., 2004).

Table 4.2: Lithology of sediments retrieved from Eagle and Platypus Tarns.

Tarn	Depth interval (cm)	Description
Eagle	42-129	Light grey mud
	129-160	Dark brown gyttja
	160-195	Light grey mud (diatomaceous sediments)
	195-299	Light brown mud
	299-310	Dark brown gyttja
	310-332	Brown mud
	332-374	Dark brown gyttja
	374-410	Light brown mud
	410-420	Banded light brown mud
	420-439	Clay with silt bands
Platypus	41-225	Banded dark brown gyttja
	225-240	Light grey mud (diatomaceous sediment)
	240-249	Dark brown gyttja
	249-275	Light grey mud (diatomaceous sediment)
	275-307	Clay with silt bands

The upper 42 and 41 cm of Eagle and Platypus Tarns, respectively, were unconsolidated and extruded into Whirlpaks® on site.

Chapter 5 Southern Westerly Winds submit to the ENSO regime: A multi-proxy paleohydrology record from Lake Dobson, Tasmania

Abstract

The El Niño/Southern Oscillation (ENSO) and Southern Westerly Winds (SWW) have a profound impact on global climate. ENSO influences a host of economically valuable resources, ranging from South American fish stocks to crop yields in the south-eastern United States. Tropical climate anomalies are propagated to higher latitudes where the SWW become a major player. These winds possess distinct zonal symmetry (i.e., homogeneous flow along lines of latitude) and dominate extratropical climate. Although many studies have invoked either mechanism to explain trends in proxy data, few have demonstrated the breakdown of zonally symmetric SWW flow in the wake of enhanced El Niño activity, postulated to have occurred 5 cal ka BP; Tasmania is ideally situated to examine this issue. Currently, El Niño (La Niña) events result in drier (wetter) conditions island-wide. Further, Tasmania houses north-south trending mountain ranges near its western coast. As a result of orographic lift, areas west of the mountains exhibit a positive correlation between SWW flow and precipitation, whereas eastern regions possess a negative relationship. We collected grain size measurements, chironomid (Insecta: Diptera) remains, charcoal, and geochemical proxies to investigate the paleohydrological history of Lake Dobson, a site located in south-central Tasmania. The SWW controlled rainfall from 12 to 4.9 cal ka BP, fluctuating from generally wet to dry conditions around 8.4 cal ka BP. An abrupt shift in climate at 4.9 cal ka BP demarked the

onset of enhanced ENSO activity, highlighting the teleconnections between the equatorial Pacific and southern Australasia.

Introduction

The El Niño/Southern Oscillation (ENSO) and Southern Westerly Winds (SWW) are important controls of climate south of the equator. ENSO exerts particularly strong amplitude signatures over the equatorial Pacific Ocean and adjoining landmasses, producing trans-Pacific Ocean oscillations in sea surface temperature (SST) and sea-level pressure (SLP). The phenomenon is characterized by the Southern Oscillation Index (SOI), which is the standardized difference between mean SLP over Darwin, Australia and Tahiti. Climatological anomalies resulting from ENSO activity are propagated into the sub- and extratropical domains of both hemispheres by mechanisms that operate at higher latitudes, like the Southern Annular Mode (SAM) (Hill et al., 2009). Importantly, the SWW are a major control of synoptic-scale climate at these higher latitudes.

The SWW dominate the climate of the extratropics (between 30 and 60°S) where, unlike in the Northern Hemisphere, large tracts of open ocean permit accelerated wind speeds below the 30th parallel. The extratropics are marked by zonal symmetry, homogeneous wind circulation along a line of latitude (Garreaud, 2007). These zonally symmetric winds are associated with circulation and productivity patterns of the Southern Ocean, meridional heat transport, deep-water formation, global atmospheric CO_2 levels, and terrestrial climate (Toggweiler et al., 2006; Garreaud, 2007; Toggweiler, 2009; Anderson et al., 2009; Moreno et al., 2010). Recent syntheses of palaeoenvironmental data from extratropical regions of Australia, New Zealand, and Southern South America (SSA) reveal substantial changes in the position and strength of the SWW during the postglacial period. Consequently, these areas have become the focus of considerable

effort attempting to link palaeoenvironmental trends to ENSO variability and/or changes in SWW behaviour (see McGlone et al., 1993; Shulmeister et al., 2004; Lamy et al., 2010; Fletcher and Moreno, 2011; Fletcher and Moreno 2012).

Changes in the position and strength of the SWW drove precipitation patterns throughout the postglacial, resulting in vegetation and fire-regime changes that appear to be temporally synchronous and zonally symmetric prior to about 5 cal ka BP (Fletcher and Moreno, 2011; Fletcher and Moreno, 2012). An apparent breakdown of this zonal symmetry after 5 cal ka BP corresponds to an increase in the frequency and intensity of El Niño-like flood events in the eastern equatorial Pacific region (Moy et al., 2002). Fletcher and Moreno (2012) postulated that an intensification of ENSO after this time disrupted the previous zonal symmetry driven by the SWW. Critically, while many terrestrial records from landmasses occupying the mid-latitudes support an intensification of ENSO-type conditions after 5 cal ka BP, no study displays clear evidence of the transition from SWW to ENSO dominance. Our main objective is to characterize the breakdown of zonal SWW circulation, marking the onset of the modern ENSO-dominated climate: when did the breakdown occur, and how long was the transition between different these modes of climate?

Current regional precipitation patterns of Lake Dobson, Tasmania, are significantly correlated to ENSO and the SWW (Hendon et al., 2007; Meneghini et al., 2007; Hill et al., 2009). The site is positioned within the transitional zone between the hyper-humid western region, where moisture is strongly associated with SWW speed and the SAM, and the sub-humid eastern zone of Tasmania, where current rainfall patterns are correlated with the SOI. Therefore, Lake Dobson is ideally positioned to address

questions regarding the dynamic interplay between the SWW and ENSO through time. We use chironomid remains, charcoal, and sediment geochemical analyses to reconstruct precipitation changes throughout the Holocene, with a particular focus on the hypothesized 5 cal ka BP juncture.

Material and methods

Small, open lakes with perennial water supplies and steep basins provide ideal settings for recording sediment transport caused by precipitation (Parris et al., 2010). Lake Dobson (lat 42°41.019 S, long 146°35.478 E, elev 1030 m a.s.l., surface area 5.6 ha) is a moraine-bound cirque lake located in the subalpine zone of Mount Field National Park, south-central Tasmania. The site possesses one out-flowing and two in-flowing streams, with the main in-flow originating from the adjacent Mawson Plateau, 240 m higher in elevation (Fig. 5.1); outflow is determined by a sill of glacial till that has been scarcely eroded. Lake Dobson's basin is simple with a broad littoral bench that narrows into a 5.7 m deep cone. We retrieved a 1047 cm sediment core from the deep cone during January of 2009 and developed a chronology from ten terrestrial plant macrofossil samples (Table 5.1). We calibrated the radiocarbon dates in R v3.0.2 (R Development Core Team, 2012) using CLAM v2.2 (Blaauw, 2010) and compiled a variety of proxies from the sediment core to reconstruct late Pleistocene and Holocene precipitation.

During periods of intense rainfall, increased stream velocity and discharge entrain coarse-grained sediment from uplands surrounding Lake Dobson, while a steep-sloped catchment facilitates the erosion of soil as surface runoff. To reconstruct these two processes, we both measured grain sizes every 10 cm, following Geological Survey of

Canada - Atlantic (GSCA) standard procedures, and conducted ITRAX runs at L'Institut National de la Recherche Scientifique (INRS), Québec City using a 2 mm sampling resolution and 20 s exposure times. ITRAX uses X-ray fluorescence to estimate the abundance of roughly 20 elements (Croudace et al., 2006) and, because Lake Dobson's catchment predominantly consists of Jurassic dolerite, elements like iron, calcium, and titanium are good indicators of surface runoff (Bromfield et al., 2007). All three elements were positively correlated throughout the late Pleistocene and Holocene, so we only present the Fe profile. We also used fire history to assess trends in precipitation.

We disaggregated charcoal samples (2 and 4 cm^3 for the surface and long cores, respectively) in 40 mL of 10% KOH for 24 hours, then added 40 mL of 6% sodium hypochlorite. After one hour, we gently washed the samples through sieves with 250 and 150 μm meshes and enumerated the fraction retained on the 150 μm-mesh sieve with a stereoscope at about 17x magnification (Long et al., 1998; Enache and Cumming, 2007; Walsh et al., 2010). We used CharAnalysis (Higuera et al., 2009) to both identify fires occurring within a 1 km radius of Lake Dobson and assess the difference between fire regimes for statistical significance. Although abiotic proxies like grain size, ITRAX, and charcoal are very informative, biotic proxies are also useful, independent indicators of precipitation and erosion.

Annual precipitation is a significant predictor of chironomid distributions in Tasmania (Rees et al., 2008). Chironomids (Insecta: Diptera) are among the most widespread organisms on the planet, inhabiting biotopes ranging from volcanic lakes to the harsh environments of Signy Island, Antarctica. Rees et al. (2008) identified taxa with significant, albeit complex relationships, to precipitation using generalized linear models.

We included those species, along with others possessing simple linear relationships to annual precipitation, in a qualitative index of rainfall. To improve the reliability of the index, we only included taxa whose autecology matched the statistical results. For instance, *Riethia* predominantly inhabits the depositional zone of low order streams (Trivinho-Strixino et al., 2009). Therefore, head capsules of that genus recovered from lentic environments likely indicate enhanced stream flow. We collected chironomid samples at 10 cm intervals using the standard procedures outlined by Walker et al. (1991) and used the chironomid stratigraphy to develop zones for the entire suite of lacustrine proxies. Zones were identified with Psimpoll, using optimal splitting by information content, where statistical validity is established by comparison to a broken stick model (Bennett, 2005).

Results and Discussion

The lacustrine proxies uniformly suggest increased precipitation from 12 to 8.4 cal ka BP. Sediments from this period possess the highest frequency of grains larger than 500 μm, an abundance of sand relative to clay, and, consequently, the highest median grain sizes for the entire record (Fig. 5.2c, d, e). Iron and the precipitation index follow suit, although, these profiles possess troughs at 11.4 and 10.3 cal ka BP, corresponding to elevated levels of charcoal (Fig. 5.2f, g, h). This distinct wet phase parallels local and regional changes occurring within Lake Dobson's catchment and more widely throughout eastern Tasmania.

Pollen evidence from Eagle Tarn (Fig. 5.1) reveals major shifts in catchment vegetation around 11.5 cal ka BP (9960±300 ^{14}C a BP; Macphail, 1979). *Eucalyptus*

forest, with an abundance of *Phyllocladus*, was replaced by rainforest species like *Nothofagus cunninghamii* and *N. gunnii*, suggesting that local climate became cool and wet. The wet phase from 12 to 8.4 cal ka BP also corresponds to a period of lake high-stands in Tasmania, with the majority of surveyed lakes located in the east (Harrison and Dodson, 1993) (Fig. 5.2a). Using a composite charcoal profile for western Tasmania and the paleovegetation index developed from the Lake Vera pollen record, Fletcher and Moreno (2012) argued for drier conditions in western Tasmania between 11 and 8 ka, driven by a zonally symmetric decrease in SWW flow. Considering the evidence for drier conditions in western Tasmania concurrent with wet conditions in the east, we propose that atmospheric circulation resembled the closest modern analogue - the positive phase of SAM during the summer.

The positive phase of SAM is associated with anomalously strong westerly flow along roughly 60°S contrasted by anomalously strong easterly flow along 40°S (Hendon et al., 2007). During the summer season, the westerlies are positioned farthest to the south and, when coupled with years of a positive SAM index, Tasmania experiences the weakest westerly flow. This atmospheric configuration produces atypically dry conditions in the west and wet conditions in the east (Hendon et al., 2007; Hill et al., 2009). In a survey of landmasses occupying the mid-latitudes of the Southern Hemisphere, Fletcher and Moreno (2012) argued for weakened SWW flow between 11 and 8 ka BP based on this very mechanism. They reasoned that in areas like Tasmania, where SWW speed is positively (negatively) correlated to precipitation in the west (east), periods of weakened westerlies would generate a geographical dichotomy. Western regions would archive dry conditions, and, due to reduced evaporation from foehn winds

and the penetration of moisture bearing easterlies, eastern regions would archive wet conditions. This is consistent with the lacustrine proxies of Lake Dobson and the general consensus emerging from the literature for weakened SWW flow during the early Holocene (e.g., Whitlock et al., 2007; Markgraf et al., 2007; Moreno et al., 2010; Moy et al., 2011; Fletcher and Moreno, 2012). This climate configuration began to wane around 8.4 cal ka BP.

The lacustrine proxies of Lake Dobson highlight a transition to a different mode of climate between 8.4 and 4.9 cal ka BP. The occurrences of the largest grains dwindle and sediment composition becomes equal parts sand and clay, driving the negative trend in median grain size (Fig. 5.2c,d,e); the iron content and precipitation index both generally parallel this trend (Fig. 5.2f,g); and the influx of charcoal into Lake Dobson also begins to increase around 7.5 cal ka BP (Fig. 5.2h). Together, these proxies suggest reduced erosion, likely due to diminished rainfall. This interpretation is consistent with a low percentage of full lakes in eastern Tasmania (Harrison and Dodson, 1993) (Fig. 5.2a). Based on analogues of modern climate, two competing hypotheses could produce uncharacteristically dry conditions in eastern Tasmania: enhanced ENSO activity and/or strengthened SWW flow (Hill et al., 2009).

The Laguna Pallcacocha record demonstrates ENSO activity initiated roughly 6.9 cal ka BP (Moy et al., 2002), coinciding with low lake stands in eastern Tasmania (Fig. 5.2b,c). Currently, El Niño (La Niña) events result in atypical dryness (wetness) island-wide, where enhanced SWW flow produces a dichotomous rainfall pattern: elevated precipitation in western regions corresponds to pronounced dryness in eastern regions. Therefore, if western regions emulate the dry period from roughly 8.4 to 4.9 cal ka BP in

eastern Tasmania, regional climate was likely driven by ENSO activity. On the other hand, if moisture regimes are antithetical, then SWW flow was the likely driver. This latter scenario is supported by the western Tasmania charcoal composite and Lake Vera paleovegetation index (Fletcher and Moreno, 2012). Indeed, Fletcher and Moreno (2012) argued for zonally strengthened SWW from 7 to 5 cal ka BP throughout the mid-latitudes of the Southern Hemisphere. This is generally consistent with continuously increasing strength of the SWW starting in the middle Holocene (Gilli et al., 2005; Moreno et al., 2010; Moy et al., 2011; Fletcher and Moreno, 2012). Furthermore, alternating El Niño (dry)/La Niña (wet) phases of the SOI should generate notable variability in Tasmanian proxies of erosion/precipitation. This is precisely what we see after about 4.9 cal ka BP.

The proxies of Lake Dobson indicate conditions were generally dry, though variable, from 4.9 cal ka BP to present. The largest grain size fraction virtually disappears from the record, and the sediment consists of nearly equal parts clay and sand, with relative abundances becoming irregular around 2.8 cal ka BP; this feature drives median grain sizes (Fig. 5.2c,d,e). The precipitation index and iron content highlight reduced, though fluctuating degrees of erosion (Fig. 5.2f,g), while charcoal influx is elevated and variable (Fig. 5.2h). Importantly, where CharAnalysis failed to identify a significant difference between the early and middle Holocene zones, charcoal influx during the middle to late Holocene (4.9 cal ka BP to present) is statistically unique. Together, these proxies suggest an abrupt switch to a climate regime dominated by ENSO activity.

Lake Dobson is ideally situated to detect the switch from a climate controlled by the SWW to one controlled by ENSO. Currently, ENSO cycles exhibit an island-wide effect on Tasmania, with El Niño (La Niña) causing anomalous dry (wet) years (Hill et

al., 2009). The leading empirical orthogonal function (EOF), calculated on rainfall climatology for the period between 1950 and 2005, explained 72% of the variance in the 55 year data set (Hill et al., 2009). The EOF was primarily related to ENSO, the Pacific-South American mode (PSA) and, to a lesser extent, the SAM (Hill et al., 2009). Extrapolating this pattern back to the onset of enhanced El Niño activity, we would expect the proxy record to archive an increased fire frequency and generally less erosion, coupled with distinct variability. Indeed, the Lake Dobson proxies demonstrate this pattern and fit with a hemisphere-scale trend.

A significant body of evidence purports that the frequency of El Niño events increased at about 5 cal ka BP, and the resultant effects were manifest throughout many of the landmasses occupying the Southern Hemisphere. Support for an intensification of ENSO across the Pacific sector after circa 5 cal ka BP includes: Shulmeister and Lees (1995), Donders et al. (2007), Lynch et al. (2007), Marx et al. (2009), and Quigley et al. (2010) for Australia; Hellstrom et al. (1998), McGlone and Wilmshurst (1999), and Gomez et al. (2004) for New Zealand; and Sandweiss et al. (1996), Rodbell et al. (1999), Moy et al. (2002), and Conroy et al. (2008) for South America. Importantly, Fletcher and Moreno (2012) postulated that the multi-millennial zonal symmetry of the SWW, characterizing the period from 14 to 5 ka, broke down around 6-5 ka, coinciding with the onset of ENSO variability. That breakdown was clearly captured by the proxy record archived in Lake Dobson, which responded in concert with climatological events originating in the equatorial Pacific.

Conclusions

The paleohydrology of Lake Dobson was governed by the SWW from 12 to 4.9 cal ka BP. The period from 12 to 8.4 cal ka BP was analogous to the positive mode of SAM in the summer, when the SWW are displaced towards the pole. On the other hand, the period from 8.4 to 4.9 cal ka BP was comparable to negative SAM years, when western (eastern) regions of Tasmania are anomalously wet (dry). The final phase of Lake Dobson's paleohydrological history was dominated by ENSO. The interval of more mean El Niño-like conditions at Laguna Pallcacocha, starting around 5 cal ka BP, closely matches the climatology associated with Lake Dobson's catchment, suggesting a tight link between Tasmania and the equatorial Pacific. The transition from a SWW- to ENSO-dominated climate was abrupt, transpiring within centuries, and occurred roughly 4.9 cal ka BP.

Acknowledgments

We would like to thank Michael-Shawn Fletcher for his invaluable help interpreting the data, Maarten Blaauw for his advice with CLAM, Owen Brown for assisting with the collection and interpretation of the grain size data, and Pierre Francus for consulting with the ITRAX results. John Southon provided the radiocarbon dates. We are also grateful to Greg Jordan and Vera Markgraf for providing helpful comments on earlier drafts. This research was supported by a Natural Sciences and Engineering Research Council of Canada (NSERC) Discovery grant to Les C. Cwynar and an NSERC Postgraduate Scholarship to Andrew B.H. Rees.

References

Anderson, R.F., Ali, S., Bratmiller, L.I., Nielsen, S.H.H., Fleisher, M.Q., Anderson, B.E., Burkle, L.H., 2009. Wind-driven upwelling in the Southern Ocean and the deglacial rise in atmospheric CO_2. Science 323, 1443-1448.

Bennett, K.D., 2005. Documentation for Psimpoll 4.25 and Pscomb 1.03: C programs for plotting pollen diagrams and analysing pollen data. Software manual. Uppsala Universitet, Uppsala.

Blaauw, M., 2010. Methods and code for 'classical' age-modelling of radiocarbon sequences. Quaternary Geochronology 5, 512-518.

Bromfield, K., Burrett, C.F., Leslie, R.A., Meffre, M., 2007. Jurassic volcaniclastic - basaltic andesite - dolerite sequence in Tasmania: new age constraints for fossil plants from Lune River. Australian Journal of Earth Sciences 54, 965-974.

Conroy, J.L., Overpeck, J.T., Cole, J.E., Shanahan, T.M., Steinitz-Kannan, M., 2008. Holocene changes in eastern tropical Pacific climate inferred from a Galápagos lake sediment record. Quaternary Science Reviews 27, 1166-1180.

Croudace, I.W., Rindby, A., Rothwell, R.G., 2006. ITRAX: description and evaluation of a new multi-function X-ray core scanner. Special Publication - Geological Society of London 267, 51.

Donders, T.H., Haberle, S.G., Hope, G., Wagner, F., Visscher, H., 2007. Pollen evidence for the transition of the Eastern Australian climate system from the post-glacial to the present-day ENSO mode. Quaternary Science Reviews 26, 1621-1637.

Enache, M.D., Cumming, B.F., 2007. Charcoal morphotypes in lake sediments from British Columbia (Canada): an assessment of their utility for the reconstruction of past fire and precipitation. Journal of Paleolimnology 38, 347-363.

Fletcher, M.-S., Moreno, P.I., 2011. Zonally symmetric changes in the strength and position of the Southern Westerlies drove atmospheric CO_2 variations over the past 14 k.y. Geology 39, 419-422.

Fletcher, M.-S., Moreno, P.I., 2012. Have the Southern Westerlies changed in a zonally symmetric manner over the last 14,000 years? A hemisphere-wide take on a controversial problem. Quaternary International 253, 32-46.

Garreaud, R.D., 2007. Precipitation and circulation covariability in the extratropics. Journal of Climate 20, 4789-4797.

Gilli, A., Ariztegui, D., Anselmetti, F.S., McKenzie, J.A., Markgraf, V., Hajdas, I., McCulloch, R.D., 2005. Mid-Holocene strengthening of the Southern Westerlies in South America - Sedimentological evidences from Lago Cardiel, Argentina (49°S). Global and Planetary Change 49, 75-93.

Gomez, B., Carter, L., Trustrum, N.A., Palmer, A., Roberts, A., 2004. El Niño-Southern Oscillation signal associated with middle Holocene climate change in intercorrelated terrestrial and marine sediment cores, North Island, New Zealand. Geology 32, 653-656.

Harrison, S.P., Dodson, J.R., 1993. Climates of Australia and New Guinea since 18,000 yr B.P. In: Wright Jr., H.E., Kutzbach, J.E., Webb III, T., Ruddiman, W.F., Street-Perrot, F.A., Bartlein, P.J. (Eds.), Global Climates Since the Last Glacial Maximum. University of Minnesota Press, Minneapolis, MN, pp. 265-293.

Hellstrom, J., McCulloch, M., Stone, J., 1998. A detailed 31,000-year record of climate and vegetation change, from the isotope geochemistry of two New Zealand speleothems. Quaternary Research 50, 167-178.

Hendon, H.H., Thompson, D.W., Wheeler, M.C., 2007. Australian rainfall and surface temperature variations associated with the Southern Hemisphere annular mode. Journal of Climate 20, 2452-2467.

Higuera, P.E., Brubaker, L.B., Anderson, P.M., Hu, F.S., 2009. Vegetation mediated the impacts of postglacial climate change on fire regimes in the south-central Brooks Range, Alaska. Ecological Monographs 79, 201-219.

Hill, K.J., Santoso, A., England, M.H., 2009. Interannual Tasmanian rainfall variability associated with large-scale climate modes. Journal of Climate 22, 4383-4397.

Hogg, A.G., Hua, Q., Blackwell, P.G., Niu, M., Buck, C.E., Guilderson, T.P., Heaton, T.J., Palmer, J.G., Reimer, P.J., Reimer, R.W., Turney, C.S.M., Zimmerman, S.R.J., 2013. SHCal13 southern hemisphere calibration, 0 - 50,000 cal BP. Radiocarbon 55, doi:10.2458/azu_js_rc.55.16783.

Lamy, F., Kilian, R., Arz, H.W., Francois, J.-P., Kaiser, J., Prange, M., Steinke, T., 2010. Holocene changes in the position and intensity of the southern westerly wind belt. Nature Geosciences 3, 695-699.

Long, C.J., Whitlock, C., Bartlein, P.J., Millspaugh, S.H., 1998. A 9000-year fire history from the Oregon Coast Range, based on a high-resolution charcoal study. Canadian Journal of Forest Research 28, 774-787.

Lynch, A.H., Beringer, J., Kershaw, A.P., Marshall, A., Mooney, S., Tapper, N., Turney, C., van der Kaars, S., 2007. Using the palaeorecord to evaluate climate and fire

interactions in Australia. Annual Review of Earth and Planetary Sciences 35, 215-239.

Macphail, M.K., 1979. Vegetation and climates in southern Tasmania since the Last Glaciation. Quaternary Research 11, 306-341.

Markgraf, V., Whitlock, C., Haberle, S., 2007. Vegetation and fire history during the last 18,000 cal yr BP in Southern Patagonia: Mallín Pollux, Coyhaique, Province Aisén (45 41′ 30 ″S, 71 50′ 30 ″W, 640 m elevation). Palaeogeography, Palaeoclimatology, Palaeoecology 254, 492-507.

Marx, S.K., McGowan, H.A., Kamber, B.S., 2009. Long-range dust transport from eastern Australia: a proxy for Holocene aridity and ENSO-induced climate variability. Earth and Planetary Science Letters 282, 167-177.

McGlone, M.S., Wilmshurst, J.M., 1999. A Holocene record of climate, vegetation change and peat bog development, east Otago, South Island, New Zealand. Journal of Quaternary Science 14, 239-254.

McGlone, M.S., Salinger, M.J., Moar, N.T., Kutzbach, J.E., Webb III, T., Ruddiman, W.F., Street-Perrott, F.A., Bartlein, P.J., 1993. Paleovegetation studies of New Zealand's climate since the last glacial maximum. In: Wright Jr., H.E., Kutzbach, J.E., Webb III, T., Ruddiman, W.F., Street-Perrot, F.A., Bartlein, P.J. (Eds.), Global Climates Since the Last Glacial Maximum. University of Minnesota Press, Minneapolis, MN, pp. 294-317.

Meneghini, B., Simmonds, I., Smith, I.N., 2007. Association between Australian rainfall and the Southern Annular Mode. International Journal of Climatology 27, 109-121.

Moreno, P.I., Francois, J.P., Moy, C.M., Villa-Martinez, R., 2010. Covariability of the Southern Westerlies and atmospheric CO_2 during the Holocene. Geology 39, 727-730.

Moy, C.M., Seltzer, G.O., Rodbell, D.T., Anderson, D.M., 2002. Variability of El Niño/Southern Oscillation activity at millennial timescales during the Holocene epoch. Nature 420, 162-165.

Moy, C.M., Dunbar, R.B., Guilderson, T.P., Waldmann, N., Mucciarone, D.A., Recasens, C., Ariztegui, D., Austin Jr., J.A., Anselmetti, F.S., 2011. A geochemical and sedimentary record of high southern latitude Holocene climate evolution from Lago Fagnano, Tierra del Fuego. Earth and Planetary Science Letters 302, 1-13.

Parris, A.S., Bierman, P.R., Noren, A.J., Prins, M.A., Lini, A., 2010. Holocene paleostorms identified by particle size signatures in lake sediments from the northeastern United States. Journal of Paleolimnology 43, 29-49.

Quigley, M.C., Horton, T., Hellstrom, J.C., Cupper, M.L., Sandiford, M., 2010. Holocene climate change in arid Australia from speleothem and alluvial records. Holocene 20, 1093-1104.

R Core Team (2013). R: A language and environment for statistical computing. R Foundation for Statistical Computing, Vienna, Austria. URL http://www.R-project.org/.

Rees, A.B.H., Cwynar, L.C., Cranston, P.S., 2008. Midges (Chironomidae, Ceratopogonidae, Chaoboridae) as a temperature proxy: a training set from Tasmania, Australia. Journal of Paleolimnology 40, 1159-1178.

Rodbell, D.T., Seltzer, G.O., Anderson, D.G., Abbott, M.B., Enfield, D.B., Newman, J.H., 1999. An ~15,000-year record of El Niño-driven alluviation in southwestern Ecuador. Science 283, 516-520.

Sandweiss, D.H., Richardson III, J.B., Reitz, E., Rollins, H.B., Maasch, K.A., 1996. Geoarchaeological evidence from Peru for a 5000 years B.P. onset of El Niño. Science 273, 1531-1533.

Shulmeister, J., Lees, B.G., 1995. Pollen evidence from tropical Australia for the onset of an ENSO-dominated climate at c. 4000 B.P. Holocene 5, 10-18.

Shulmeister, J., Goodwin, I., Renwick, J., Harle, K., Armand, L., McGlone, M.S., Cook, E., Dodson, J., Hesse, P.P., Mayewski, P., Curran, M., 2004. The Southern Hemisphere westerlies in the Australasian sector over the last glacial cycle: a synthesis. Quaternary International 118-119, 23-53.

Toggweiler, J.R., 2009. Climate change: Shifting Westerlies. Science 323, 1434-1435.

Toggweiler, J.R., Russell, J.L., Carson, S.R., 2006. Midlatitude westerlies, atmospheric CO_2, and climate change during the ice ages. Paleoceanography 21, PA2005.

Trivinho-Strixino, S., Roque, F.O., Cranston, P.S., 2009. Redescription of *Riethia truncatocaudata* (Edwards, 1931) (Diptera: Chironomidae), with description of female, pupa and larva and generic diagnosis for *Riethia*. Aquatic Insects 31, 247-259.

Walker, I.R., Smol, J.P., Engstrom, D.R., Birks, H.J.B., 1991. An assessment of Chironomidae as quantitative indicators of past climatic change. Canadian Journal of Fisheries and Aquatic Sciences 48, 975-987.

Walsh, M.K., Pearl, C.A., Whitlock, C., Bartlein, P.J., Worona, M.A., 2010. An 11 000-year-long record of fire and vegetation history at Beaver Lake, Oregon, central Willamette Valley. Quaternary Science Reviews 29, 1093-1106.

Whitlock, C., Moreno, P.I., Bartlein, P., 2007. Climatic controls of Holocene fire patterns in southern South America. Quaternary Research 68, 28-36.

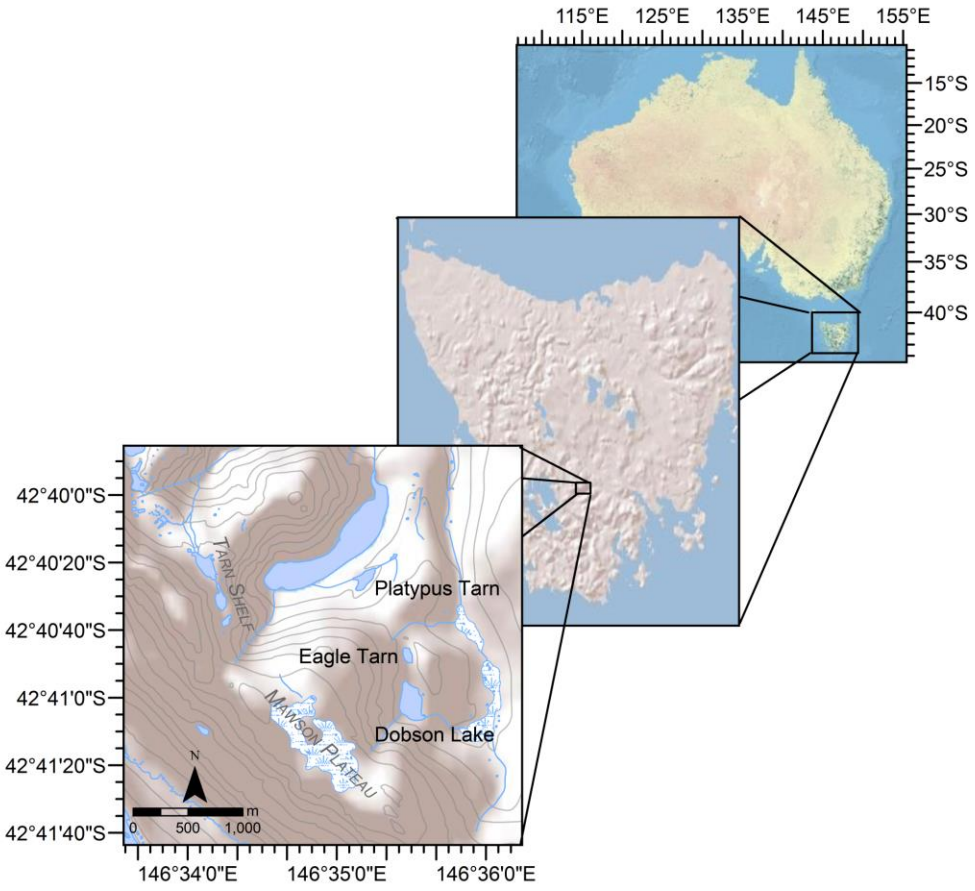

Figure 5.1: Map of the study site.

Note the proximity of Lake Dobson to other sites mentioned in the text: the Tarn Shelf, Mawson Plateau, and Eagle Tarn.

Figure 5.2: Summary figure including a) the percentage of full lakes in eastern and central Tasmania (Harrison and Dodson, 1993) and b) the number of El Niño events at Laguna Pallcacocha, Ecuador in 100-a overlapping windows (Moy et al., 2002). The figure also includes the suite of lacustrine proxies from Lake Dobson, namely: c) the percentage of grains larger than 500 µm (log scale); d) the percentage of sand and clay constituting each sample; e) the median grain size of the sediment; f) the precipitation index calculated from fossil chironomid taxa; g) iron content; and h) charcoal influx rates with background levels (grey line), threshold limits (red line), and fires (red plus symbols). The dashed line in b denotes the minimum number of events needed to produce an ENSO band, and solid grey lines in e, f, and g represent running averages. We objectively derived the zones from the chironomid data with Psimpoll (Bennett, 2005).

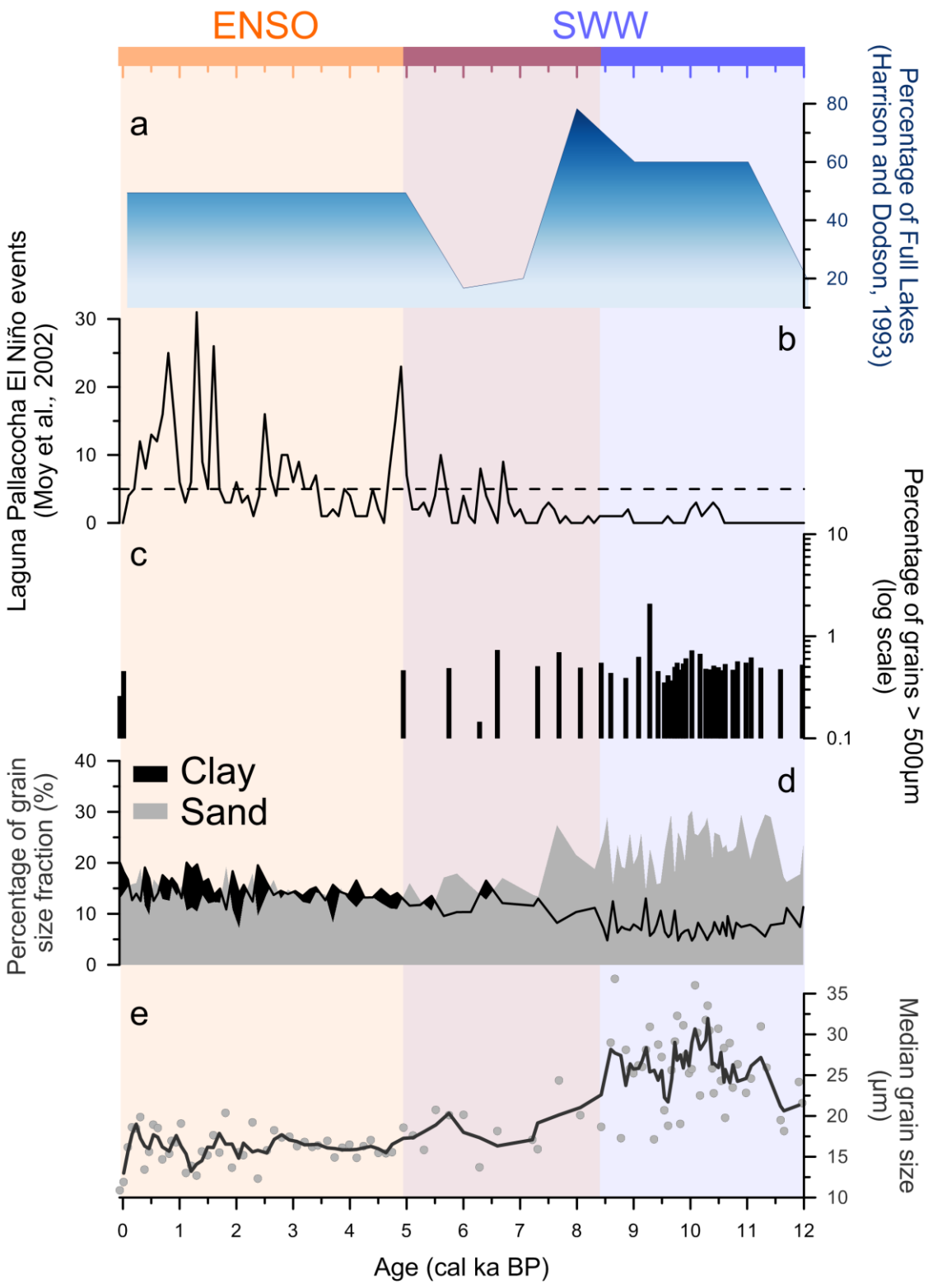

Figure 5.2: Summary figure.

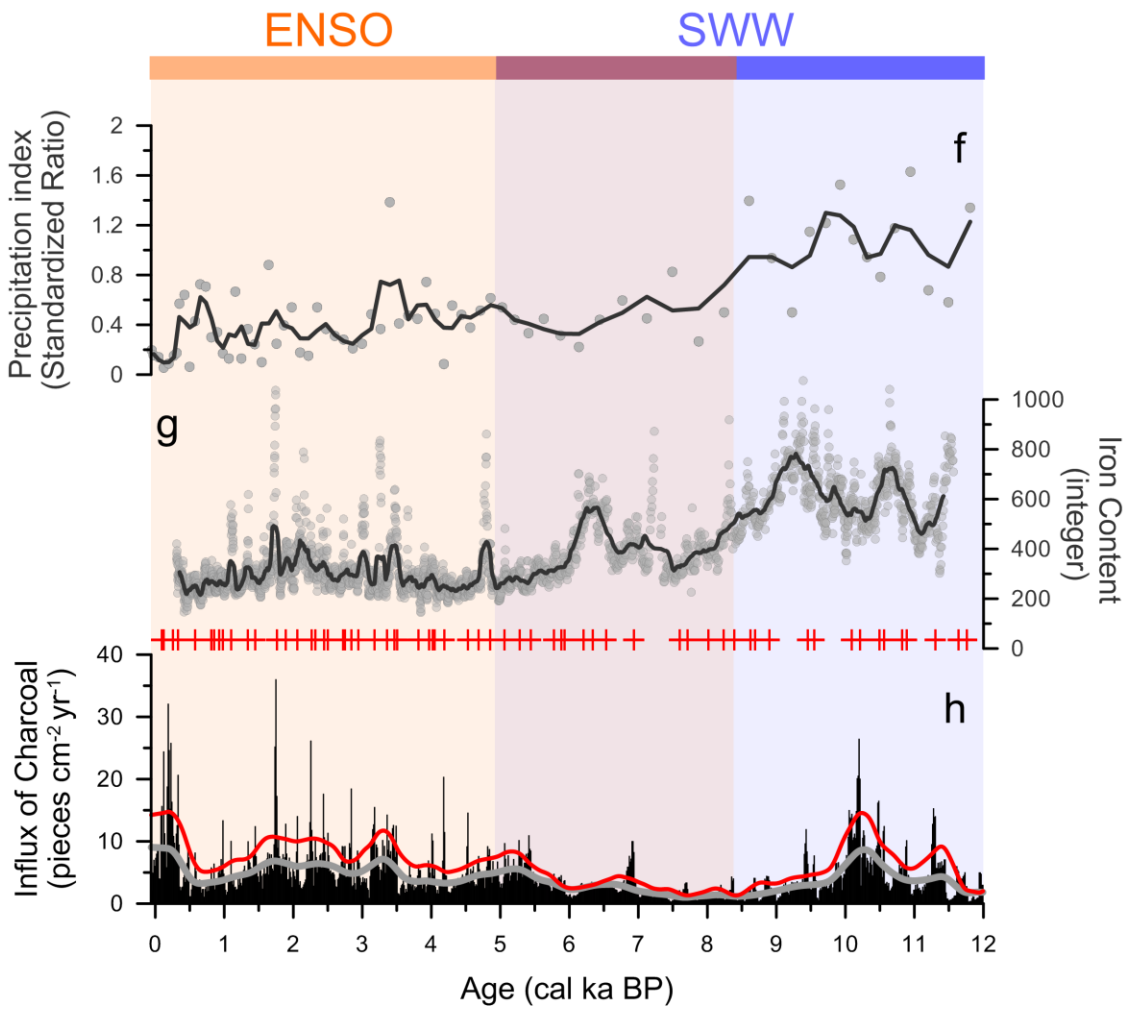

Figure 5.2: Summary figure (continued).

Table 5.1: Radiometric dates from Lake Dobson, Mount Field National Park, Tasmania.

Lab code	Sample depth (cm)	Sample Description	^{14}C age (a BP)	95% C.I.[a] (min)	95% C.I.[a] (max)	HPD[b]
76880	116.7-118.7	leaf & wood fragments	955±20	767	905	95.0
76881	204.9-206.9	leaf fragments	1795±20	1595	1601	2.0
				1606	1715	92.9
76882	284.4-286.0	leaf fragments	2555±20	2490	2604	52.0
				2606	2643	15.5
				2653	2668	2.3
				2676	2739	25.2
76883	392.2-394.2	leaf fragments, stems	3750±25	3932	3941	1.5
				3969	4104	79.1
				4106	4149	14.3
76884	529.0-531.0	wood fragments	5790±20	6468	6638	95.0
76885	598.0-600.0	wood fragments	8235±25	9029	9259	95.0
76886	695.8-697.8	leaf & wood fragments	9795±35	11110	11111	0.3
				11122	11242	94.6
76887	777.1-782.1	leaf & wood fragments	12035±35	13741	13988	95.0
76888	824.0-826.0	leaf & wood fragments	12240±30	13969	14210	95.0
76889	927.0-928.0	leaf & wood fragments	12555±35	14406	15079	95.0

Ten terrestrial macrofossil samples were collected from Lake Dobson for AMS ^{14}C dating and submitted to the UCI Keck Carbon Cycle AMS Program at the University of California, Irvine, USA. Calibrations were made in CLAM v2.2 (Blaauw, 2010) using the SHCal13 calibration curve (Hog et al., 2013).
[a]C.I. = confidence interval
[b]HPD = highest probability density

Chapter 6 Conclusion and synthesis

Specific conclusions and data chapter synthesis

The "paleo approach" draws on our knowledge of the present to interpret the past. Accordingly, my thesis centers on understanding the modern environment of Tasmania in order to investigate two major transitions: 1) the most recent deglaciation and 2) the transition from a SWW- to ENSO-dominated climate. The building blocks focus on developing the neoecology and understanding modern chironomid-environment relationships.

In the neoecology chapters (Chapters 2 and 3), I found that chironomids possess significant relationships to pH and temperature in Tasmania. From a hierarchical perspective, the fauna can be divided into two groups corresponding to the geological provinces delineated by Tyler's Line. That is, at the largest scale, assemblages reflect the congruent changes in climate, vegetation, and geology that define the 146th meridian. This explains why pH is the most important predictor of chironomid distributions in Tasmania. However, within either province, mean temperature of the warmest quarter (TWARM) explains the most variance in the species data. Consequently, chironomids are a useful proxy of temperature and a valuable tool for reconstructing past climates; therefore I developed a chironomid-based transfer function to reconstruct TWARM during the last deglaciation.

In the paleoecology chapters, I applied the knowledge garnered from modern chironomid-environment relationships to develop templates of past temperature and precipitation for the Mount Field region of Tasmania. In Chapter 4, I applied the

TWARM transfer function to a pair of fossil chironomid records dating to about 16 cal ka BP. From a climatological perspective, one of the most interesting periods is the transition from the late Pleistocene to the Holocene; conditions rapidly switched from maximum glacial development to a more or less modern state. One simple, though profound, question immediately arises - does Tasmania possess a transition resembling the Northern Hemisphere, with a Younger Dryas (YD) signal, the Southern Hemisphere, with an Antarctic Cold Reversal (ACR), or something completely unique. From my results, the last scenario appears to be the case with Tasmania registering a deglacial sequence that is unique from Northern and Southern Hemisphere ice cores. Importantly, there is little evidence of the ACR and no evidence of the YD. Shortly after deglaciation, TWARM reached modern values and remained high until roughly 12.5 cal ka BP, supporting evidence from cosmogenic dates and sea surface temperatures. After a generally cool phase, temperatures began to increase around 8 cal ka BP, reaching a mid-Holocene thermal maximum sometime between 6.7 and 4.6 cal ka BP. After the thermal maximum, temperatures once again became cool in the Mount Field region.

The second paleoecology chapter attempts to characterize the transition from a SWW- to ENSO-controlled climate, postulated to have occurred about 5 ka BP. Rainfall was elevated between 12 and 8.4 cal ka BP, with conditions analogous to a modern day positive SAM during the summer. That is, the westerlies were weak and displaced farthest to the south. Weakened westerlies enhance effective moisture in eastern Tasmania by two mechanisms: reduced foehn winds 1) lessen the impact of evaporation and 2) permit the incursion of moisture-bearing easterlies. Strong SWW flow resumed between 8.4 and 4.9 cal ka BP, driving drier (wetter) conditions in the east (west). The

onset of an El Niño-dominated climate at 4.9 cal ka BP was abrupt and marked an increased fire frequency in the Mount Field region, characterizing a variable, though generally drier catchment at Lake Dobson.

General conclusions and reflections

The "paleo approach" has much to recommend it and, with the advancement of statistical techniques, it is possible to quantify the past. Reconstructing environmental change serves three powerful, though related functions: 1) extending the historical record, 2) contextualizing modern ecosystems by providing baseline references, and 3) fine-tuning climate models by comparing simulations to results obtained from paleolimnological techniques. These functions are primary to creating templates of environmental change, from which hypotheses are developed and subsequently tested. However, without the ability to directly observe past phenomena, it is difficult to gauge the reliability of baselines generated by the "paleo approach". Many studies boil down to a weight-of-evidence argument, where agreement between multiple proxies equates to a more robust picture of the past (e.g., Chapter 5). But, with the advancement of statistical techniques, single proxy reconstructions are becoming increasingly more reliable (e.g., the diagnostics from Chapter 4). Returning to the big picture, these two features, namely the development of templates of environmental change and the incorporation of complex statistics into paleolimnology, deserve further attention.

This thesis outlines a template of late Pleistocene/Holocene climate (i.e., temperature and precipitation) change for the Mount Field region of Tasmania. Until recently, few paleolimnological studies have been conducted in the Southern

Hemisphere. Most of the previous research from Tasmania is pollen-based and qualitative to semi-quantitative in nature. This thesis presents one of the first quantitative models for the region though, more importantly, the model was made using a new, independent proxy - chironomids. I applied the transfer function to some of the best constrained and well-dated chronologies from Tasmania, developed using modern techniques. Further, unlike most of the previous research, I assessed the reliability of estimates generated by the model. All of this is to say that much of this thesis is ground work, building the foundation for further research and more pointed research questions. I essentially developed two late Pleistocene/Holocene reconstructions: one for temperature of the warmest quarter (quantitative) and another for precipitation (qualitative). Combined with interpretations from the pollen records, or from proxies yet to be applied in Tasmania, my work should provide a point of reference for broad scale trends and help elucidate a finer understanding of past climates.

For instance, one of the most interesting findings of this thesis is that the chironomid-based temperature estimates suggest TWARM was above average from about 16 to 12 cal ka BP; this is in stark contrast to temperatures inferred from pollen evidence. The chironomid-based estimates appear to be reliable and cosmogenic dates from moraines in the catchment along with sea surface temperatures (SST) from the adjacent ocean corroborate this feature (see Chapter 4). One potential explanation is that forest development at Mount Field was delayed until ~11.5 cal ka BP due to moisture availability (see Chapter 5). Another possibility is that summer temperatures were warm while winter temperatures were cool during this period, triggering a seasonal threshold for chironomids, but not for vegetation. Either way, the contribution of a template derived

from an independent line of evidence (i.e., chironomids) lets us refine our understanding of past environments, generate clear hypotheses, and highlight specific time intervals worth investigating in higher resolution. However, not every reconstruction is reliable, which brings me to the next point - the incorporation of numerical techniques into paleolimnology.

The integration of statistics into paleolimnology during the course of this thesis has been staggering. In their new book on data handling in paleolimnology, Birks et al. (2012) described complex methods ranging from Bayesian age-depth models to artificial neural networking. Considering one of the earliest applications of quantitative techniques in paleolimnology occurred in 1975, when Pennington and Sackin applied principal components analysis to down-core pollen and geochemical data, it seems the adoption of numerical methods by the field has been nothing short of viral. However, the integration of statistics is a double-edged sword. With the proliferation of software packages and an ever increasing suite of environmental proxies (limited only by the investigator's imagination), it is all too easy to create reconstructions with inappropriate methods and/or without understanding underlying mechanisms governing a proxy's deposition. The mantra, "Garbage in, garbage out" holds particularly true nowadays, when powerful computers can spew out piles of erroneous data in a short period of time. With the popularity of the transfer function approach, the temptation to publish reconstructions without proper scrutiny seems too alluring for many and is a pitfall I encountered during my project.

To elaborate, the main objective of this thesis was to develop a consensus reconstruction of TWARM for the Mount Field region using records from Lake Dobson

and Eagle and Platypus Tarns; obviously that objective was not met. Consensus reconstructions have the benefit of highlighting major trends by using multiple sites, thereby reducing noise. After running the reconstruction diagnostics, it was clear that the fossil chironomids from Lake Dobson were not responding to TWARM throughout the late Pleistocene and Holocene; consequently I explored other relationships that ultimately resulted in the material comprising Chapter 5. Not only is this an example of how projects evolve, but it emphasizes the value of scrutinizing results. It would have been easier (and quicker) to run the fossil assemblages from Lake Dobson through the transfer function and include the results in a consensus reconstruction; however, as previously mentioned - garbage in, garbage out!

Future directions

The Southern Hemisphere is an exciting region for the pursuits of Quaternary research and paleolimnology. Recently, robust climate event stratigraphies, covering the last 30 ka, have been developed for New Zealand (Alloway et al., 2007) and Australia (Petherick et al., 2013) while an unprecedented number of studies are being conducted in Southern South America (SSA). Further, advances in methodologies permit more complex questions and the ability to reconstruct more complex phenomena, like seasonality and precipitation.

Seasonality is simultaneously a major control of biological communities and one of the most difficult variables to reconstruct. Nevertheless, seasonality could explain a discrepancy between my results and the literature. The chironomid record at Mount Field indicates above-modern temperatures during the Antarctic Cold Reversal - starkly

contrasting with pollen inferences. However, the chironomid communities could have responded to warmer summer temperatures, while the vegetation was responding to cooler winter or annual temperatures. Degree-days play an important role in the chironomid lifecycle (Brooks et al., 2007), and the vegetation of Tasmania is known to be highly sensitive to frosts and prolonged cold periods (Reid et al., 2005). Ecosystem process models could be used to exploit this apparent seasonal contrast between chironomids and pollen. In these exploratory tests, ecosystem models of forest dynamics are used to determine climate settings that produce the best match between simulation results and fossil pollen records (McGlone et al., 2011). Chironomid-based reconstructions could be used to constrain summer temperatures, thereby refining the climate parameters of model runs. Consequently, coupling both biological proxies could provide valuable insights regarding seasonality during the transition from the late Pleistocene to the Holocene as well as during other periods of interest.

Like seasonality, precipitation is another important control of biological proxies that is difficult to reconstruct. Gains have been made through isotope analysis, carbon to nitrogen ratios (C/N), and indirectly through diatom transfer functions designed to reconstruct salinity. For instance, Moy et al. (2011) recently employed geochemical analyses (e.g., C/N) to understand the Holocene climate of Tierra del Fuego, SSA. In the case of Tasmania, north-south transects could inform on the migration or expansion/contraction of the SWW, while west-east transects could inform on the strength of circulation. As previously mentioned, regions west of large mountain ranges typically possess a positive correlation between zonal wind speed and precipitation, resulting in hyper-humid conditions. East of the mountain ranges, the correlation between

wind speed and rainfall either disappears or becomes negative, producing sub-humid to semi-arid rain-shadows (Garreaud, 2007). Consequently, if SWW flow is strong, proxies from western regions should archive greater rainfall while those from eastern regions should record less. On the other hand, if SWW strength is attenuated, the opposite would be true. Determining trends in precipitation and seasonality during the ACR would be very useful; however, the ACR is not the only period warranting further investigation.

Traditionally, the Last Glacial Maximum is considered to have occurred between about 24 and 18 cal ka BP. However, in New Zealand, evidence for an early onset of the LGM, beginning around 29-28 ka, has prompted terms like "extended LGM" (eLGM; Newnham et al., 2007) in the literature. The eLGM was interrupted by a warming complex between 27 and 21 ka (Alloway et al., 2007). Questions remain regarding the scale of this phenomenon; for instance how far-reaching was the eLGM? As Tasmania is one of the closest major landmasses to New Zealand, occupying similar latitudes and also possessing a maritime climate, one might expect this phenomenon to register in Tasmanian archives.

With templates of long term climate change emerging from landmasses occupying the Southern Ocean, it is possible to address more complex phenomena during specific climate events. Seasonality and precipitation are among a few of the more difficult variables submitting to reconstruction, while the expression of the LGM in Australasia, along with the transition from the late Pleistocene to the Holocene, are among a few of the interesting events. The advancement of methodological and statistical techniques has complimented the development of templates of environmental change, making it truly a great time to be a Quaternary researcher!

References

Alloway, B.V., Lowe, D.J., Barrell, D.J.A., Newnham, R.M., Almond, P.C., Augustinus, P.C., Bertler, N., Carter, L., Litchfield, N.J., McGlone, M.S., Shulmeister, J., Vandergoes, M.J., Williams, P.W., 2007. Towards a climate event stratigraphy for New Zealand over the past 30 000 years (NZ-INTIMATE project). Journal of Quaternary Science 22, 9-35.

Birks, H.J.B., Lotter, A.F., Juggins, S., Smol, J.P., 2012. Tracking Environmental Change using Lake Sediments. Data Handling and Numerical Techniques, vol 5. Springer, Dordrecht, Netherlands.

Brooks, S.J., Langdon, P.G., Heiri, O., 2007. Using and Identifying Chironomid Larvae in Palaeoecology. QRA Technical Guide no. 10. Quaternary Research Association, London, UK.

Garreaud, R.D., 2007. Precipitation and circulation covariability in the extratropics. Journal of Climate 20, 4789-4797.

Reid, J.B., Hill, R.S., Brown, M.J., Hovenden, M.J., 2005. Vegetation of Tasmania. Australian Biological Resources Study, Tasmania, Australia.

McGlone, M.S., Hall, G.M., Wilmshurst, J.M., 2011. Seasonality in the early Holocene: Extending fossil-based estimates with a forest ecosystem process model. The Holocene 21, 517-526.

Moy, C.M., Dunbar, R.B., Guilderson, T.P., Waldmann, N., Mucciarone, D.A., Recasens, C., Ariztegui, D., Austin Jr., J.A., Anselmetti, F.S., 2011. A geochemical and sedimentary record of high southern latitude Holocene climate evolution from Lago Fagnano, Tierra del Fuego. Earth and Planetary Science Letters 302, 1-13.

Newnham, R.M., Lowe, D.J., Giles, T., Alloway, B.V., 2007. Vegetation and climate of Auckland, New Zealand, since ca. 32 000 cal. yr ago: support for an extended LGM. Journal of Quaternary Science 22, 517-534.

Pennington, W., Sackin, M., 1975. An application of principal components analysis to the zonation of two Late-Devensian profiles. New Phytologist 75, 419-453.

Petherick, L., Bostock, H., Cohen, T.J., Fitzsimmons, K., Tibby, J., Fletcher, M., Moss, P., Reeves, J., Mooney, S., Barrows, T., 2013. Climatic records over the past 30 ka from temperate Australia - a synthesis from the Oz-INTIMATE workgroup. Quaternary Science Reviews, in press.

Curriculum Vitae

Candidate's full name:

Andrew Benjamin Herbert Rees

Universities attended (with dates and degrees obtained):

Bachelor of Science, Biology, University of New Brunswick 2005

Bachelor of Arts, Philosophy, University of New Brunswick 2005

Publications:

Cwynar, L.C., **Rees, A.B.H.**, Pedersen, C.R., Engels, S., 2012. Depth distribution of chironomids and an evaluation of site-specific and regional lake-depth inference models: a good model gone bad? Journal of Paleolimnology 48, 517-533.

Engels, S., Cwynar, L.C., **Rees, A.B.H.**, Shuman, B.N., 2012. Chironomid-based water depth reconstructions: an independent evaluation of site-specific and local inference models. Journal of Paleolimnology 48, 693-709.

Irvine, F., Cwynar, L.C., Vermaire, J.C., **Rees, A.B.H.**, 2012. Midge-inferred temperature reconstructions and vegetation change over the last~ 15,000 years from Trout Lake, northern Yukon Territory, eastern Beringia. Journal of Paleolimnology 48, 133-146.

Rees, A.B.H., Cwynar, L.C., 2010. Evidence for early postglacial warming in Mount Field National Park, Tasmania. Quaternary Science Reviews 29, 443-454.

Rees, A.B.H., Cwynar, L.C., 2010. A test of Tyler's Line - response of chironomids to a pH gradient in Tasmania and their potential as a proxy to infer past changes in pH. Freshwater Biology 55, 2521-2540.

Rees, A.B.H., Cwynar, L.C., Cranston, P.S., 2008. Midges (Chironomidae, Ceratopogonidae, Chaoboridae) as a temperature proxy: a training set from Tasmania, Australia. Journal of Paleolimnology 40, 1159-1178.

Conference Presentations:

Rees, A.B.H., Cwynar, L.C., Fletcher, M.-S., 2013. Southern Westerly Winds submit to the ENSO regime: A multi-proxy paleohydrology record from Lake Dobson, Tasmania. International Oral Presentation: International Union for Quaternary Research (INQUA) Early Career Researchers meeting, Wollongong, Australia.

Rees A.B.H., Cwynar L.C., Vandergoes M.J., 2011. Assessing chironomid-based temperature reconstructions from Tasmania, Australia - the devil is in the details. International Oral Presentation: 18th INQUA Congress, Bern, Switzerland.

Rees A.B.H., Cwynar L.C., Vandergoes M.J., 2011. A continuous sediment record encompassing marine isotope stages 1 to 6 from Lake Selina, Tasmania. National Oral Presentation: CANQUA-IAH Joint Meeting, Quebec City, Canada.

Rees A.B.H., Cwynar L.C., 2010. Lateglacial and Holocene chironomid-inferred temperature records from Tasmania, Australia. International Oral Presentation: 6th Southern Connections Congress, Bariloche, Argentina.

Rees A.B.H., Cwynar L.C., 2009. Paleotemperature reconstructions from Mount Field National Park, Tasmania. International Oral Presentation: Past Climates

Symposium and INTIMATE (Integration of Ice core, Marine and Terrestrial Records) meeting, Wellington, New Zealand.

Rees A.B.H., Cwynar L.C., 2007. A chironomid-based transfer function to reconstruct the paleoclimate of Tasmania. International Poster Presentation: 17th INQUA Congress, Cairns, Australia.

Rees A.B.H., Cwynar L.C., 2007. An inference model for reconstructing mean summer temperature in Tasmania using fossil chironomids. National Poster Presentation: CANQUA meeting, Ottawa, Canada.